DRAFT

Sparrows Point Shoreline Reclamation Project
Hydrodynamic Model of Baltimore Harbor

4/22/94
WILL CORRECT
PER BOB SMITH

Prepared for

~~Maryland Environmental Service~~
MARYLAND PORT ADMINISTRATION
CONTRACT NO. 593917

Final Report Submitted to

The Maryland Department of the Environment
Chesapeake Bay and Watershed Management Administration

by

Shenn-Yu Chao

University of Maryland System
Center for Environmental and Estuarine Studies
Horn Point Environmental Laboratory

March, 1994

DRAFT

DRAFT

Sparrows Point Shoreline Reclamation Project Hydrodynamic Model of Baltimore Harbor

Prepared for

~~Maryland Environmental Service~~

Final Report Submitted to

The Maryland Department of the Environment
Chesapeake Bay and Watershed Management Administration

by

Shenn-Yu Chao

University of Maryland System
Center for Environmental and Estuarine Studies
Horn Point Environmental Laboratory

March, 1994

DRAFT

TABLE OF CONTENTS

LIST OF FIGURES

ACKNOWLEDGEMENTS

The development of the hydrodynamic model for Baltimore Harbor would not have been possible without the financial support of the Maryland Port Administration. Nauth Panday of Chesapeake Bay and Watershed Management Administration (CBWMA) provided much needed logistics to make this effort successful. Bob Smith of Maryland Environmental Service patiently followed every step of the progress and provided valuable advices including the final editing of this report. Harry Wang of Waterways Experiment Station, Army Corps of Engineers derived boundary conditions of Baltimore Harbor from the upper Chesapeake Bay hydrodynamic model for us timely and conscientiously.

I was also indebted to Sunny Wu and Debra Willey for executing day-to-day operations faithfully and cheerfully, to my colleagues Bill Boicourt and Larry Sanford for providing helpful comments, to Santha Kurian of CBWMA for providing Patapsco River inflow data, and to Jeff Liang, Visty Dalal and Liz Casman of CBWMA for general and editorial comments.

SUMMARY

In 1992, the State of Maryland proposed a wetland creation project near Bethlehem Steel, Sparrows Point, MD. An assessment of the environmental impact of the possible shoreline alteration necessitates computer simulations of Baltimore Harbor circulation. To meet this goal, a three-dimensional hydrodynamic model for the upper Chesapeake Bay and a high-resolution hydrodynamic model for Baltimore Harbor are utilized in this project. The upper Chesapeake Bay model, developed by Waterways Experiment Station (WES) of the Army Corps of Engineers, provided boundary conditions for the high-resolution Baltimore Harbor model. The high-resolution Baltimore Harbor model was developed by the Horn Point Environmental Laboratory of the University of Maryland, and was used to simulate Harbor circulation in 1984, 1985, and 1986.

The investigation led to the following major conclusions.

(1) The proposed wetland creation has virtually no effect on the harborwide circulation, as the relative volumetric change of the Baltimore Harbor caused by the shoreline alteration is negligible.

(2) The instantaneous Harbor circulation near the surface and over shallows is primarily driven by winds and secondarily driven by tides. Winds along the longitudinal axis of the Harbor are more effective in producing windward currents than cross-harbor winds.

(3) The two embayments to the east and west of Sparrows Point have incompatible flushing time scales. Being shallow and wide, waters in the Old Road Bay are renewed with e-folding time scales ranging from 8 to 13 days. By comparison, the residence time of waters in the much narrower and deeper Sparrows Point Channel is much shorter, having an e-folding scale of about 2 days.

(4) In terms of flushing rates in the two adjacent embayments, the environmental impact of the proposed wetland creation to the south of Sparrows Point is quite low. To quantify further, if the local shoreline is displaced southward by (360 m, 720 m, 1080 m), the respective delay in flushing rate will be less than (1–2%, 2–3%, 3–5%) in the Old Road Bay, and less than (1%, 7%, 10%) in the Sparrows Point Channel. The larger percentage change in Sparrows Point Channel should not be alarming, because the existing e-folding time scale is quite short (~2 days).

(5) The intra-annual variation of tidally averaged longitudinal circulation along the major axis of the Harbor seems to be driven by low-frequency salinity variations at the Harbor mouth. In 1984, our numerical simulation suggests that continuous freshening from January to July drives an inflow at the top and outflow at depths. Thereafter, the progressively saltier water entering the Harbor drives a reverse circulation pattern. This annual variation is in qualitative agreement with that observed in 1979.

1. Introduction

Baltimore Harbor is a tributary embayment situated on the western side of the upper Chesapeake Bay. In the upper (westernmost) reaches, the Harbor receives a small amount of fresh water from the Patapsco River; the amount of freshening is generally too insignificant to drive a classical two-layer estuarine circulation (Stroup, Pritchard and Carpenter; 1961). The Harbor is periodically flushed by tidal currents at the mouth. Garland (1952) suggested a flushing time scale of about 60 days on the basis of the tidal prism exchange.

The subtidal circulation of the Baltimore Harbor appears to be induced by the stratification of the adjacent Chesapeake Bay. Pritchard and Carpenter (1960) envisioned a three-layer flow pattern inside the Harbor. The vertically averaged salinity and density are essentially constant from the mouth to the head of the Harbor. Furthermore, there is less vertical variation in salinity within the Harbor than there is in the adjacent Chesapeake Bay. The surface waters of the Harbor are more saline than the surface waters in the Bay just outside the Harbor. However, the deep waters in the Harbor are less saline than waters at the corresponding depth in the adjacent Bay. On this basis, Pritchard and Carpenter inferred that both surface and bottom layers must exhibit a net inflow to the Harbor, while the water at mid-depth flows out of the Harbor into the open Bay. The evidence for this type of circulation pattern, according to Pritchard and Carpenter, should be strongest after a period of high discharge from the Susquehanna River, when the vertical stratification is large, and weakest after a period of low flow, when the stratification is small. There is some indication that the strength of this circulation is greatest in winter and early spring, and least in summer and fall.

Direct long-term flow measurements were conducted in 1978–1979 (Boicourt and Olson, 1982) mainly along the deep channel of the Baltimore Harbor. To verify the three-layer circulation, current data were averaged over long periods to partially remove meteorologically and tidally induced circulations. The results suggested that the three-layer circulation might exist occasionally, but was not as persistent as one would like to see. In particular, the outflow at mid-depth could be as large as 5 cm/s, often extending to the bottom and overwhelming the bottom inflow. The surface inflow at the top 2 m of the water column appeared to be elusive, often being masked by meteorologically driven noises. Moreover, Patapsco River freshets could, on occasion, produce conditions in which the three-layer circulation is over-ridden by the classical two-layer estuarine circulation.

Not much is previously known about the wind-driven circulation inside the Baltimore Harbor. Wind events are generally episodic over short time intervals (up to 10 days). In fall and winter months, winds are mostly northwesterly or northerly. In summer months the northwesterly or northerly winds are more frequently disrupted by southerly wind events lasting several days each. The wind-driven circulation often dominates other circulation components over short time intervals, and is particularly prominent near the Harbor head (Middle Branch) and in the three principal tributaries (Northwest Branch, Curtis Creek, and Bear Creek) (Boicourt and Olson, 1982).

In 1992, the State of Maryland proposed a wetland creation project ~~near~~ on Bethlehem Steel property, Sparrows Point. An assessment of the environmental impact of the possible shoreline alteration necessitates computer simulations of Baltimore Harbor circulation. To meet this goal, a three-dimensional hydrodynamic model for the upper Chesapeake Bay and a high-resolution hydrodynamic model for the Baltimore Harbor are utilized in this project.

The U.S. Army Corps of Engineers Waterways Experiment Station (WES) had developed a 3-D hydrodynamic model of the upper Chesapeake Bay for the Maryland Department of Natural Resources. The model was completed in July 1989 with the unique feature of curvilinear coordinates that permit the adoption of more realistic and economical grid schematization (Johnson, 1989). The horizontal resolution of WES model is high enough to provide quality boundary conditions at the mouth of the Baltimore Harbor, but is insufficient to resolve the optimum geometry of the proposed wetlands and adjacent embayments. To meet the latter goal, the bulk of the present project is devoted to the development of a high resolution hydrodynamic model for the Baltimore Harbor, which is driven by the boundary conditions provided by the WES model. The Blumburg-Mellor hydrodynamic model (Mellor, 1990) provides the framework for the construction of the high-resolution model.

The model was developed under the auspices of Maryland Port Administration and was used to simulate the 3-dimensional Baltimore Harbor circulation in 1984, 1985 and 1986. Among the three years, 1984 is considered as a wet year, with excessive freshwater discharge from the Susquehanna River. By comparison, 1985 is a dry year and 1986 should be regarded as an average year. After completion of the 3 year simulation, the average year (1986) was selected as a model year to determine the flushing time scales and characteristics of the two small embayments east and west of the shoreline reclamation area as functions of altered shoreline configurations. A wet month and a dry month in 1986 were chosen for this concentrated study. Here "dry" and "wet" refer to low and high discharges from Patapsco River, respectively. Finally, vertical profiles of salinity and longitudinal flow along the main channel were examined to clarify the nature of three-layer circulation in the Baltimore Harbor.

Section 2 outlines the specifics of the high-resolution hydrodynamic model. Section 3 discusses dominant forcing functions driving the Harbor circulation in 1984, 1985 and 1986. Section 4 discusses the simulated surface flow in 1984, 1985 and 1986. Section 5 describes how the proposed wetland creation affects the flushing rate of the two adjacent embayments and the Harbor itself. In section 6, the nature of the three-layer circulation as seen from the hydrodynamic model is clarified. Section 7 summarizes and concludes this work. Suggestion for future studies is given in section 8.

2. Model formulation

2.1 Basic equations

Let x, y, z be the conventional right-handed cartesian coordinates, x and z being seaward and upward, respectively. The water is confined below by a variable bottom topography ($z = -H(x, y)$) and bounded above by a free surface ($z = \eta(x, y, t)$). The basic equations have been cast in a bottom-following, sigma coordinate system defined by

$$\sigma = (z - \eta) / D \tag{1}$$

where $D = H + \eta$ is the local water depth. Thus, σ ranges from $\sigma = 0$ at $z = \eta$ to $\sigma = -1$ at $z = -H$.

The hydrodynamic model solves for three velocity components ((u, v, ω) in (x, y, σ) directions, respectively), free surface (η), salinity (S) and a neutrally buoyant tracer (C). The governing equations may be written

$$\frac{\partial \eta}{\partial t} + \frac{\partial uD}{\partial x} + \frac{\partial vD}{\partial y} + \frac{\partial \omega}{\partial \sigma} = 0 \tag{2}$$

$$\frac{\partial uD}{\partial t} + \frac{\partial u^2 D}{\partial x} + \frac{\partial uvD}{\partial y} + \frac{\partial u\omega}{\partial \sigma} - fvD + gD\frac{\partial \eta}{\partial x} = \frac{\partial}{\partial \sigma}\left(\frac{K_M}{D}\frac{\partial u}{\partial \sigma}\right) - \frac{gD^2}{\rho_o}\int_\sigma^o \left[\frac{\partial \rho}{\partial x} - \frac{\sigma}{D}\frac{\partial D}{\partial x}\frac{\partial \rho}{\partial \sigma}\right] d\sigma + F_x \tag{3}$$

$$\frac{\partial vD}{\partial t} + \frac{\partial uvD}{\partial x} + \frac{\partial v^2 D}{\partial y} + \frac{\partial v\omega}{\partial \sigma} + fuD + gD\frac{\partial \eta}{\partial y} = \frac{\partial}{\partial \sigma}\left(\frac{K_M}{D}\frac{\partial v}{\partial \sigma}\right) - \frac{gD^2}{\rho_o}\int_\sigma^o \left[\frac{\partial \rho}{\partial y} - \frac{\sigma}{D}\frac{\partial D}{\partial y}\frac{\partial \rho}{\partial \sigma}\right] d\sigma + F_y \tag{4}$$

$$\frac{\partial SD}{\partial t}+\frac{\partial SuD}{\partial x}+\frac{\partial SvD}{\partial y}+\frac{\partial S\omega}{\partial \sigma}=\frac{\partial}{\partial \sigma}\left[\frac{K_H}{D}\frac{\partial S}{\partial \sigma}\right]+F_s \tag{5}$$

$$\frac{\partial CD}{\partial t}+\frac{\partial CuD}{\partial x}+\frac{\partial CvD}{\partial y}+\frac{\partial C\omega}{\partial \sigma}=\frac{\partial}{\partial \sigma}\left[\frac{K_H}{D}\frac{\partial C}{\partial \sigma}\right]+F_C \tag{6}$$

where ρ is the water density, ρ_o is a reference (constant) water density, f is the Coriolis parameter, g is the gravitation constant, and (K_M, K_H) are coefficients of vertical viscosity and diffusivity, respectively. The equation of state for the sea water follows that of Knudsen (1901).

The horizontal viscosity and diffusion terms are defined according to:

$$F_x=\frac{\partial}{\partial x}(D\tau_{xx})+\frac{\partial}{\partial y}(D\tau_{xy}) \tag{7a}$$

$$F_y=\frac{\partial}{\partial x}(D\tau_{xy})+\frac{\partial}{\partial y}(D\tau_{yy}) \tag{7b}$$

where

$$\tau_{xx}=2A_M\frac{\partial u}{\partial x} \tag{8a}$$

$$\tau_{xy}=A_M\left(\frac{\partial u}{\partial y}+\frac{\partial v}{\partial x}\right) \tag{8b}$$

$$\tau_{yy}=2A_M\frac{\partial v}{\partial y} \tag{8c}$$

Also,

$$F_\phi = \frac{\partial}{\partial x}(Dq_x) + \frac{\partial}{\partial y}(Dq_y) \tag{9}$$

where

$$q_x = A_H \frac{\partial \phi}{\partial x} \tag{10a}$$

$$q_y = A_H \frac{\partial \phi}{\partial y} \tag{10b}$$

and where ϕ represents S or C. Coefficients of horizontal viscosity and diffusivity (A_M and A_H) are determined by the Smagorinsky's formula.

$$(A_M, A_H) = (C_M, C_H)\, \Delta x\, \Delta y\, \frac{1}{2} \left| \nabla v + (\nabla v)^T \right| \tag{11}$$

Normally, values of (C_M, C_H) like 0.1 have been used in ocean modeling. However, if the grid spacing is small enough, (C_M, C_H) can be null (Oey et al, 1985). In the present model, the horizontal grid spacing is 360 m, small enough to warrant the use of very small values (C_M = 0.001 and C_H = 0.00001). In fact, such values are practically null, as further decreases do not result in visible changes in our results. Although we did not attempt to use zero value of A_m and A_H, our general feeling is that such a practice will not jeopardize the stability of the computation.

Coefficients of vertical viscosity and diffusivity (K_M and K_H) are determined by the local turbulence intensity level, using the 2-1/2-level turbulence closure scheme as described by Mellor and Yamada (1982).

2.2 Vertical boundary conditions

The vertical boundary conditions on eq.(2) are

$$\omega(0) = \omega(-1) = 0. \tag{12}$$

The boundary conditions on equations (3) and (4) are

$$\frac{K_M}{D}\left(\frac{\partial u}{\partial \sigma}, \frac{\partial v}{\partial \sigma}\right) = (\tau_x, \tau_y)/\rho_o, \quad \sigma = 0 \tag{13a}$$

and

$$\frac{K_M}{D}\left(\frac{\partial u}{\partial \sigma}, \frac{\partial v}{\partial \sigma}\right) = C_z(u^2+v^2)^{1/2}(u,v), \quad \sigma = -1 \tag{13b}$$

where (τ_x, τ_y) are wind stresses in (x, y) directions, and C_z is a dimensionless bottom drag coefficient derived from a logarithmic boundary layer and generally ranges from 0.0025 to 0.02. The boundary conditions on equations (5) and (6) are

$$\frac{\partial}{\partial \sigma}(T, C) = 0 \qquad \sigma = 0 \text{ and } -1 \tag{14}$$

The horizontal resolution (Δx and Δy) of the Baltimore Harbor model is small enough to be computationally time-consuming, but is nevertheless too large compared to the width of the Patapsco River mouth. To render the model computationally stable, freshwater discharge from the Patapsco is injected into the basin at the surface over 4 cells adjacent to the river mouth.

2.3 Horizontal boundary conditions

All coastline boundaries are impermeable to salinity and tracer. The boundary conditions require the velocities normal to the land be set to zero. The landward tangential velocities in the horizontal friction terms are also set to zero.

A set of open boundary conditions prescribed at the harbor mouth are derived from the output of the hydrodynamic model for the upper Chesapeake Bay. The terms u and v are defined as velocities normal and tangential to the open boundary, respectively. The vertical averages of (u, v) are (U, V), respectively. At the boundary of the harbor mouth, (U, V) and deviations from vertical means, (u', v') = (u–U, v–V) are treated differently (Mellor, 1990). The boundary value of u' is extrapolated from the interior, so that

$$\frac{\partial u'}{\partial x} = 0 \quad \textit{on the open boundary.} \tag{15}$$

The vertically averaged inflow and outflow are largely fixed at a prescribed value (U_b) as derived from the upper Chesapeake bay model, with the exception that a small amount is allowed to fluctuate with surface gravity waves during periods of outflow, so that

$$U = U_b \quad \textit{for inflow} \tag{16a}$$

$$U = U_b + 0.1\sqrt{gH}(\eta - \eta_o)/H \quad \textit{for outflow} \tag{16b}$$

In (16b), η_o is the prescribed mean sea level height. Note that the gravity wave correction term in (16b) is used to avoid overaccumulation of high-frequency gravity waves in the harbor proper, which occasionally destabilize the computation. Open boundary conditions for v', V, S and C are advective, so that

$$\frac{\partial v'}{\partial t} + u\frac{\partial v'}{\partial x} = 0 \tag{17}$$

$$\frac{\partial V}{\partial t} + U\frac{\partial V}{\partial x} = 0 \tag{18}$$

$$\frac{\partial S}{\partial t} + u\frac{\partial S}{\partial x} = 0 \tag{19}$$

$$\frac{\partial C}{\partial t} + u\frac{\partial C}{\partial x} = 0 \tag{20}$$

In implementing (19) and (20), salinity and tracer values outside the Harbor mouth (S_b and C_b) must be prescribed during inflow periods. For salinity, S_b is derived from the output of the upper Chesapeake Bay model. Further, since we are interested in tracer released from within the Harbor, it is reasonable to eliminate sources of tracer coming in from outside the harbor mouth by requiring that $C_b = 0$.

The set of open boundary conditions described herein drives the harbor circulation through boundary-imposed velocity and salinity. This is different from the conventional, less restrictive and hence less concise boundary conditions in estuarine modeling, in which the sea level and salinity are imposed on the open boundary to drive the circulation. The changeover from one set to the other should be straightforward.

2.4 Model specifics

The horizontal resolution (Δx and Δy) of the present model is 360 m. Vertically, there are 12 layers, each one having the thickness of 1/12 of the local water depth. The model resolves barotropic and baroclinic components of the flow with the time steps of 120 s and 15 s, respectively. A 1-month simulation takes about 17 hours on a Silicon Graphics IRIS workstation with 4 processors, or equivalently, about 1.1 hours on a CRAY Y-MP computer.

The initial conditions for the Harbor are also derived from the upper Chesapeake Bay model, using the mean hydrographic condition with zero velocities. These conditions, although idealized, are quickly overwhelmed by boundary conditions at the harbor mouth in about one-month time due to strong tidal flushing.

3. Forcing functions

Figs. 1, 2 and 3 show the wind speeds and directions derived from the Washington-Baltimore International Airport for 1984, 1985, and 1986, respectively, plotted as vectors with north directed toward the top of each diagram. Wind events were dominated by periods ranging from 2 to 7 days. In general, northwesterly winds dominated the winter (November–February) months. Southerly winds became common during summerlike months (May–September). Wind stress vectors (τ_x, τ_y) were derived from wind data (W_x, W_y) using the conventional quadratic law,

$$(\tau_x, \tau_y) = \rho_{air} C_a (W_x^2 + W_y^2)^{1/2} (W_x, W_y) \qquad (21)$$

In c.g.s. units, ρ_{air} = 0.00122 gm/cm^3 , C_a = 0.0013, (Wx,Wy) are in cm/s and (τ_x, τ_y) are in dyne/cm^2.

Figs. 4, 5 and 6 show the Patapsco River discharge in cubic feet per second (cfs) for 1984, 1985 and 1986, respectively. The daily data were measured by USGS and provided to us by MDE. The wet year 1984 resulted in several spikes of river discharge. Otherwise, the discharge throughout the 3-year period are quite small (less than 500 cfs).

Figs. 7, 8 and 9 show the hourly volumetric flux data in and out of the Harbor mouth derived from the upper Chesapeake Bay model for 1984, 1985 and 1986, respectively. In general, inflow (negative) and outflow (positive) were below 5000 m^3/s, dominated by semidiurnal tides with a period of 12.42 hrs. One exception occurred in early December, 1985 (see Fig.8), when a strong Susquehanna River discharge and strong northerly winds over the upper Chesapeake Bay triggered a large fluctuation in volumetric flux.

Figs. 10, 11 and 12 show the hourly sea level fluctuations at the Harbor mouth derived from the upper Chesapeake Bay model for 1984, 1985 and 1986, respectively. The fluctuations about the mean sea level rarely exceeded 1 m, and were dominated by semi-diurnal tides. On one brief occasion (March, 1986), the sea level rose above mean sea level by 2m.

4. Surface circulation

Snapshots of instantaneous surface flow field are shown in Figs. 13 (a)–(l) at 30-day intervals for 1984. It is quite evident that the surface circulation in the Harbor was largely dominated by episodic wind events. At days 30, 60, 90, 150, 270 and 330, the northwesterly or northerly winds on or prior to these days generate seaward flows that mostly follow the longitudinal axis of the Harbor. At day 120, the southerly and southeasterly winds produce a longitudinal surface flow toward the inner Harbor. At days 180 and 240, winds were essentially from the southwest, driving a northeastward cross-harbor flow. Winds at day 210 were quite weak and in consequence, surface currents appear weak and disorganized. At days 300 and 360, winds contained strong southwesterly (cross-harbor) components, but there were also velocity components towards the Harbor mouth; the consequent surface flow is toward the main stem of the Chesapeake Bay.

The foregoing interpretations point out several basic features of surface circulation inside the Harbor. Longitudinal winds are very effective in driving surface flows in the windward directions. Cross-harbor winds are capable of driving windward currents, but, if accompanied by even weak longitudinal winds, the longitudinal currents driven by the latter could overwhelm those forced by the former.

Figs. 14 (a)–(l) show surface flows for 1985 at 30-day intervals. Compared with 1984, winds near the end of each 30 days were frequently weak or in the cross-harbor directions, and the currents became more tidally dominant. At days 30 and 120, for example, winds were sufficiently weak and flood tides dominated; driving the flow towards the inner harbor. At days 60, 150 and 210, winds were predominately in the cross-harbor directions and tidal currents prevail. At days 90, 240, 270, 300 and 360, winds contain sufficiently strong

components toward the mouth of the Harbor, driving seaward outflows. At day 180, the wind component directed towards the inner Harbor drives a surface inflow.

Figs. 15 (a)–(l) show instantaneous surface currents for 1986 at 30-day intervals. At days 30, 150, 180, 210, 240, 300 and 360, the downchannel winds drive surface currents toward the Chesapeake Bay. At days 270 and 330, winds were primarily in the cross-harbor directions and surface currents are dominated by flood and ebb tidal currents, respectively. At days 90 and 120, the essentially upchannel winds drive the surface current toward the inner Harbor.

Summarizing the 36 instantaneous flow fields of 1984–1986, one gets the distinct impression that as far as the surface circulation is concerned, about 70 percent of the circulation patterns can be explained by wind forcing. About 30 percent can be attributed to tides during occasions when winds are either too weak or too perpendicular to the longitudinal axis of the Harbor, and when tidal currents are strong. Cross-harbor winds are ineffective in driving the circulation because of the short fetch in the windward direction.

5. Shoreline alteration assessment

The proposed wetland creation off Sparrows Point spans a cross-shore distance ranging from 300 m to about 1 km southward of the existing shoreline. The effects of this shoreline alteration on the Harbor circulation and the environment quality of adjacent embayments (Old Road Bay and Sparrows Point Channel) are assessed as follows. A wet period (day 30-60) and a dry period (day 120-150) in 1986 were selected for this concentrated study. Fig.16 shows the existing shoreline (0) in solid curve. Each alternative pushes the shoreline southward by $n\Delta y$, where n=0,1,2,3 is a shoreline index number and Δy=360 m is the grid spacing of the hydrodynamic model. For each shoreline configuration, including the baseline case, neutrally buoyant dye is uniformly distributed in one of the two adjacent embayments at the beginning of the wet or dry period. The total dye concentration inside the embayment in question is then traced for 30 days to determine its retention rate. Experiments are denoted by nE or nW, where n is the shoreline index number and E or W represents whether the east (Old Road Bay) or west (Sparrows Point Channel) embayment is dyed. With n ranging from 0 to 3, there are 8 experiments each for the wet and dry periods.

Fig.17 shows the percentage of total dye concentration retained in the Old Road Bay as a function of time in February 1986. In general, the total dye concentration decays exponentially in time with an e-folding time scale of about 13 days. The e-folding time scale is the time needed for the total dye concentration to decrease by a factor of e=2.71828. As the coastline protrudes progressively southward, the residence time of the dye in the Old Road Bay increases slightly. To quantify further, if the coastline expands southward by 1080 m (as in experiment 3E), the total dye concentration in the east embayment is about 5 percent higher than the baseline calculation using the existing shoreline (as in experiment 0E) from

February 4 to 12. However, the difference diminishes thereafter. The incremental change in the difference in flushing time is approximately linear from 0E to 3E.

Fig.18 shows the percentage of total dye concentration retained in the Sparrows Point Channel as a function of time in February 1986, summarizing experiment 0W, 1W, 2W and 3W in which the dye is initially uniformly distributed in the west embayment instead. The total concentration generally decays exponentially in time with an e-folding time scale of about 2 days. The much shorter flushing time scale in the west embayment than in the east embayment can be attributed to its depth and small size. The residence time of dye concentration does not increase monotonically as the coastline protrudes progressively southward. With reference to the baseline case using the existing coastline, the residence time actually decreases by less than 3 percent if the shoreline is displaced southward by 360 m as in experiment 1W. However, if the shoreline is displaced southward by 720 m and 1080 m, then the residence time increases by less than 7 percent and 10 percent, respectively. There is no easy explanation for the fact that the flushing time scale in the west embayment does not increase monotonically with increased shoreline reclamation, noting that winds, tides and salinity difference all play a role in driving the complex system.

The dye experiments are repeated for a dry month, May 1986. Fig.19 shows the percentage of total dye concentration retained in the Old Road Bay as a function of time in May 1986. The residence time of dye concentration is considerably shorter in this period, having an e-folding decay time scale of about 8 days. The faster flushing in May can be attributed to the wind forcing, as other major forcings were comparable in February and May 1986. In February, the wind direction was frequently downchannel, driving an outflow toward the Chesapeake Bay. In May, there was a sustained period of upchannel wind driving an inflow toward the inner Harbor. For inflows, the Old Road Bay is on the upstream side of the

Sparrows Point and is therefore more susceptible to flushing, helping to explain the short residence time in May. In this period the flushing time scale is less sensitive to the shoreline alteration. Even with the maximum reclamation (1080 m southward), the flushing time scale increases by less than 3 percent.

Fig.20 shows the percentage of total dye concentration retained in the Sparrows Point Channel as a function of time in May 1986. The residence time scale in this period is comparable to that in February 1986. Interestingly, more shoreline reclamation actually enhances flushing and therefore decreases the residence time in this period. Since the difference is small, it is difficult to pinpoint the physical mechanism leading to this anomaly.

In all the foregoing experiments, dye concentration for the two embayments quickly disperses into the main channel of the Harbor, and eventually into the main stem of the Chesapeake Bay. Furthermore, whether the shoreline near Sparrows Point is altered or not leads to little or no visible changes in the circulation pattern of the Harbor. This is an expected result, as the volumetric change of the Baltimore Harbor caused by the shoreline alteration is negligible. Alteration of Sparrows Point shoreline results in little or no visible change in the circulation of Baltimore Harbor.

6. Circulation in the vertical-longitudinal section

The wet year (1984) was selected to investigate the vertical variation of longitudinal circulation along the deep channel of the Harbor. To filter out most of the tides, longitudinal currents and salinity are averaged over a 5-day period. The mean circulation is therefore dominated by wind events and density forcing from the Harbor mouth. The wet year is chosen to accentuate the density forcing from the Susquehanna River, without which the mean circulation along the major axis of the Harbor would be mostly wind-driven.

Figs.21(a)–(l) show profiles of 5-day averaged longitudinal currents along the main axis of the Harbor for 1984 at 30-day intervals. Similar profiles of 5-day averaged longitudinal salinity are shown in Figs.22(a)–(l). The mean longitudinal currents in days 30–35 (Fig.21(a)) are somewhat disorganized, suggesting that insufficient time has elapsed for the system to fully respond to boundary forcings. Circulation after the first 30 days shows organized patterns, of which the salient features are discussed as follows.

From the beginning of March to the beginning of August, it is shown in Fig.21 that there is a persistent inflow (toward the inner Harbor) near the surface and an outflow (toward the main stem of the Chesapeake Bay) at depths. The depth and strength of the two opposing currents vary from month to month. The surface inflow, being shallow and weak (~2 cm/s) most of the time, extends to mid-depth and becomes strong (~5 cm/s) at the beginning of March and June. The outflow, being usually the strongest (~5 cm/s) at mid-depth in normal months, is suppressed downward and weakened at the beginning of March and June.

From the beginning of September to the end of December, the longitudinal-vertical circulation over the major axis of the Harbor is reversed, characterized by a surface outflow

and an inflow at depths (Fig.21). The strength and depth of the two opposing currents may vary from month to month, but the general circulation pattern remains consistent.

That the 5-day averaged longitudinal-vertical circulation along the major axis of the Harbor is not wind-driven is quite clear. Although instantaneous surface circulation patterns correlate well with winds, the 5-day averaged profiles show poor correlation with winds. If one follows the wind-forced scenario, upchannel winds would drive a surface inflow and a bottom outflow, while downchannel winds would drive an opposite circulation. The poor correlation between the simulated circulation pattern and that inferred from the particular wind event during the 5-day averaging period negates the wind-forced scenario. An alternative explanation is called for.

Fig.23 shows the 5-day averaged surface and bottom salinities at the Harbor mouth as inferred from Figs.22(a)–(l) for 1984. Also included between the two curves is the average of the two. In general, freshening from the Harbor mouth continues from January to the end of July. Thereafter, waters near the Harbor mouth become progressively saltier until the end of the year. It is the annual variation of density forcing from the Harbor mouth that drives the subtidal longitudinal circulation along the main axis of the Harbor. The continuous freshening from January to the end of July drives a surface inflow and an outflow at depths. Thereafter, the buoyancy forcing from the Harbor mouth becomes progressively negative, driving a surface outflow and a bottom inflow instead. The perceived circulation patterns as driven by low-frequency density forcing from the Harbor mouth are of course modulated by higher-frequency wind events. Our results suggest that the density forcing dominates over wind forcing.

The foregoing results are to be compared with longitudinal circulation patterns observed by Boicourt and Olson in 1978–79. The 1978–79 data set does not contain enough

information for a realistic numerical simulation. On the other hand, our 1984 simulation lacks verification by a concurrent data set. The disparity between observation and simulation periods is unfortunate. This deficiency notwithstanding, there is a rather striking similarity between the observed and simulated longitudinal circulations despite the disparity in timing. The 1978–79 observations contained two long-term mooring arrays of current data over the major axis of the Harbor. One was at the Harbor mouth (mooring 3B); the other was well inside the Harbor (mooring 5M), which is used for ensuing qualitative comparison. Most of the observed currents were averaged over periods ranging from 4 to 10 days, comparable to our averaging period of 5 days.

In the period from April to the beginning of May 1979, the observed longitudinal current exhibited an outflow over a good portion of mid-depths (from 6 ft to 30 ft depths); this is consistent with our simulated current profile (Figs.21(c)–(d)). From September to November, 1979, the observed current profile at mooring 5M exhibited a top-layer outflow and a bottom-layer inflow, also in agreement with the simulated results in comparable periods. Furthermore, the observed salinity profiles at the Harbor mouth, whenever available, essentially showed progressive freshening from January to about June, 1979, and became progressively saltier from July to December, 1979. Thus, the observed intra-annual variation of longitudinal circulations over the major axis of the Harbor and its relationship to salinities at the Harbor mouth are quite consistent with our boundary forcing scenario.

7. Conclusions

A time-varying 3-D numerical hydrodynamic model of Baltimore Harbor has been developed and utilized to simulate the harborwide circulation as driven by winds, tides and density effects in 1984–86. Our objectives are two-fold: firstly to understand the basic mechanisms responsible for the Harbor circulation under realistic settings, and secondly to assess the possible environmental impacts of the proposed shoreline alteration near Sparrows Point to the two adjacent embayments and the Harbor itself. Important conclusions are the following.

(a) The proposed wetland creation has virtually no effect on the harborwide circulation, as the relative volumetric change of the Baltimore Harbor caused by the shoreline alteration is negligible.

(b) The instantaneous Harbor circulation near the surface and over shallows is primarily driven by winds and secondarily driven by tides. To quantify the statement, about 70 percent of surface currents are associated with specific wind events. The remaining 30 percent are influenced by instantaneous tidal currents.

(c) The two embayments to the east and west of Sparrows Point have incompatible flushing time scales. Being shallow and wide, waters in the Old Road Bay are renewed with e-folding time scales ranging from 8 to 13 days. By comparison, the residence time of waters in the much narrower and deeper Sparrows Point Channel is much shorter, having an e-folding scale of about 2 days.

(d) In terms of flushing rates in the two adjacent embayments, the environmental impact of the proposed wetland creation to the south of Sparrows Point is quite low. To quantify further, if the local shoreline is displaced southward by (360

(1–2%, 2–3%, 3–5%) in the Old Road Bay, and less than (1%, 7%, 10%) in the Sparrows Point Channel. The larger percentage change in Sparrows Point Channel should not be alarming, because the existing e-folding time scale is quite short (~2 days).

(e) The intra-annual variation of tidally averaged longitudinal circulation along the major axis of the Harbor seems to be driven by low-frequency salinity variations at the Harbor mouth. In 1984, our numerical simulation suggests that continuous freshening from January to July drives an inflow at the top and an outflow at depths. Thereafter, the progressively saltier water entering the Harbor drives a reverse circulation pattern. This annual variation is in qualitative agreement with that observed in 1979.

In light of the last conclusion, the classical description of a 3-layer circulation in Baltimore Harbor should be put in proper perspective. From the numerical results, a two-layer circulation is perceived as the dominant response to the density forcing at the Harbor mouth. Direct current measurements in 1978–79 confirmed, for the most part, a minimum of two layers of flows; the vertical resolution was not adequate to determine whether there was a persistent third layer on top of or beneath the 2-layer circulation. In this regard, the confirmation of a 2-layer circulation does not preclude the possibility of a third persistent layer.

8. Suggestions for future studies

With the rapid advances in instruments (particularly the ADCP), it is now possible and there is a need to resolve the circulation in the vertical much beyond previously thought to be possible. Findings from such a renewed observational effort will not only further our understanding about the Harbor circulation, but also provide a good data set against which the final (and minor) tuning of the present model can be made. In order to have a robust basis for making management decisions about water quality in the Baltimore Harbor, the latter effort seems worthwhile.

REFERENCES

Boicourt, W.C. and P. Olson, 1982: A hydrodynamic study of the Baltimore Harbor system. I. Observations on the circulation and mixing in Baltimore Harbor. The Johns Hopkins University, Chesapeake Bay Institute, Tech. Rep. 82-10, 131pp.

Garland, C.F., 1952: A study of water quality in Baltimore Harbor. Maryland Board of Natural Resources. Publ. No. 96, 132pp.

Johnson, B.H., 1989: Three-dimensional Upper-Bay hydrodynamic model, Assessment of the environmental impacts of the Hart-Miller Islands Containment Facility, 7th Annual Interpretative Report. Army Corps of Engineers, Waterways Exp. Station.

Knudsen, M., 1901: Hydrographical Tables. G.E.C.Gad, Copenhagen, Williams and Norgate, London.

Mellor, G.L., 1990: User's guide for a three-dimensional, primitive equation numerical ocean model. Atmos. and Oceanic Sciences Program, Princenton Univ., 44pp.

Mellor, G.L. and T. Yamada, 1982: Development of a turbulence closure model for geophysical fluid problems. Rev. Geophys. Space Phys., **20**, 851–875.

Oey, L.-Y., G.L.Mellor and R.I.Hires, 1985: A three-dimensional simulation of the Hudson-Raritan estuary. Part I: Description of the model and model simulations. J. Phys. Oceanogr., **15**, 1676–1692.

Pritchard, D.W. and J.H.Carpenter, 1960: Measurement of turbulent diffusion in estuarine and inshore waters. Bull. Inter. Assoc. Sc. Hydrol., **10**, 37–50.

Stroup, E.D., D.W. Pritchard and J.H.Carpenter, 1961: Chesapeake Bay Institute, Technical Report 27, Ref. 61-5, 79pp.

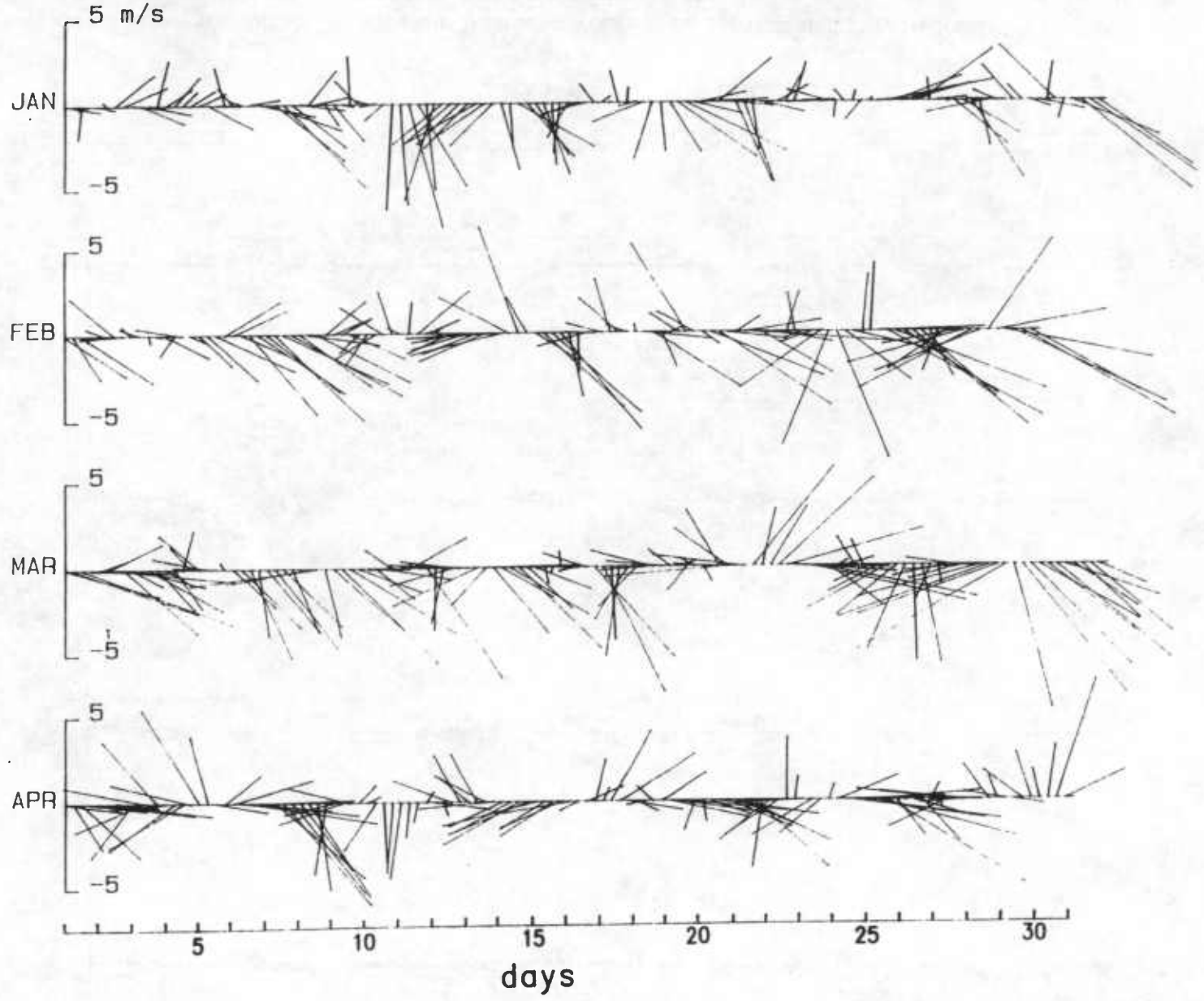

Figure 1. Low-pass filtered winds from Baltimore-Washington International Airport for 1984, plotted as vectors with north directed toward the top of the diagram.

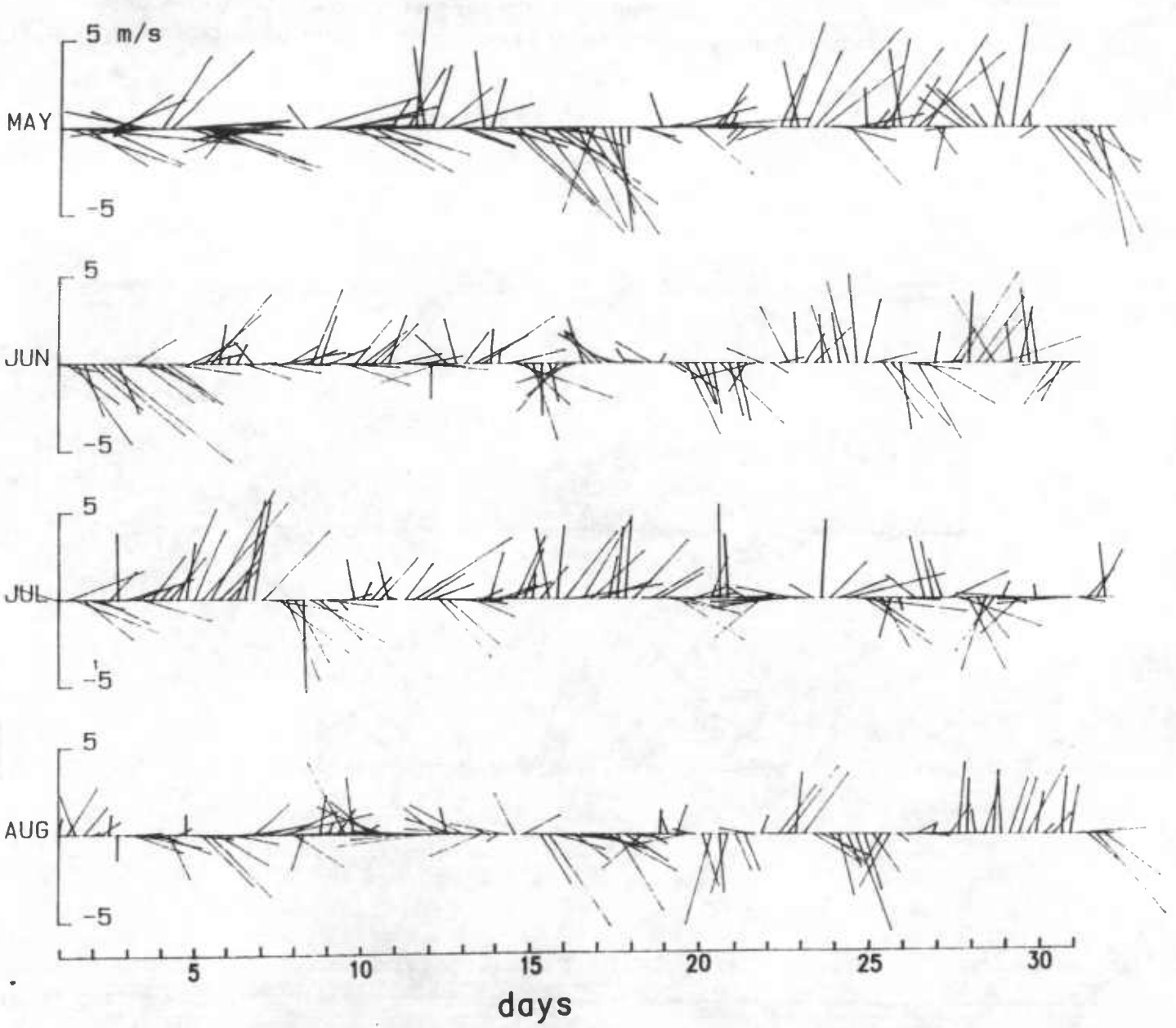

Figure 1. Low-pass filtered winds from Baltimore-Washington International Airport for 1984, plotted as vectors with north directed toward the top of the diagram.

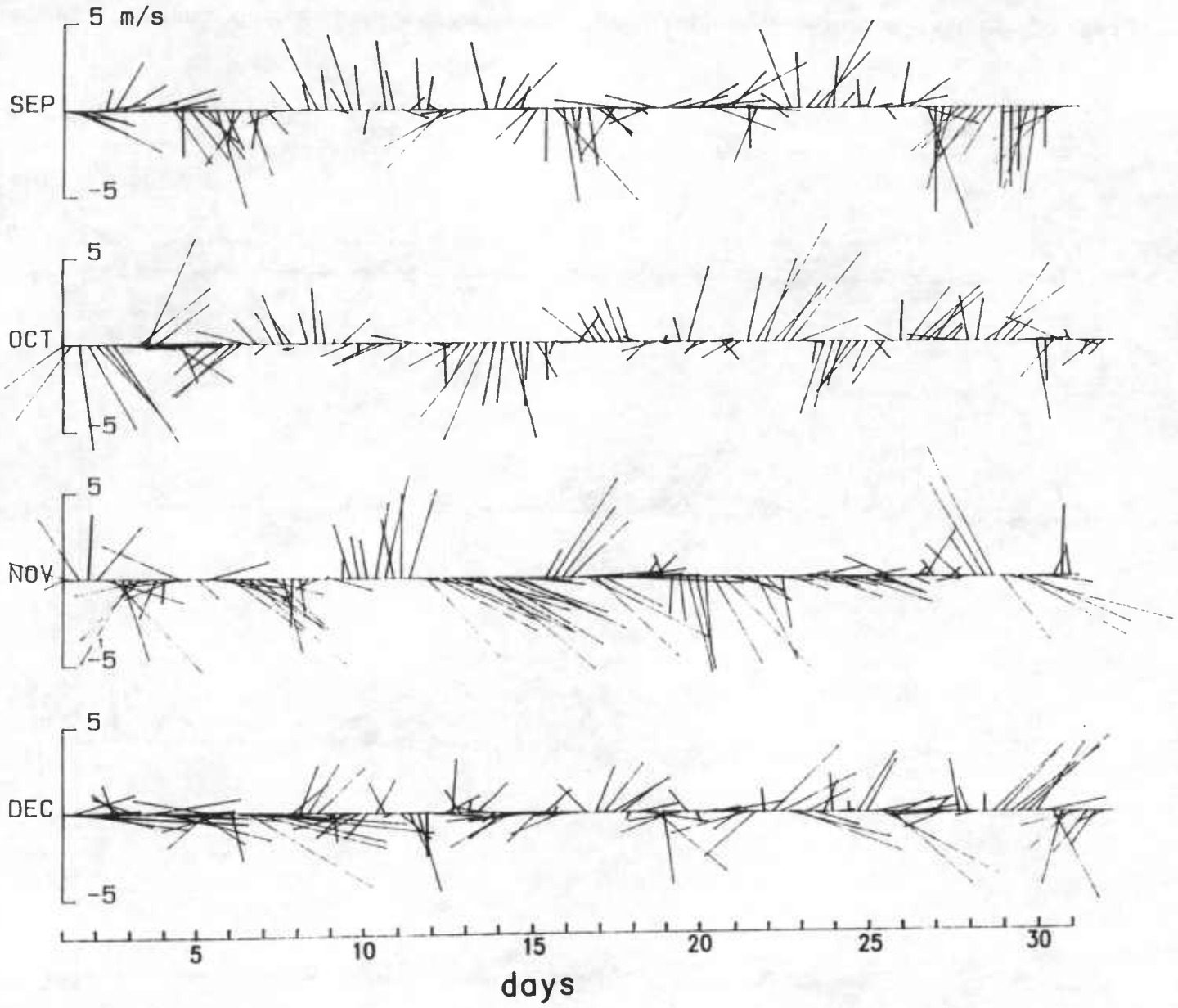

Figure 1. Low-pass filtered winds from Baltimore-Washington International Airport for 1984, plotted as vectors with north directed toward the top of the diagram.

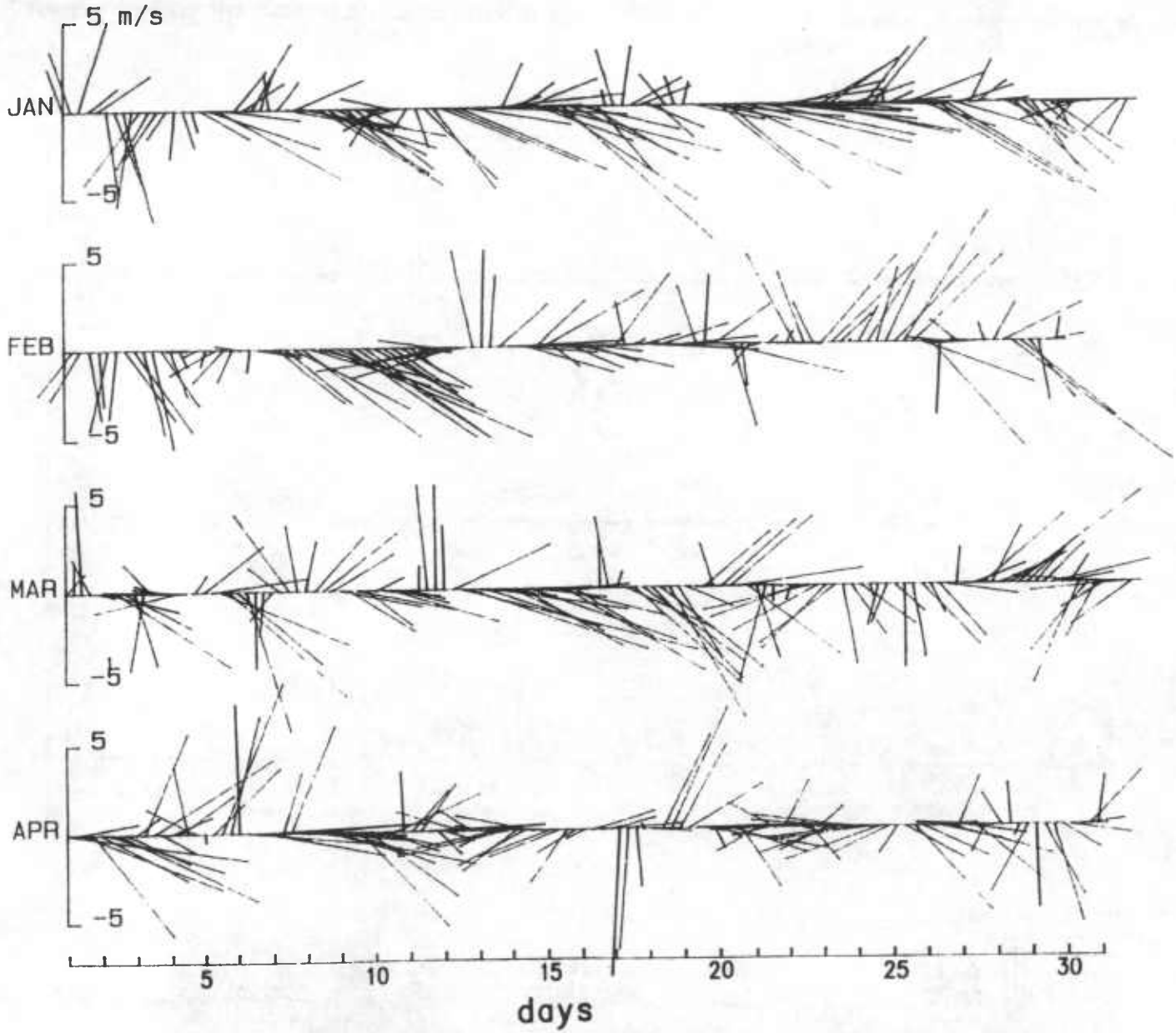

Figure 2. Low-pass filtered winds from Baltimore -Washington International Airport for 1985, plotted as vectors with north directed toward the top of the diagram.

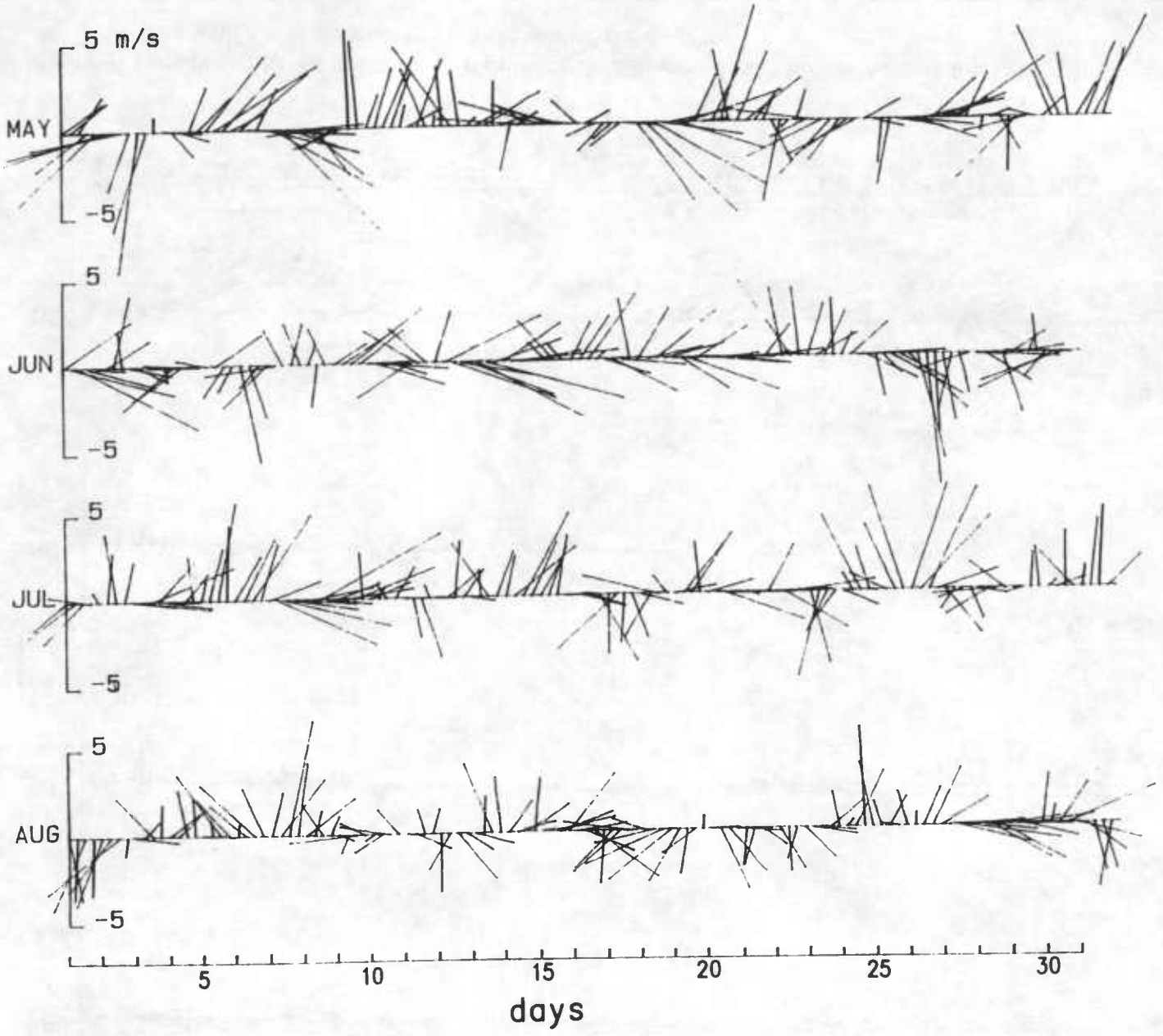

Figure 2. Low-pass filtered winds from Baltimore -Washington International Airport for 1985, plotted as vectors with north directed toward the top of the diagram.

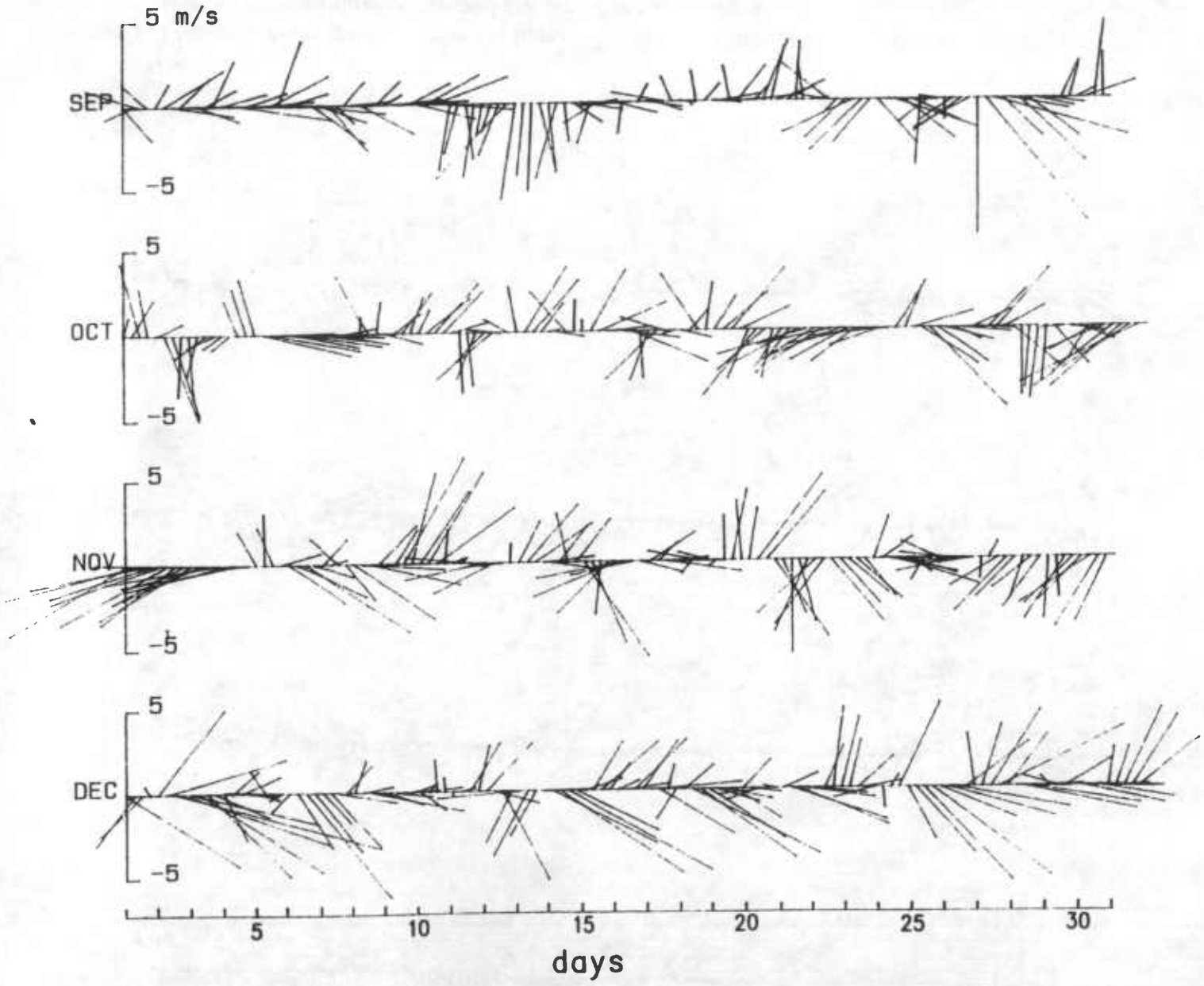

Figure 2. Low-pass filtered winds from Baltimore -Washington International Airport for 1985, plotted as vectors with north directed toward the top of the diagram.

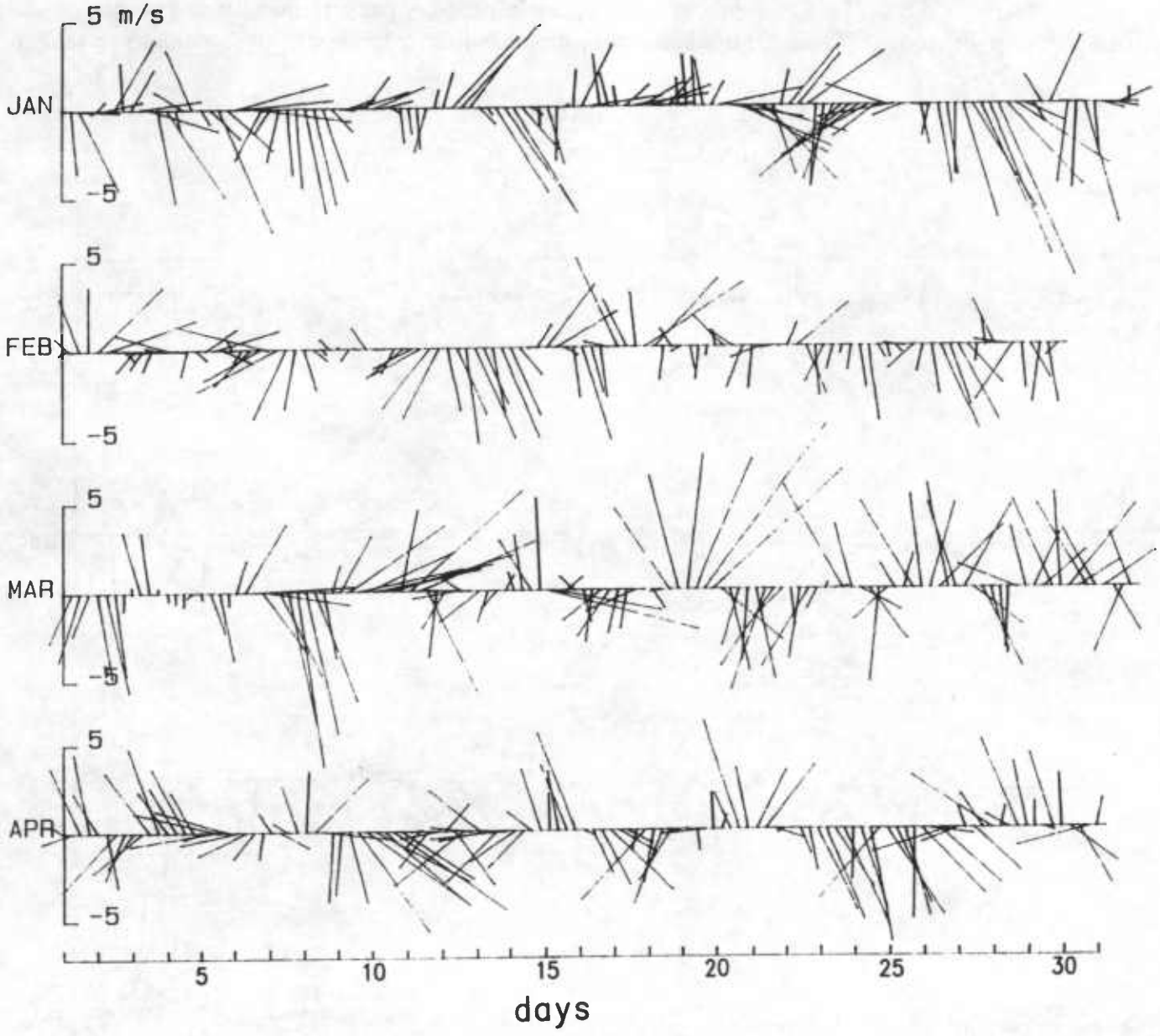

Figure 3. Low-pass filtered winds from Baltimore-Washington International Airport for 1986, plotted as vectors with north directed toward the top of the diagram.

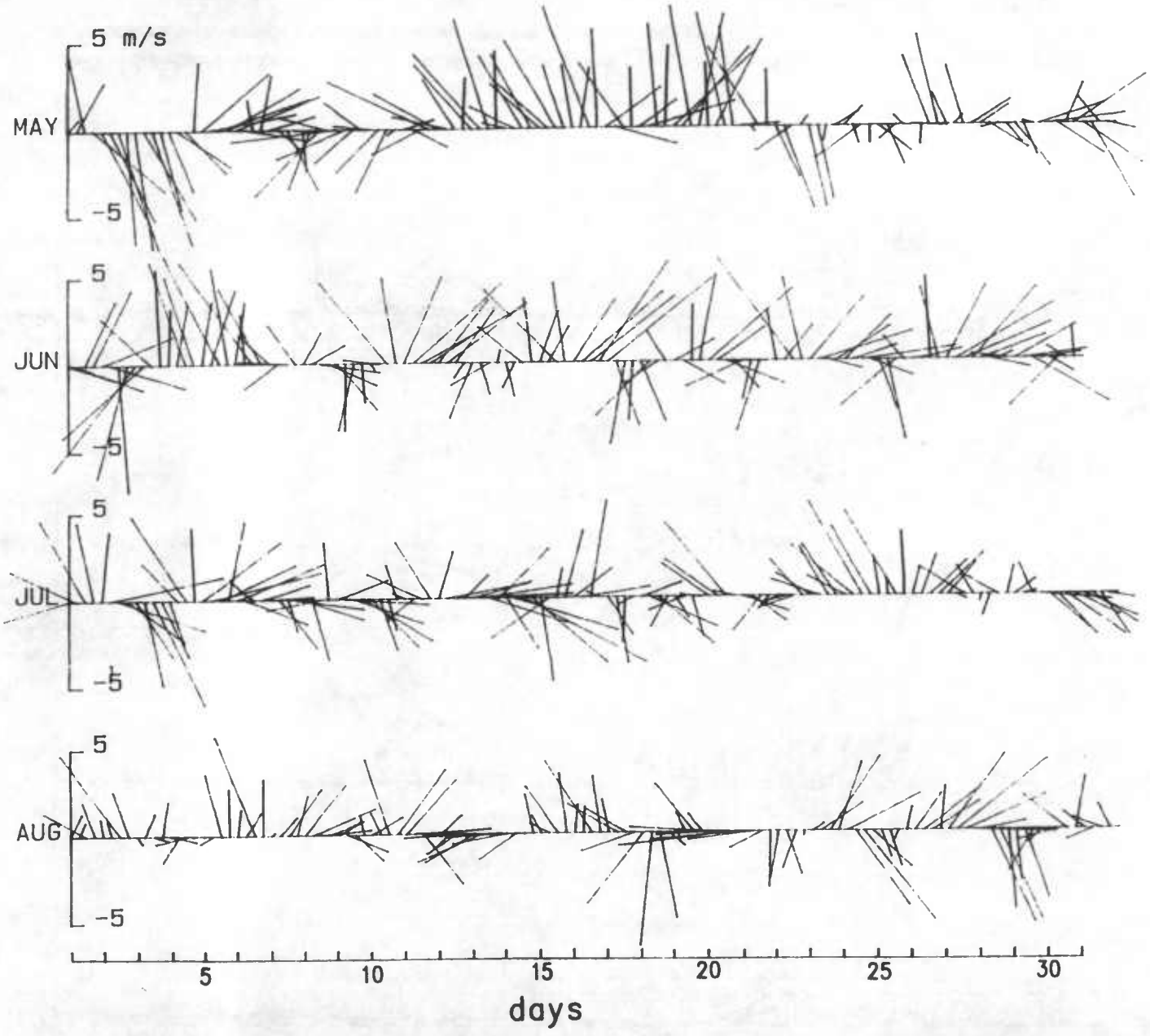

Figure 3. Low-pass filtered winds from Baltimore-Washington International Airport for 1986, plotted as vectors with north directed toward the top of the diagram.

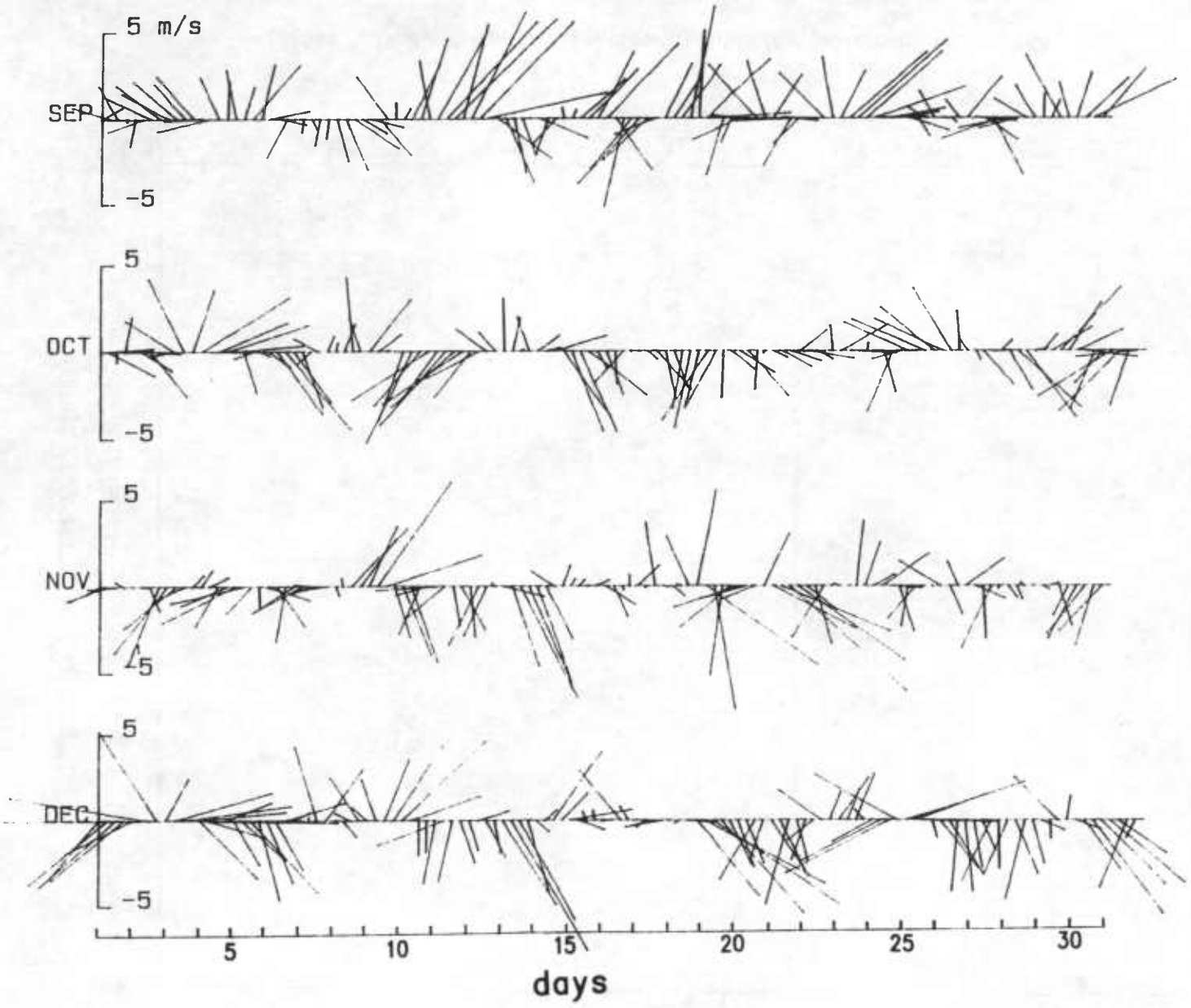

Figure 3. Low-pass filtered winds from Baltimore-Washington International Airport for 1986, plotted as vectors with north directed toward the top of the diagram.

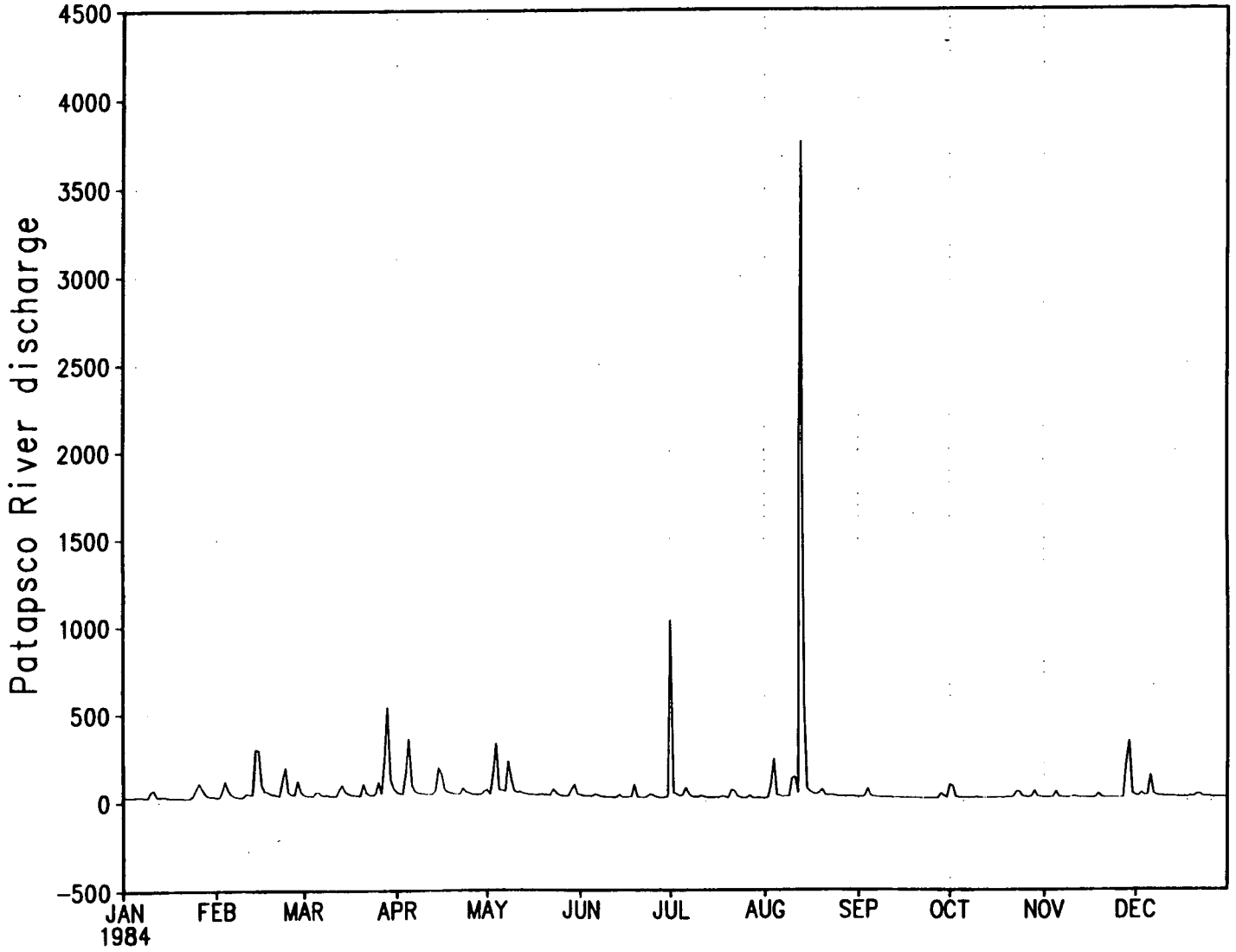

Figure 4. Daily Patapsco River flow in cubic feet per second (cfs), 1984.

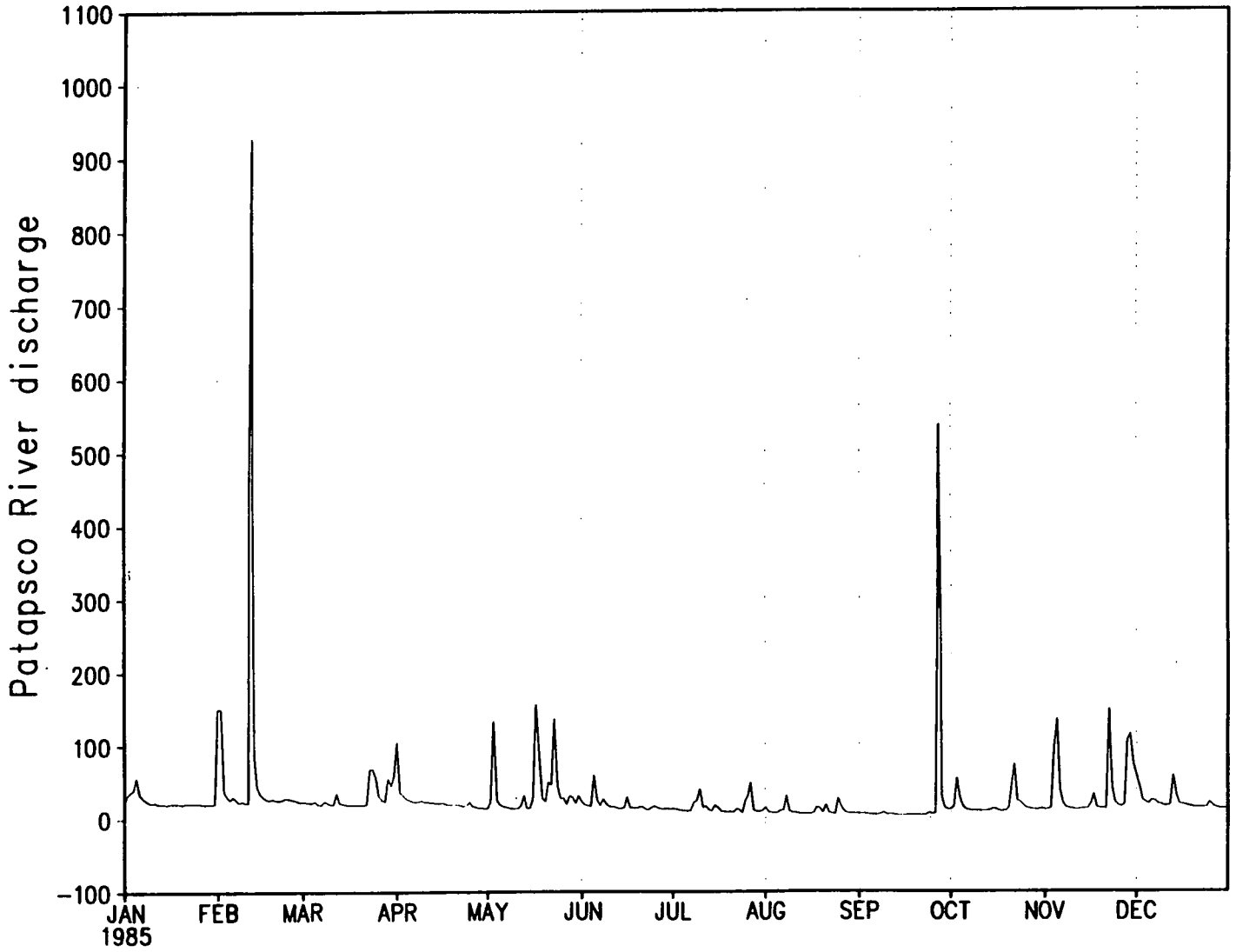

Figure 5. Daily Patapsco River flow in cubic feet per second (cfs), 1985.

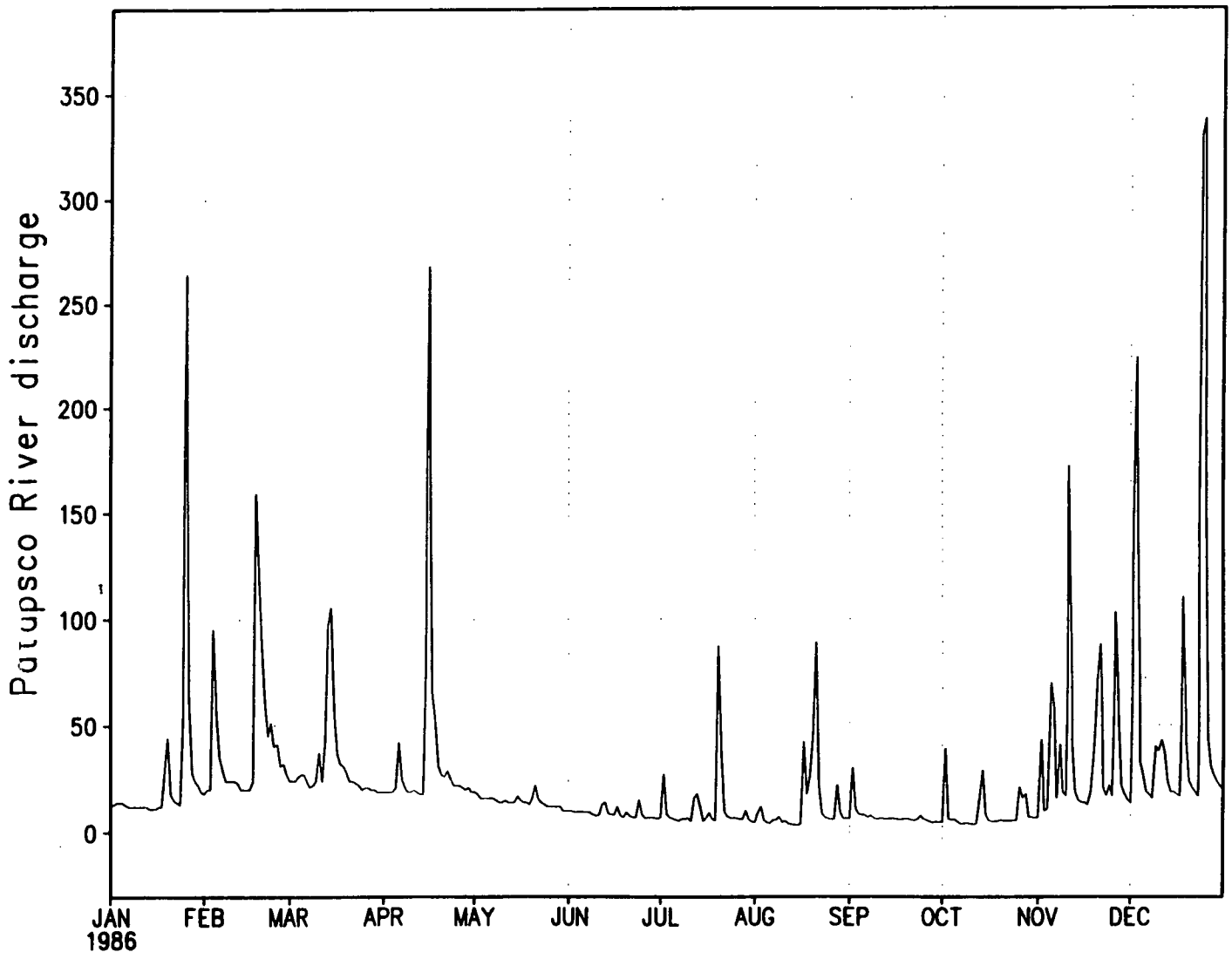

Figure 6. Daily Patapsco River flow in cubic feet per second (cfs), 1986.

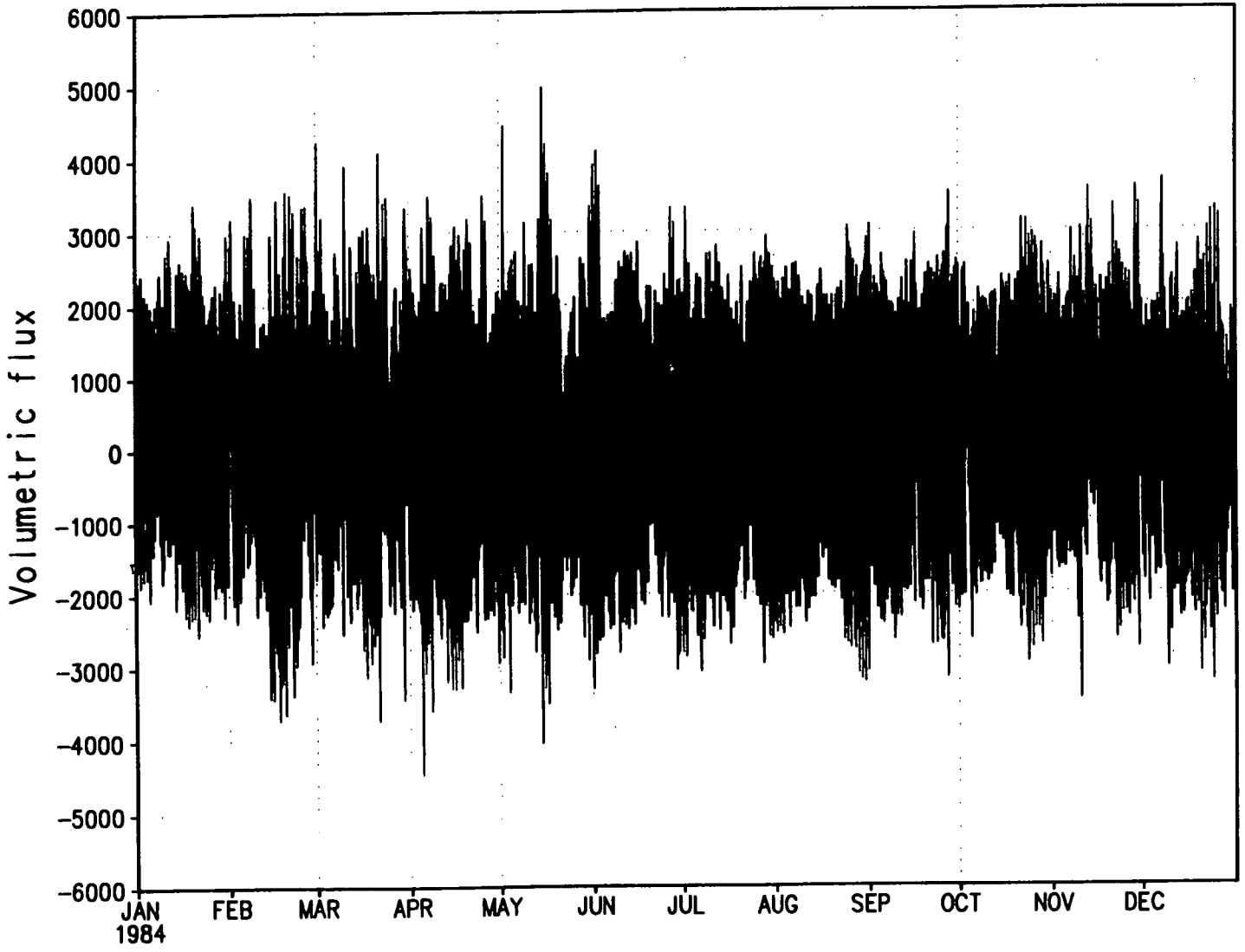

Figure 7. Volumetric flux (m^3/s) in and out of the Baltimore Harbor mouth, 1984. Positive values indicate outflows.

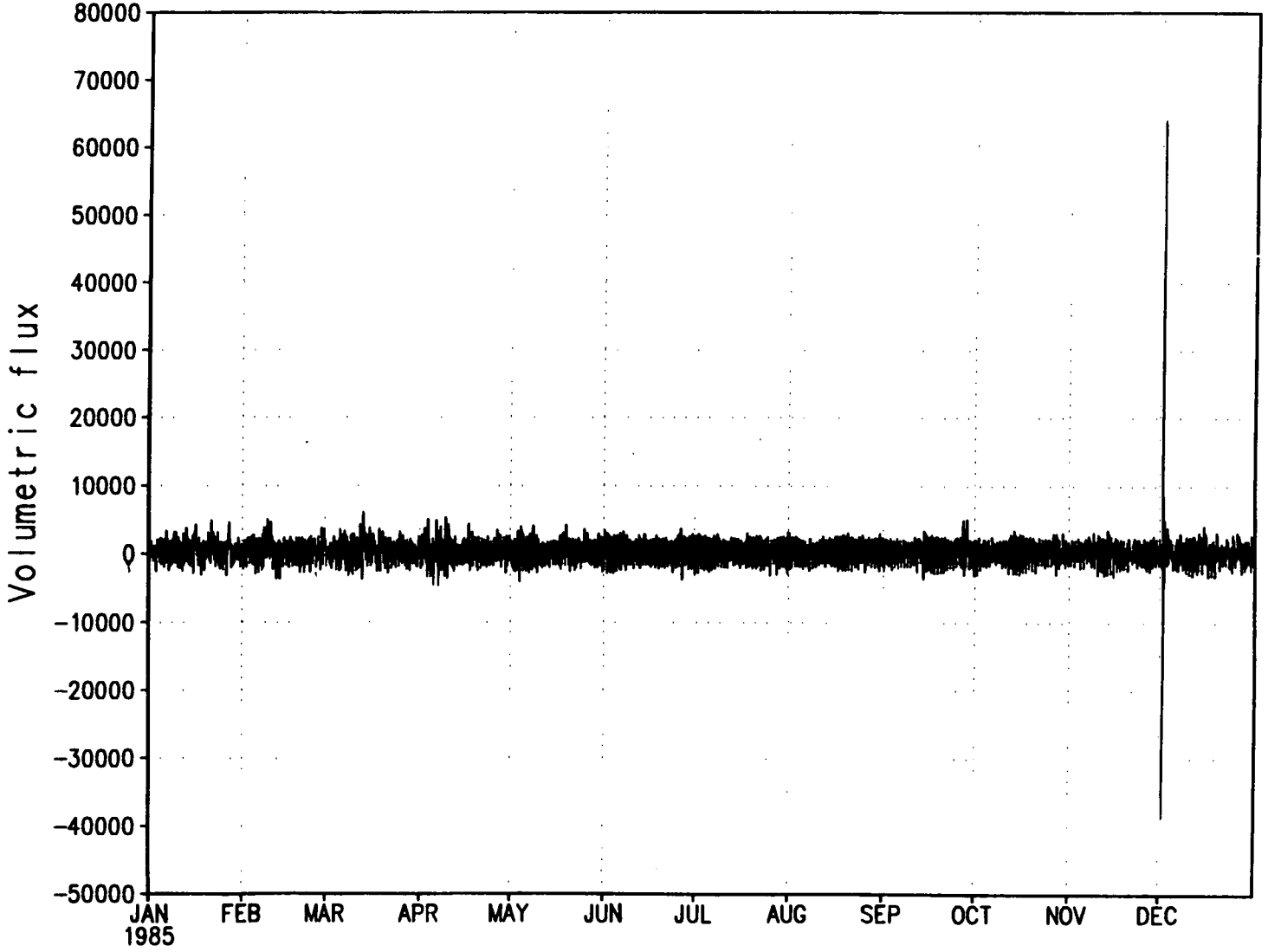

Figure 8. Volumetric flux (m^3/s) in and out of the Baltimore Harbor mouth, 1985. Positive values indicate outflows.

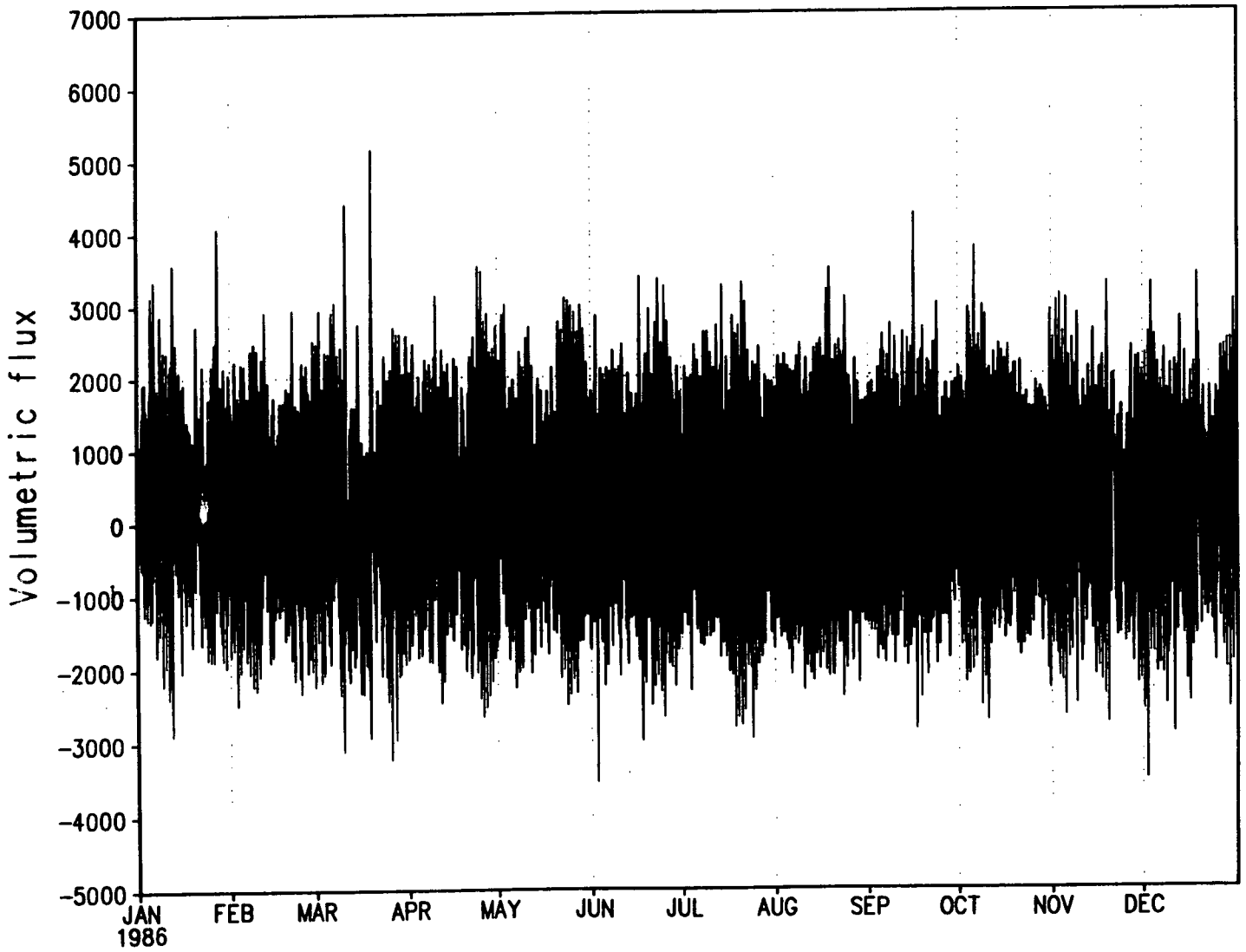

Figure 9. Volumetric flux (m^3/s) in and out of the Baltimore Harbor mouth, 1986. Positive values indicate outflows.

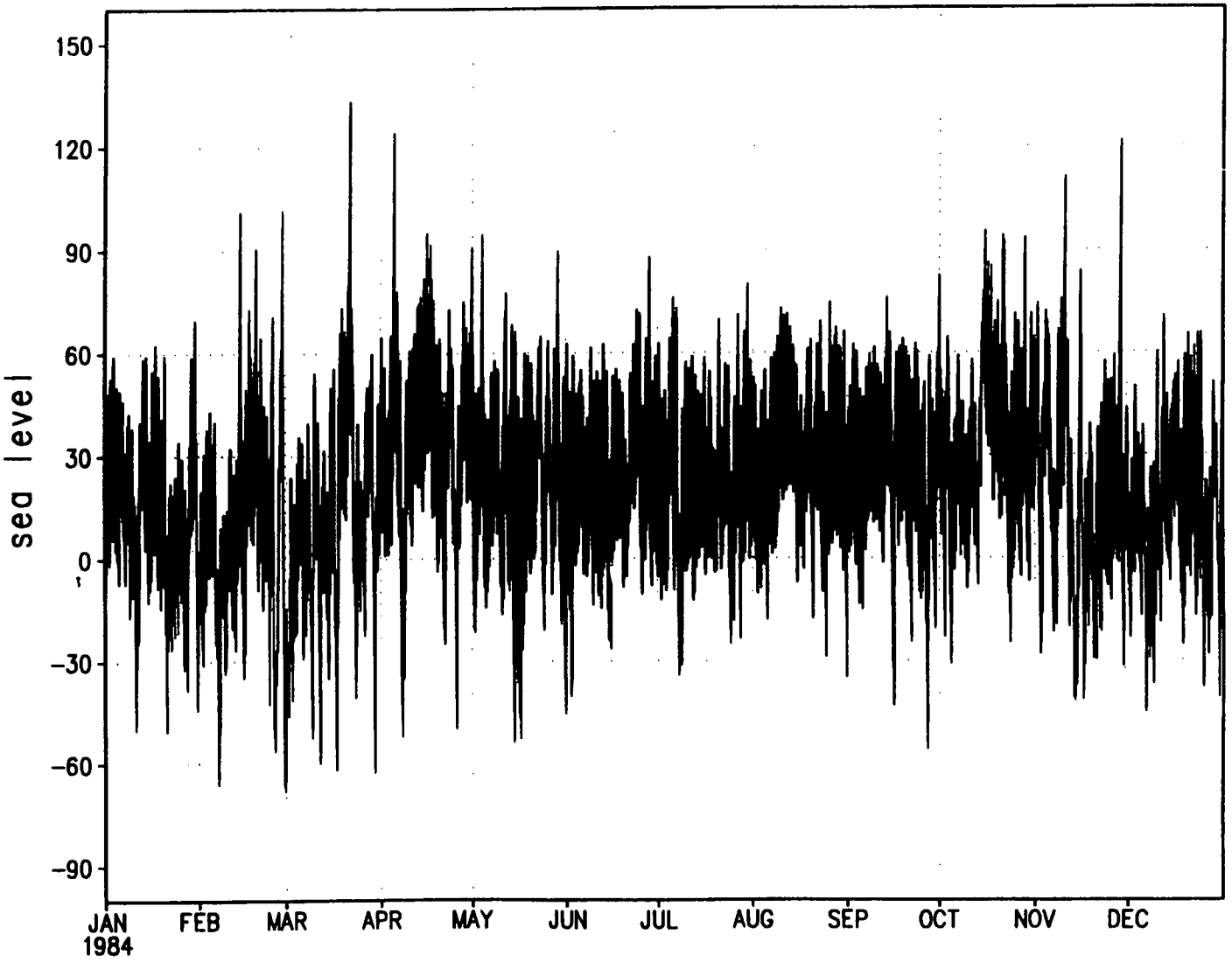

Figure 10. Sea level deviations (cm) from the mean at the Harbor mouth in 1984. Positive values indicate rises.

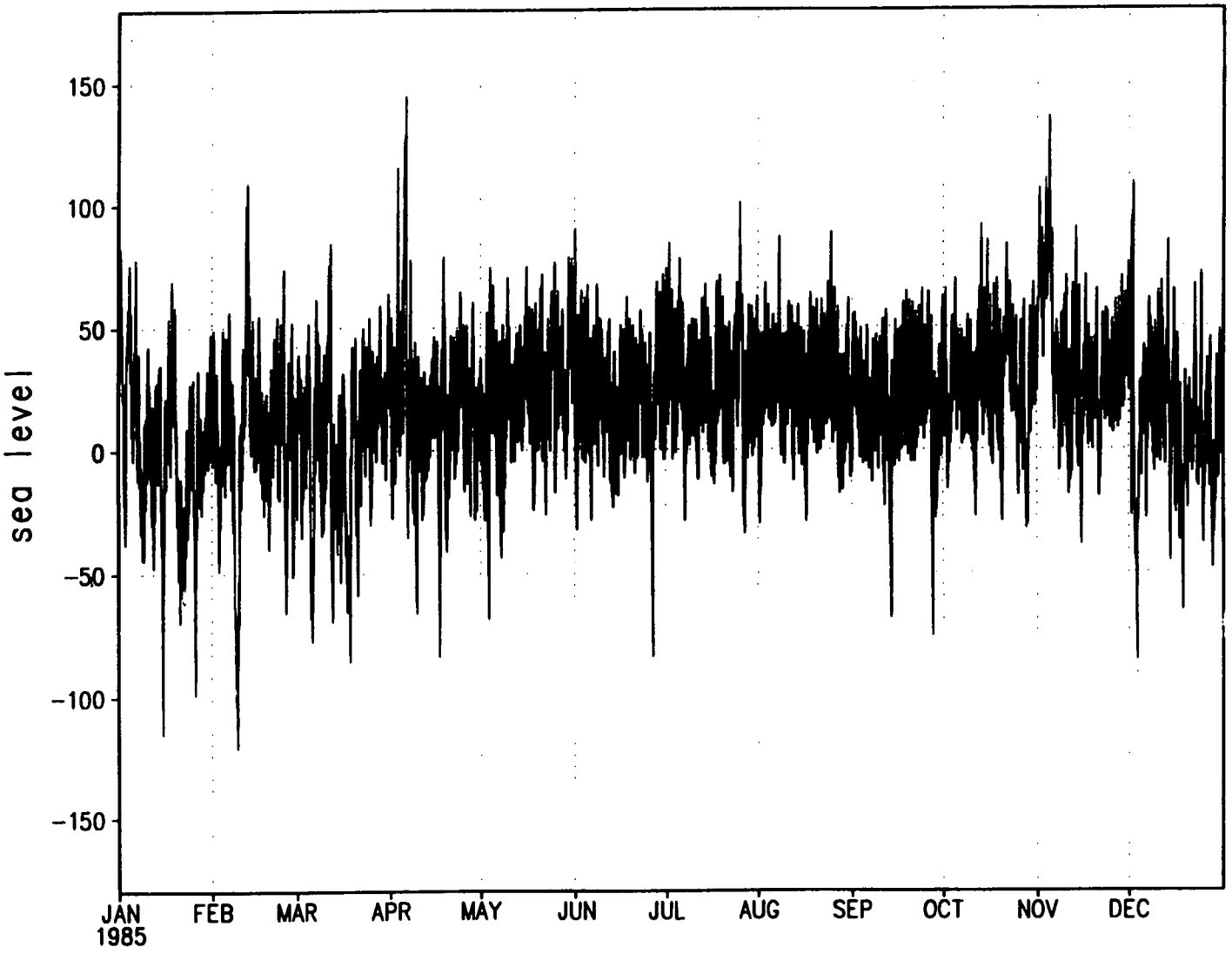

Figure 11. Sea level deviations (cm) from the mean at the Harbor mouth in 1985. Positive values indicate rises.

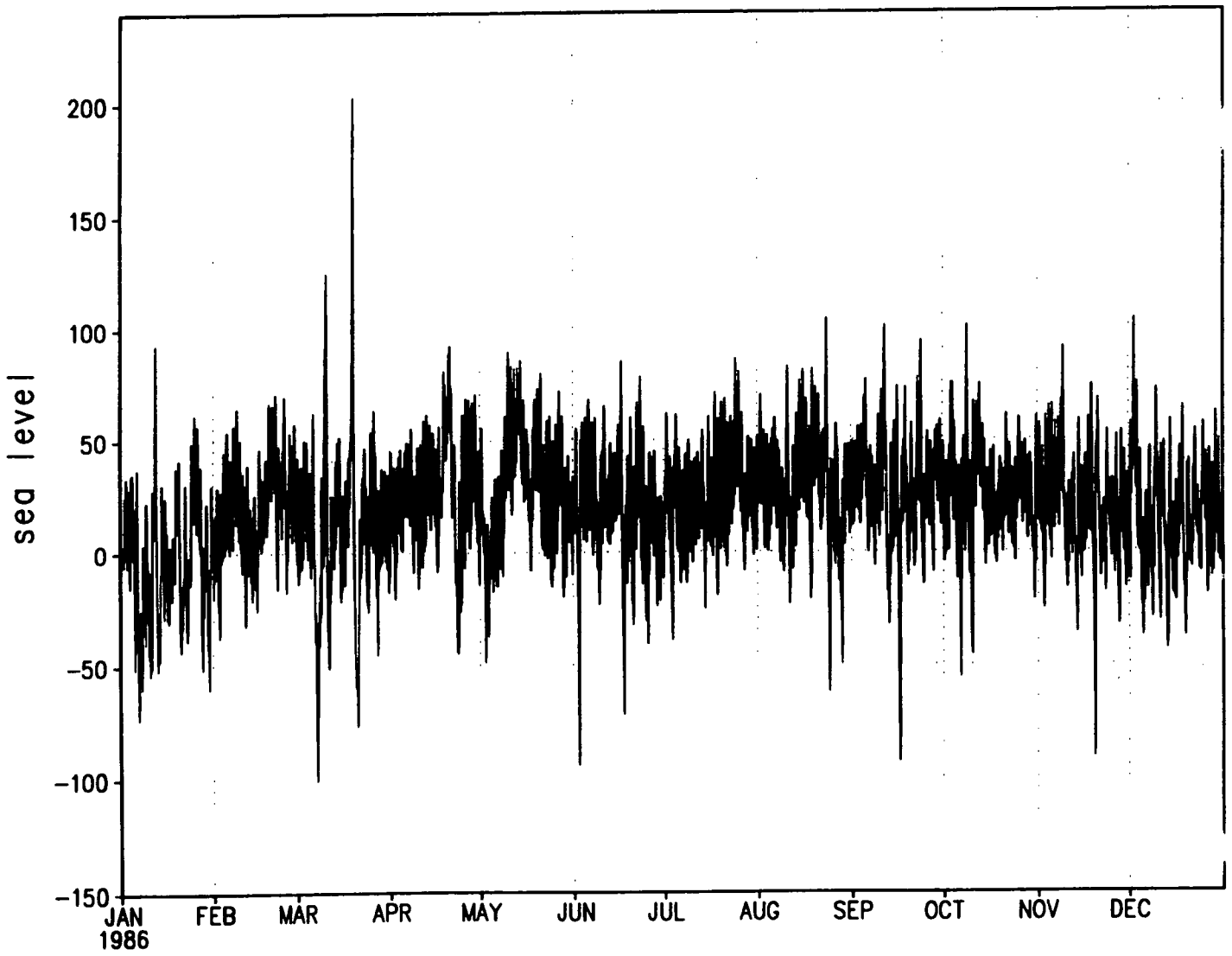

Figure 12. Sea level deviations (cm) from the mean at the Harbor mouth in 1986. Positive values indicate rises.

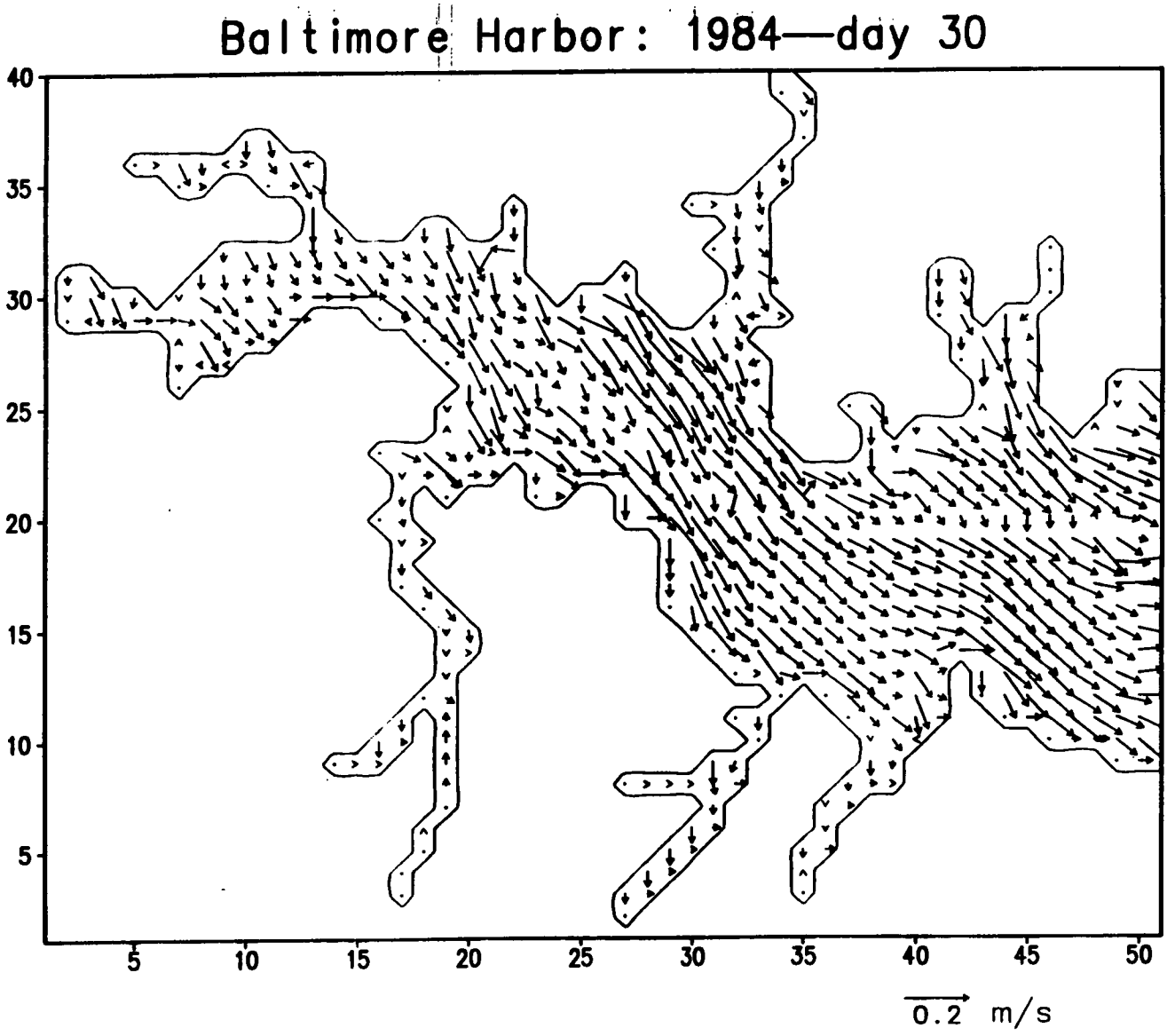

Figure 13(a). Instantaneous **surface flow of the Harbor**, day 30, 1984.

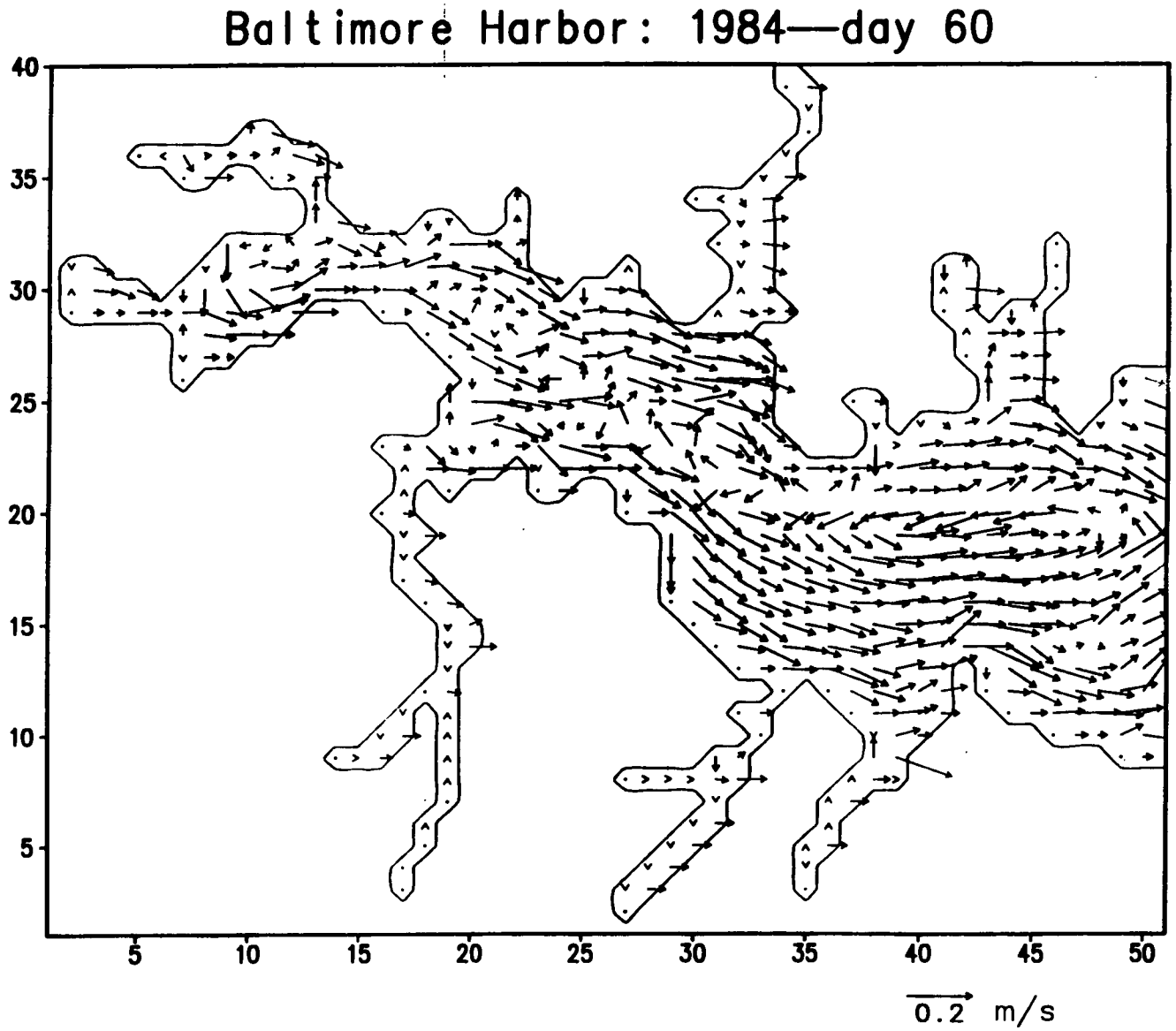

Figure 13(b). Instantaneous surface flow of the Harbor, day 60, 1984.

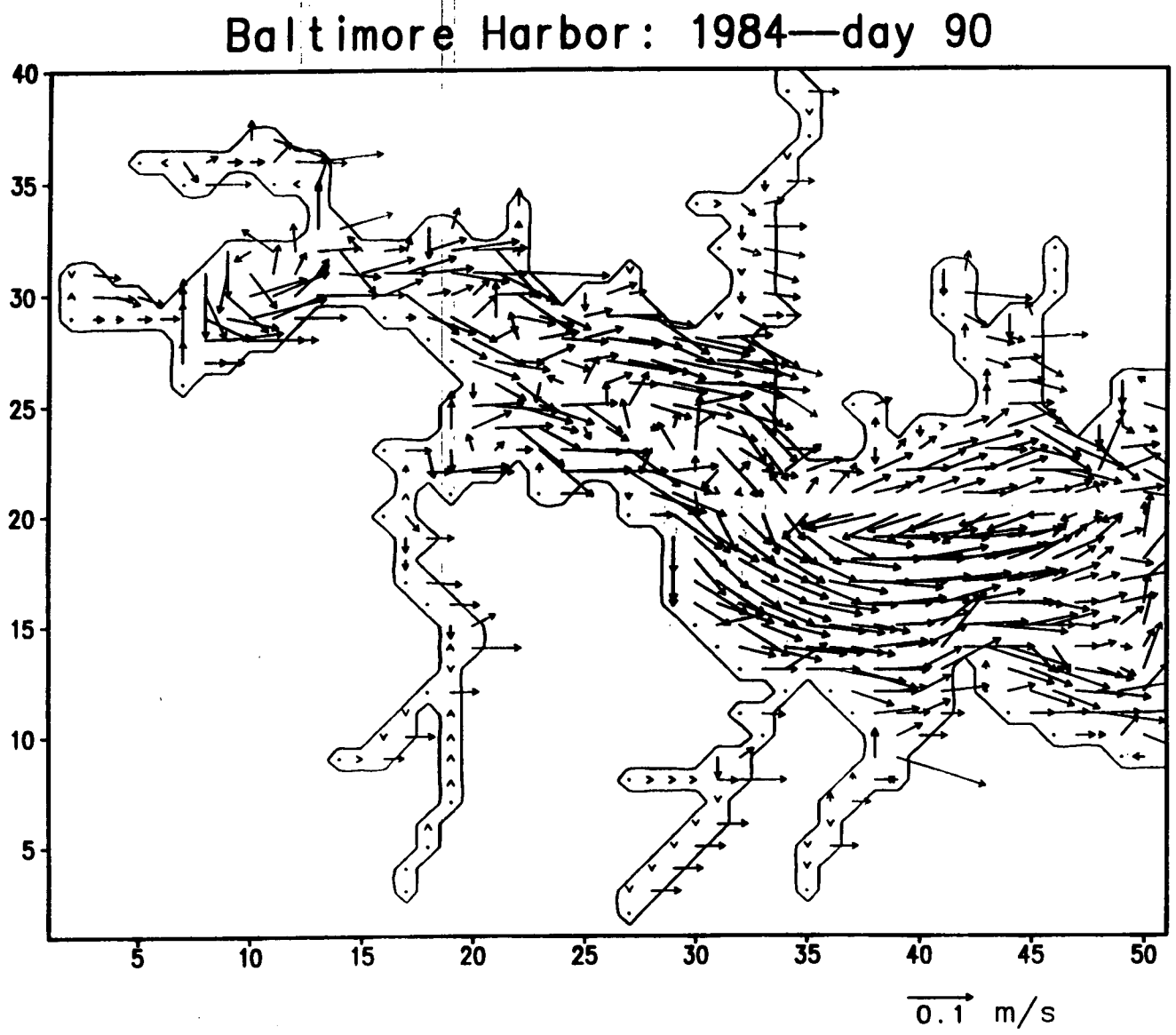

Figure 13(c). Instantaneous surface flow of the Harbor, day 90, 1984.

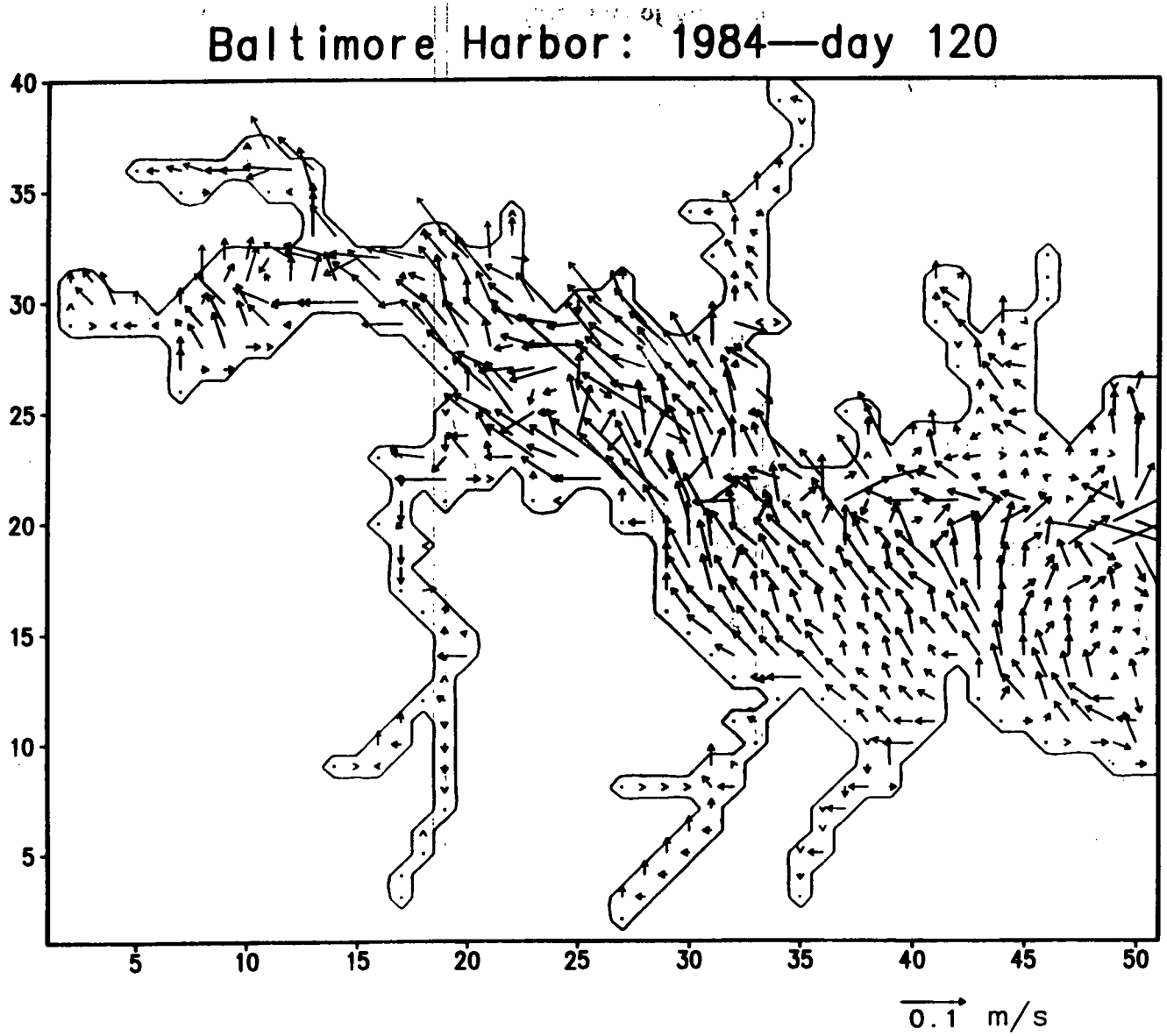

Figure 13(d). Instantaneous surface flow of the Harbor, day 120, 1984.

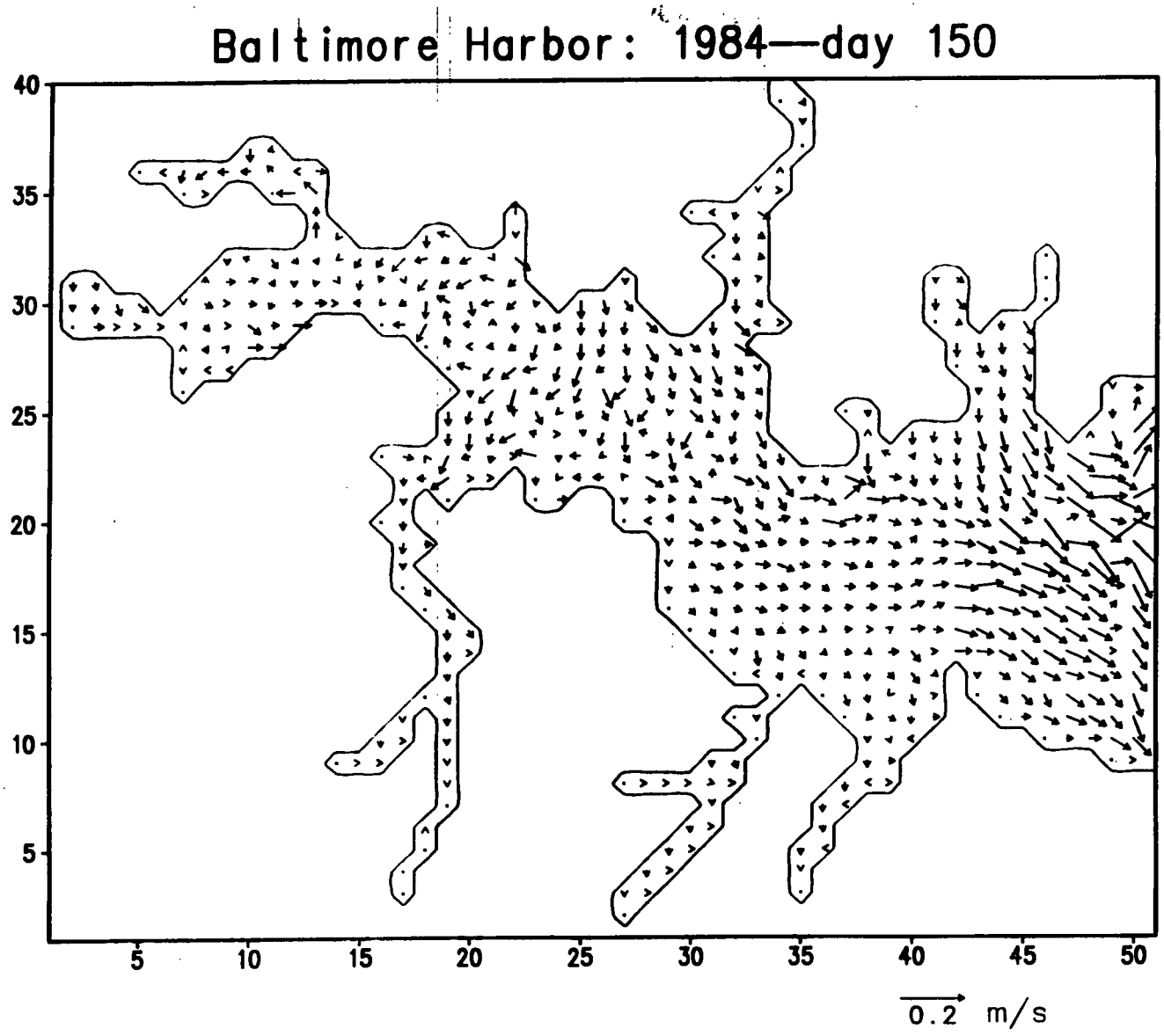

Figure 13(e). Instantaneous surface flow of the Harbor, day 150, 1984.

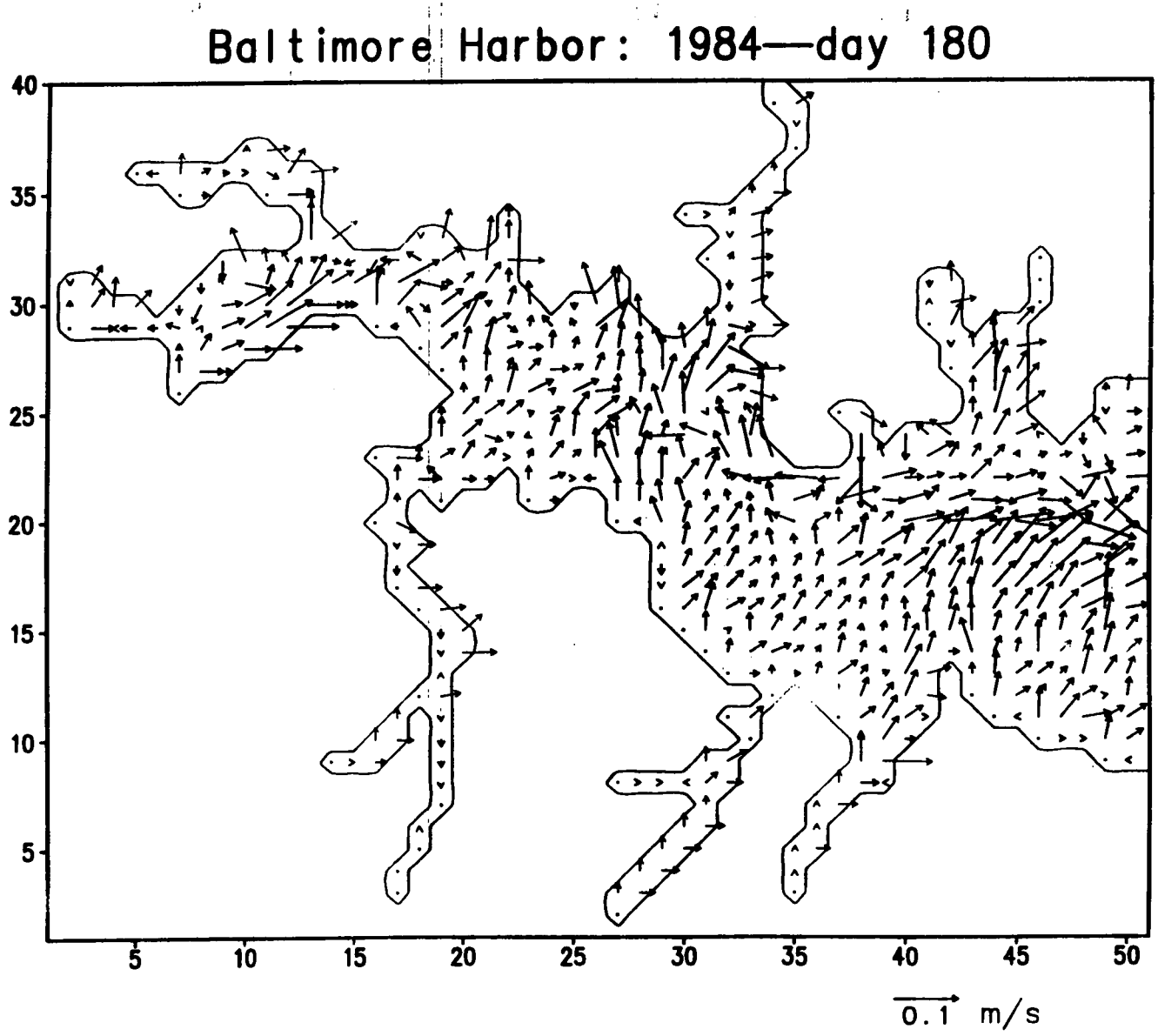

Figure 13(f). Instantaneous surface flow of the Harbor, day 180, 1984.

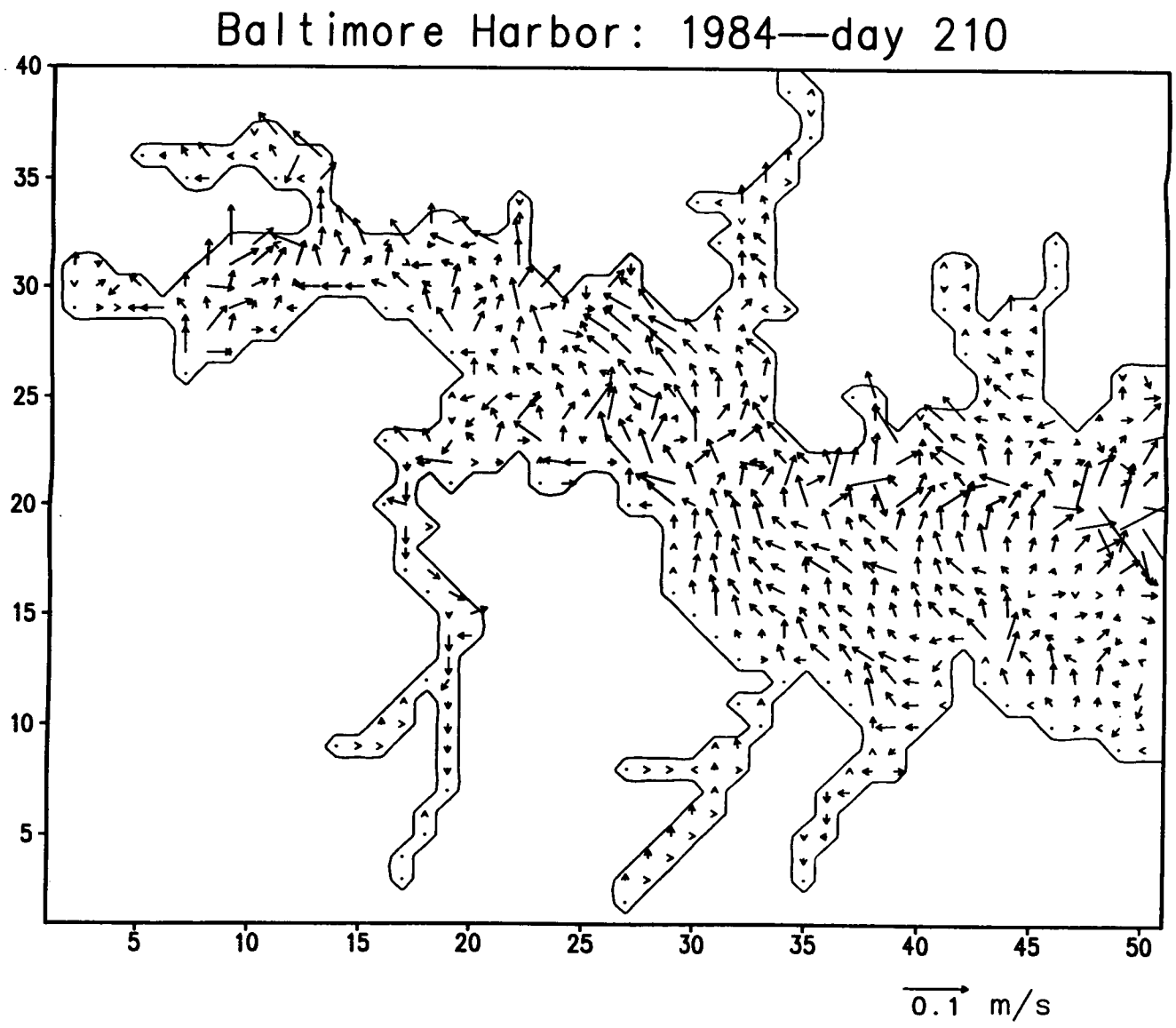

Figure 13(g). Instantaneous surface flow of the Harbor, day 210, 1984.

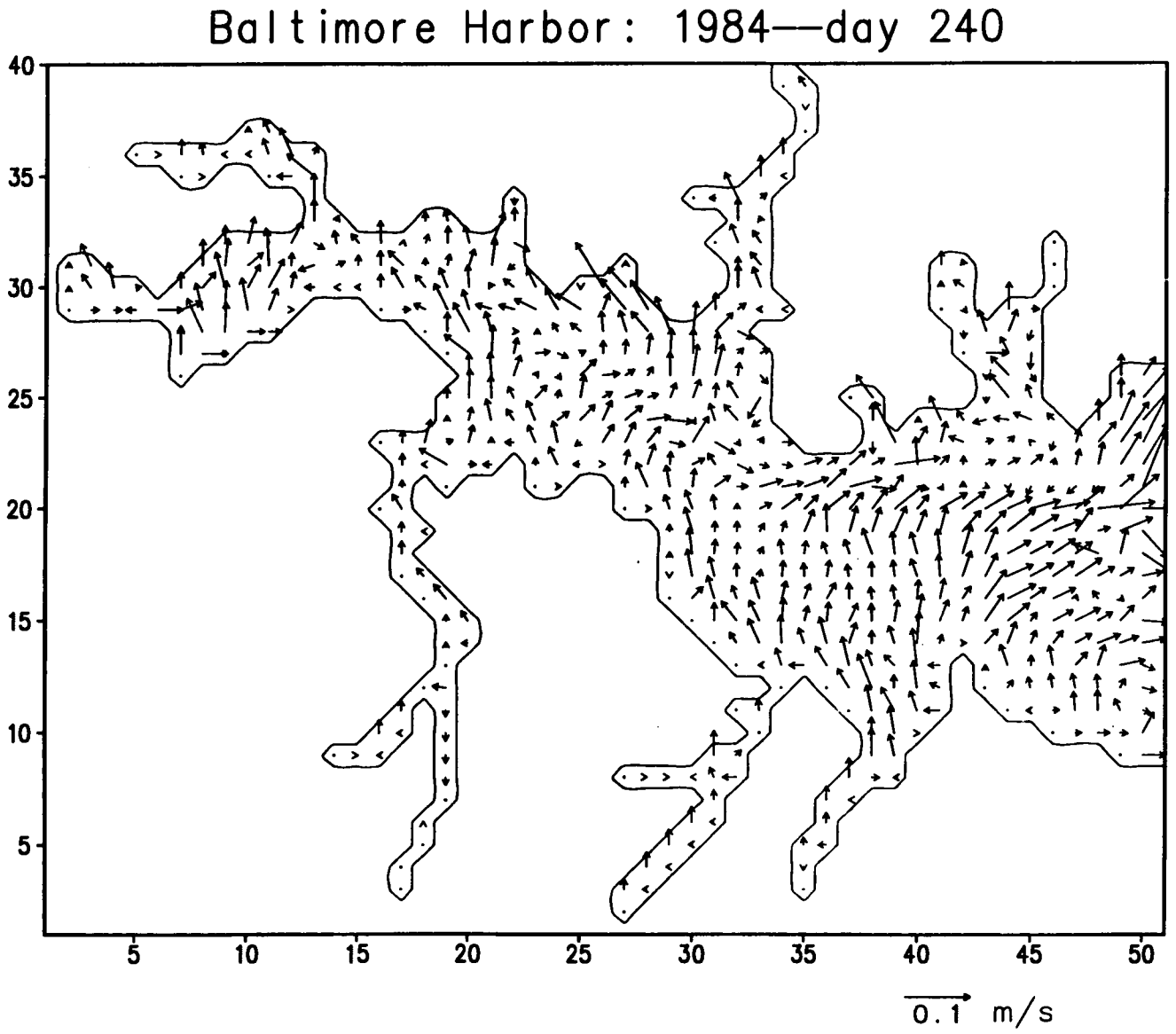

Figure 13(h). Instantaneous surface flow of the Harbor, day 240, 1984.

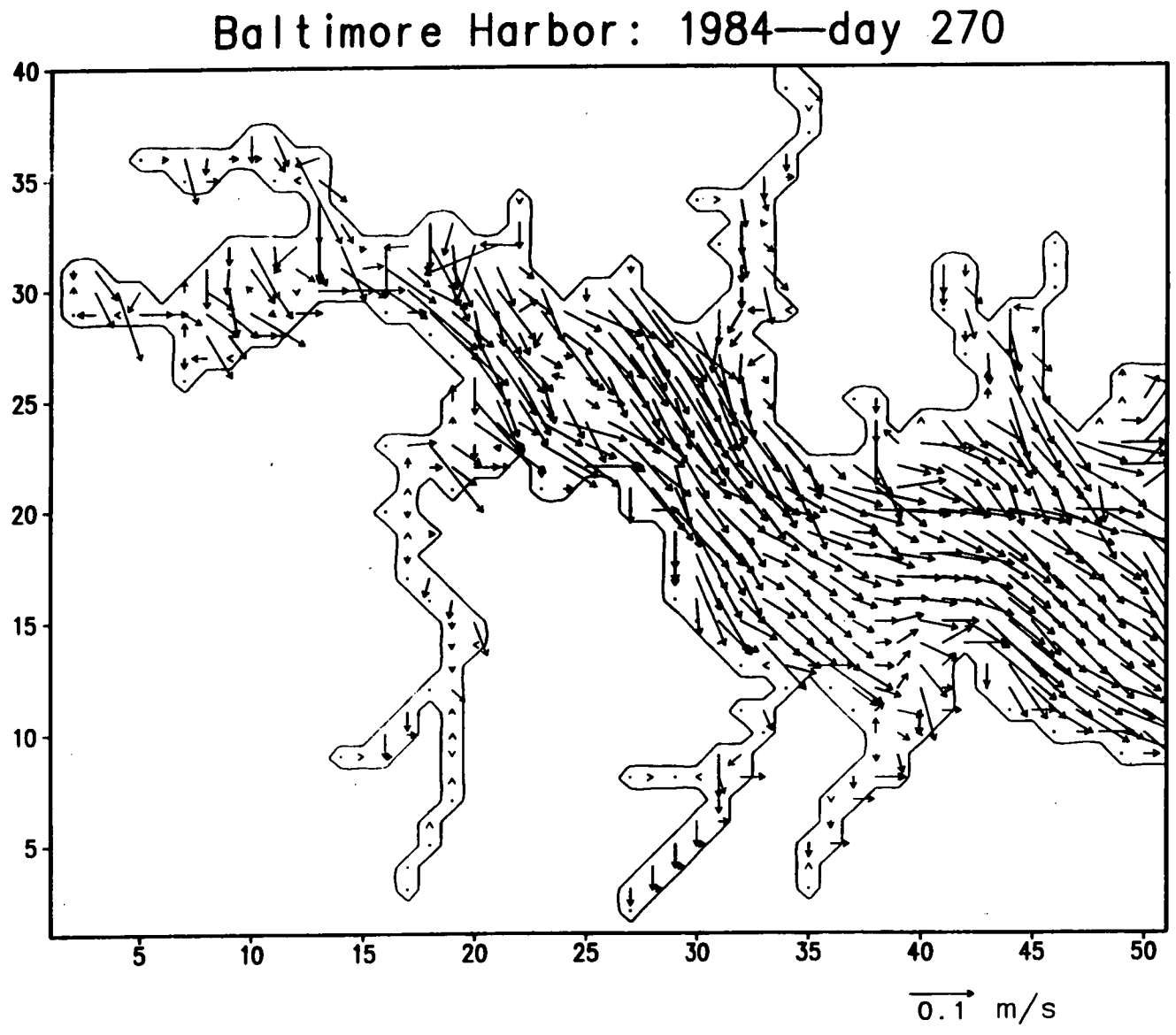

Figure 13(i). Instantaneous surface flow of the Harbor, day 270, 1984.

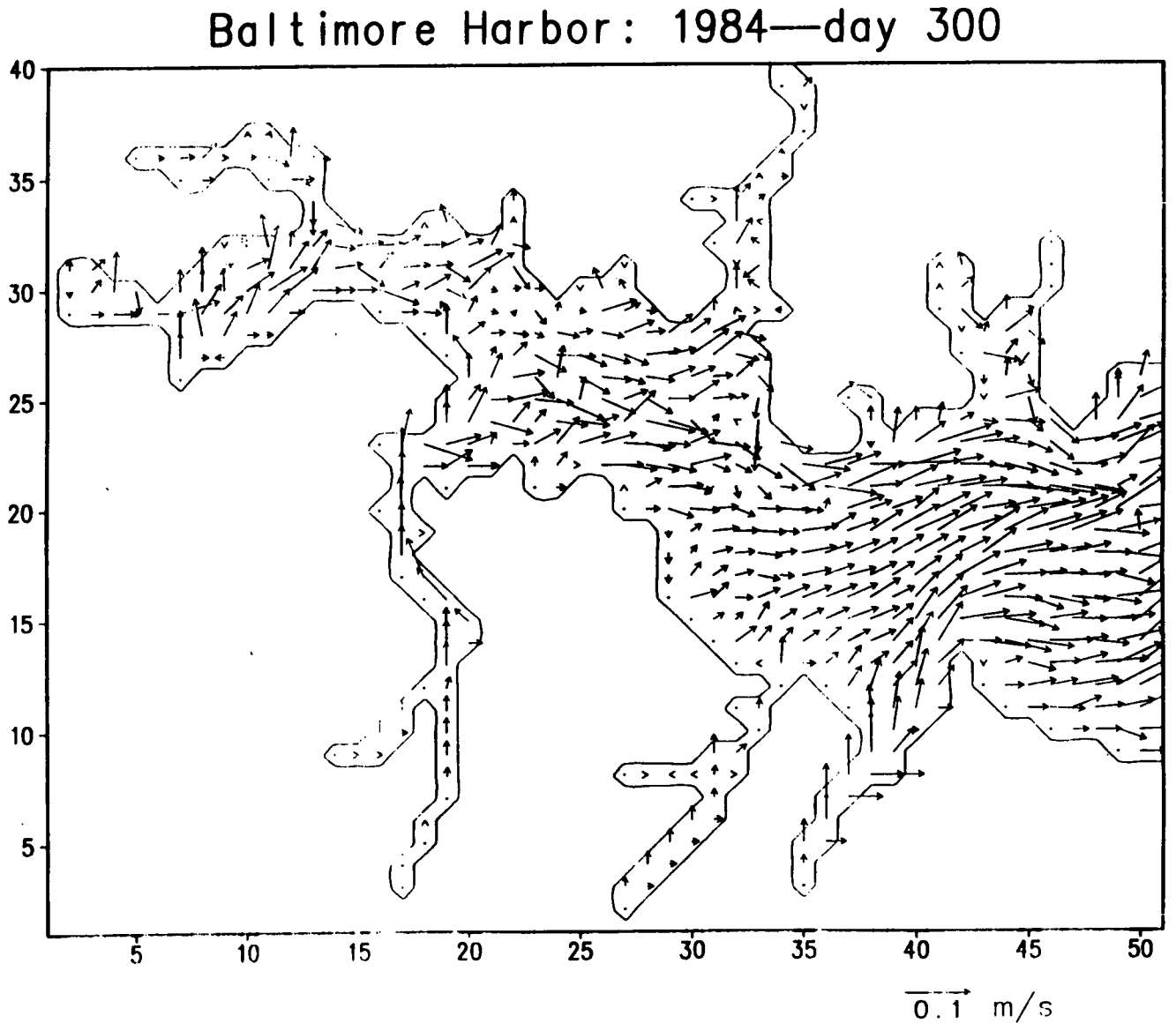

Figure 13(j). Instantaneous surface flow of the Harbor, day 300, 1984.

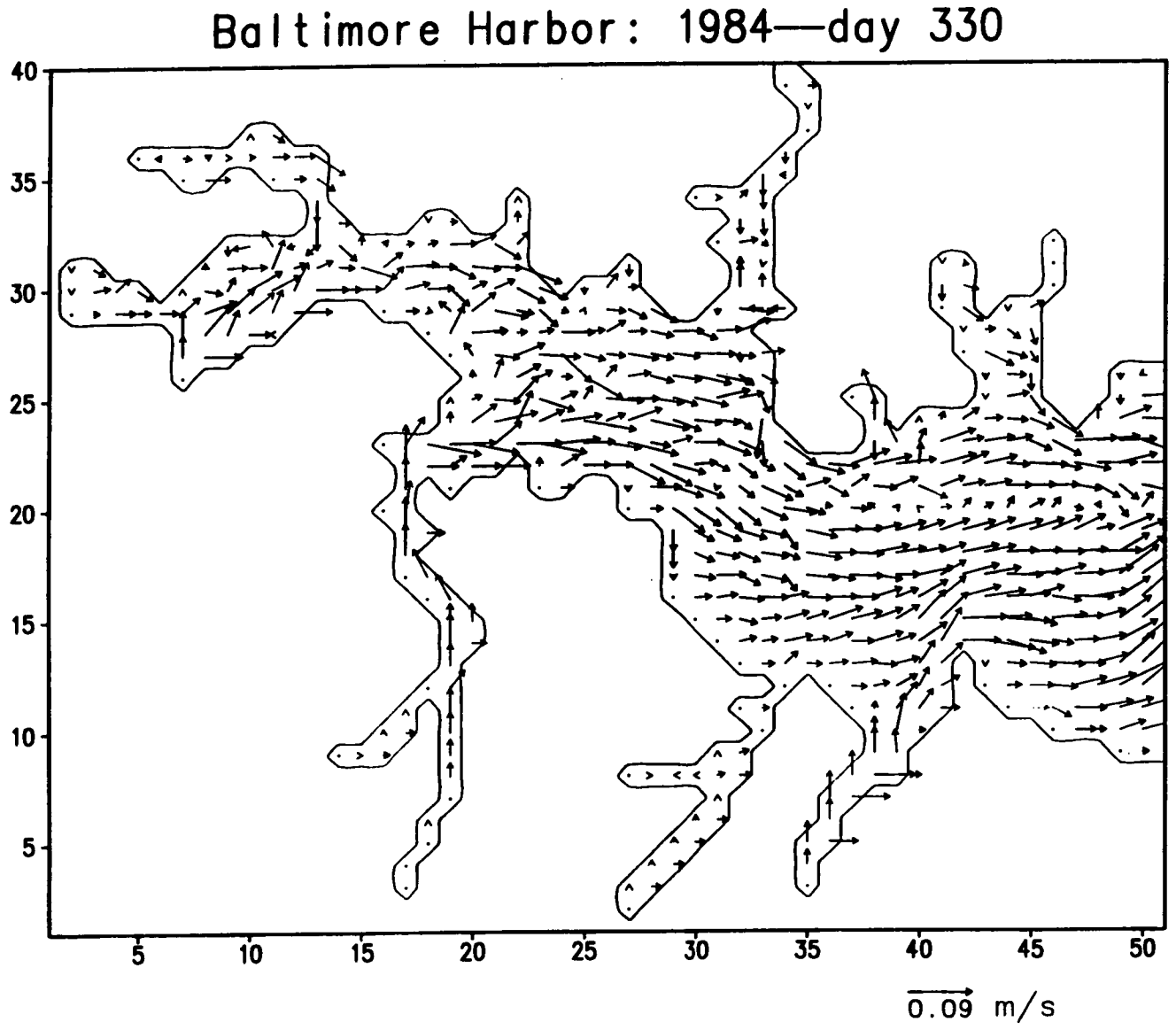

Figure 13(k). Instantaneous surface flow of the Harbor, day 330, 1984.

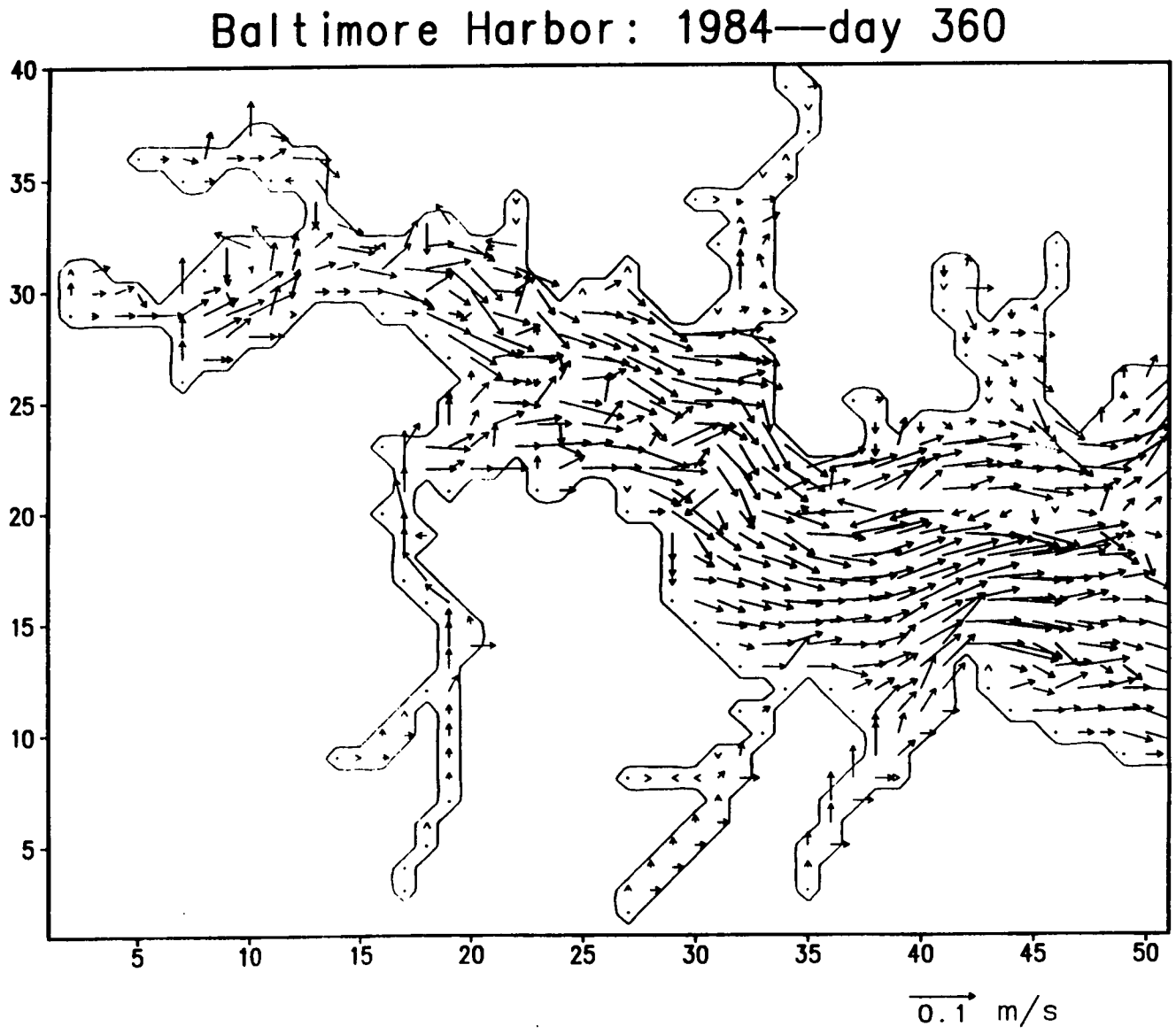

Figure 13(l). Instantaneous surface flow of the Harbor, day 360, 1984.

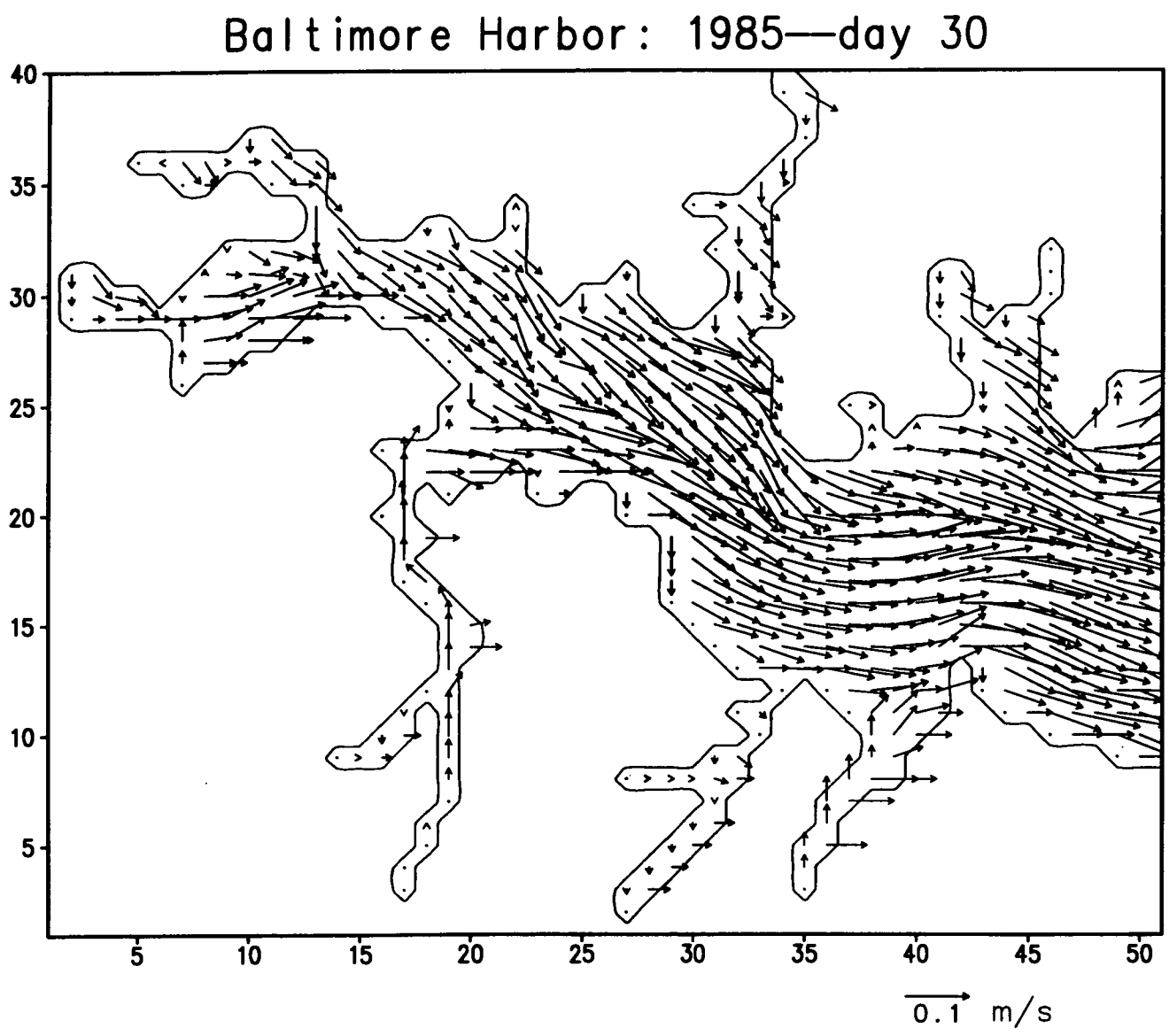

Figure 14(a). Instantaneous surface flow of the Harbor, day 30, 1985.

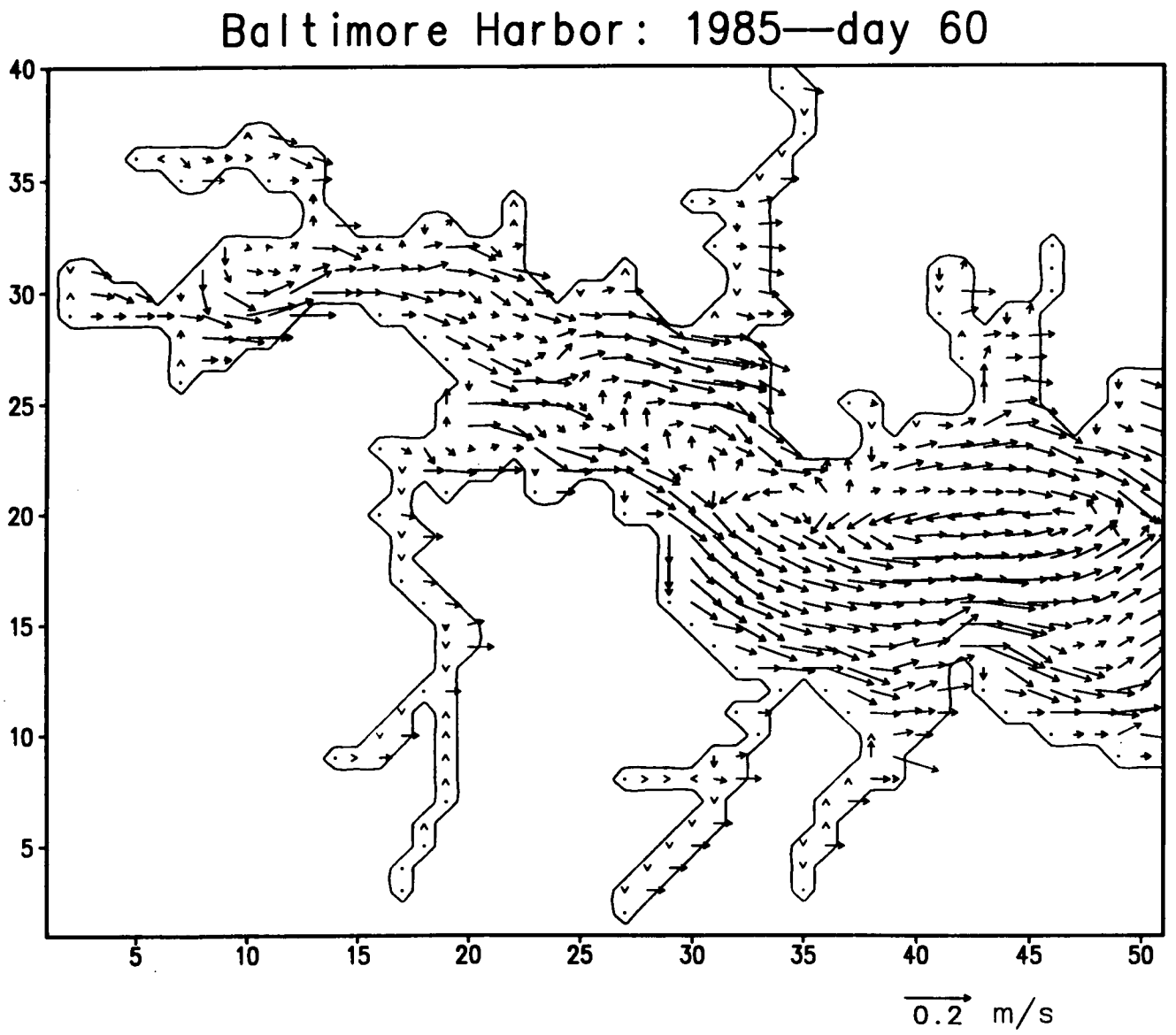

Figure 14(b). Instantaneous surface flow of the Harbor, day 60, 1985.

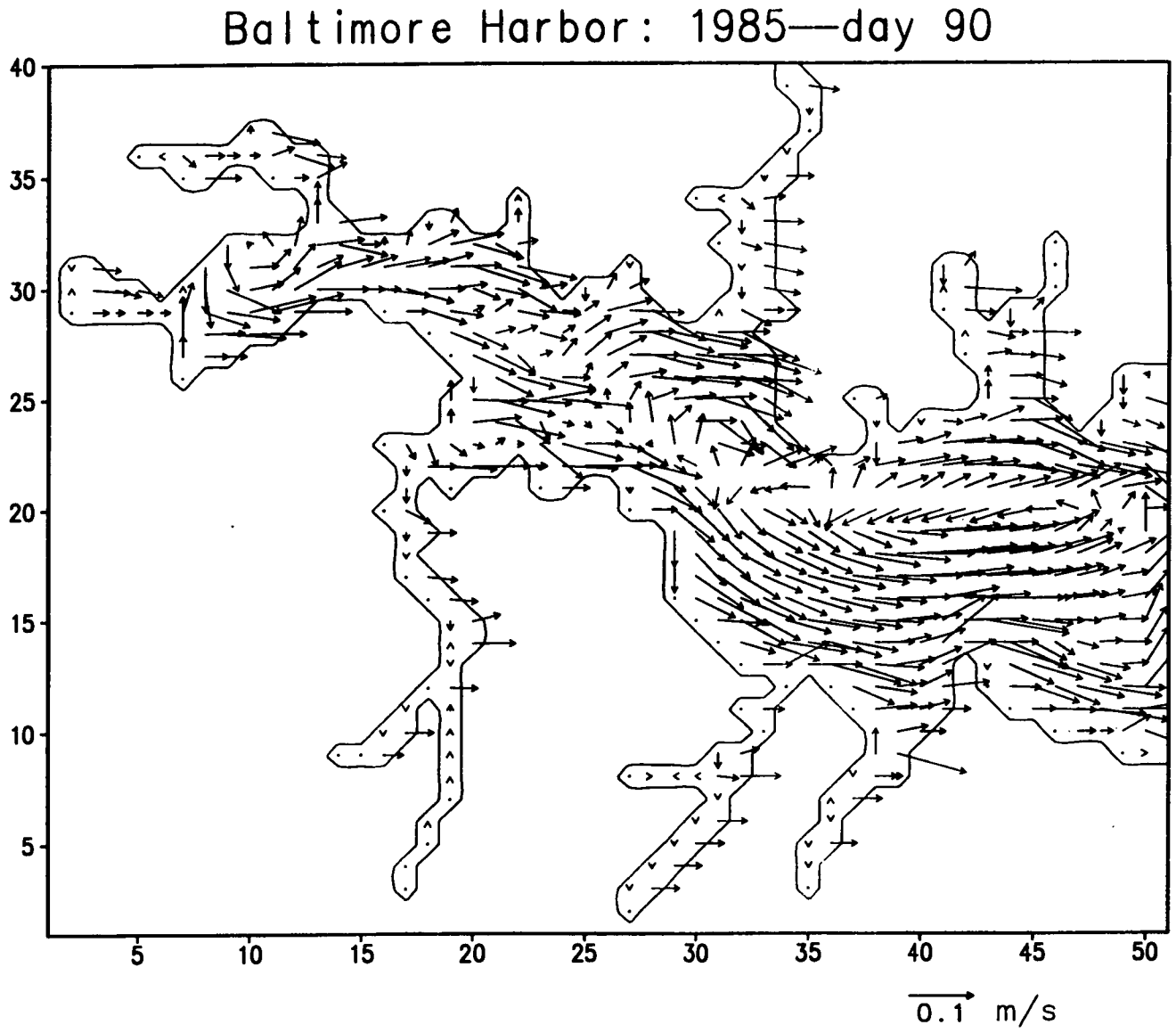

Figure 14(c). Instantaneous surface flow of the Harbor, day 90, 1985.

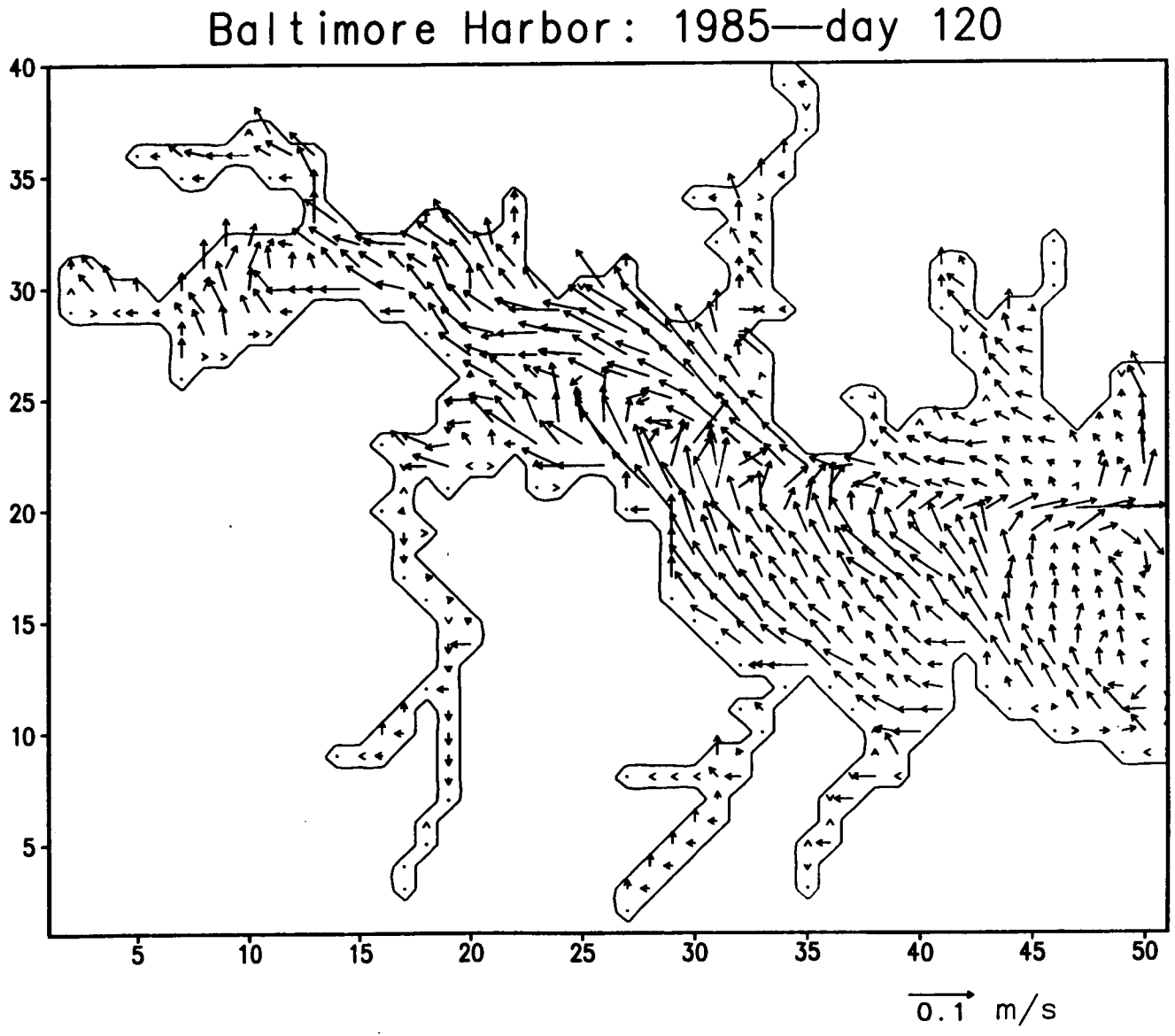

Figure 14(d). Instantaneous surface flow of the Harbor, day 120, 1985.

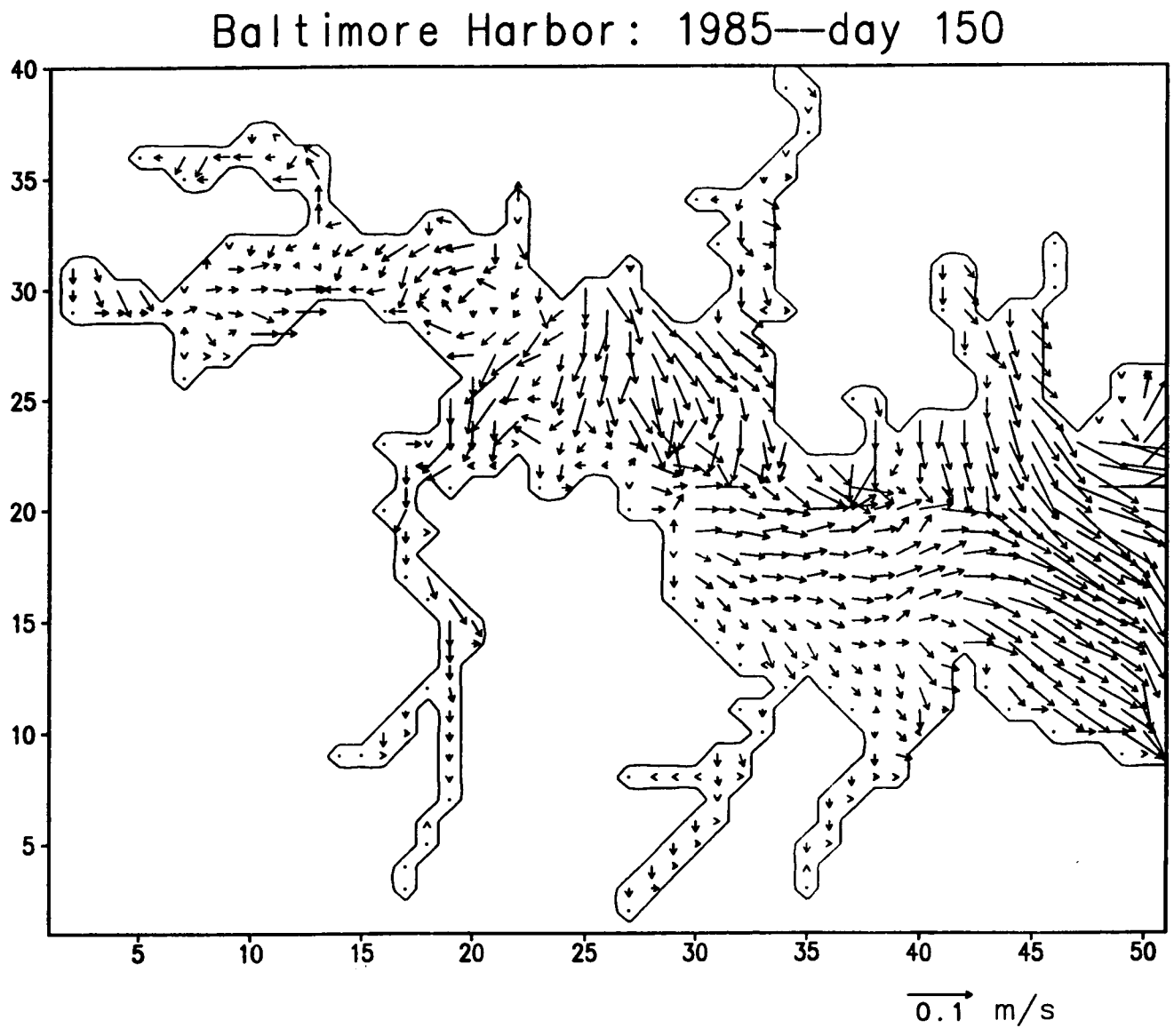

Figure 14(e). Instantaneous surface flow of the Harbor, day 150, 1985.

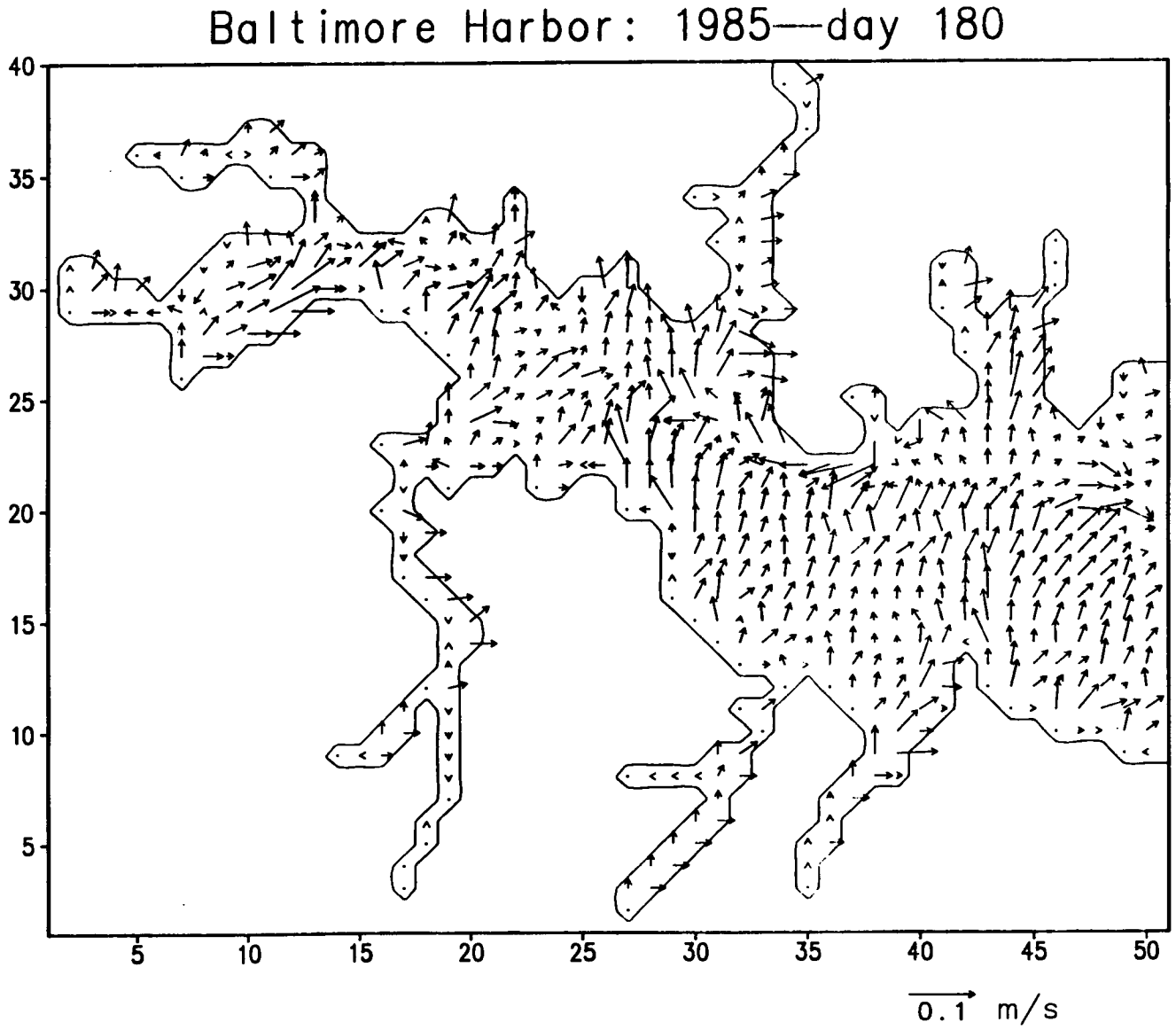

Figure 14(f). Instantaneous surface flow of the Harbor, day 180, 1985.

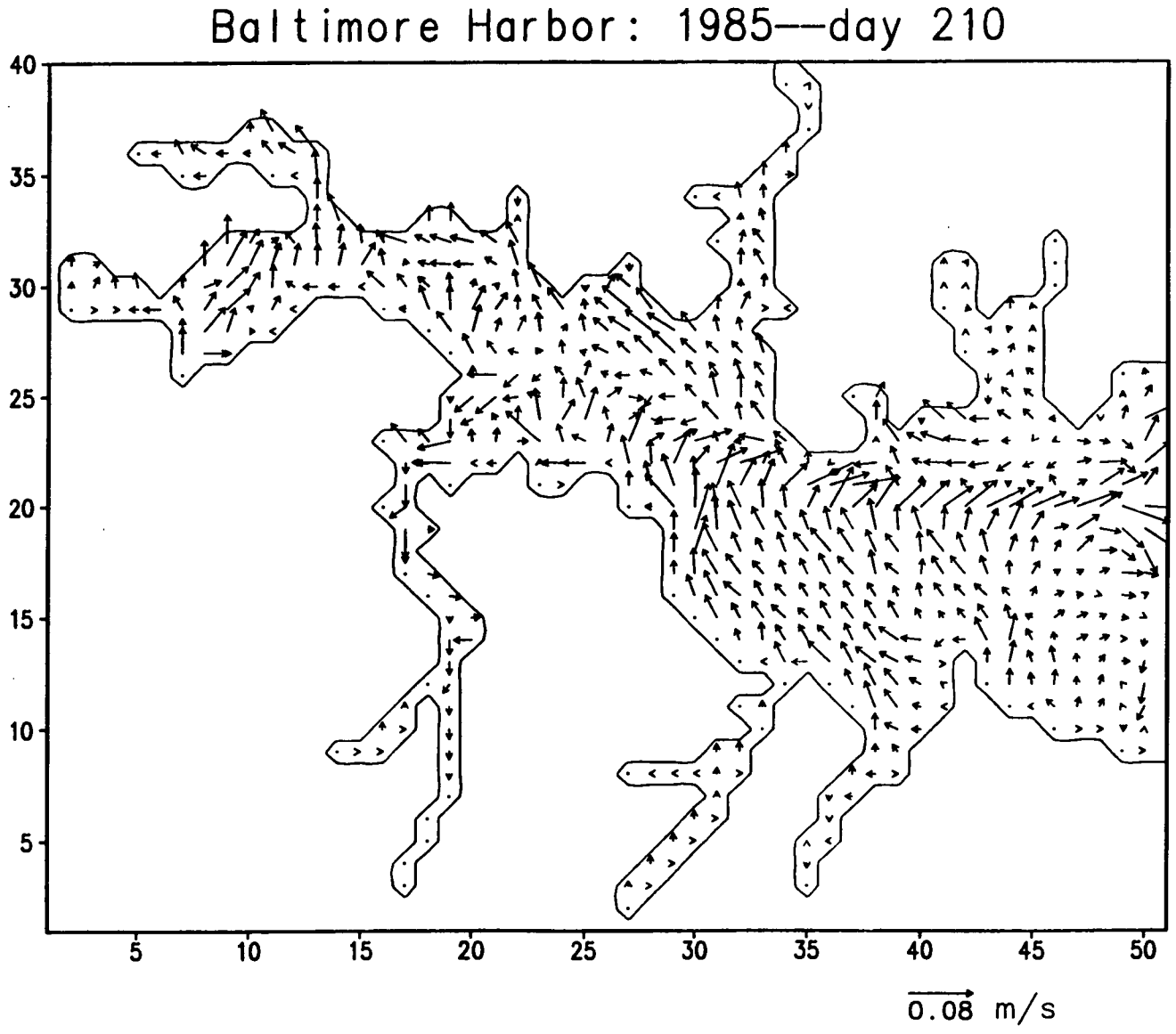

Figure 14(g). Instantaneous surface flow of the Harbor, day 210, 1985.

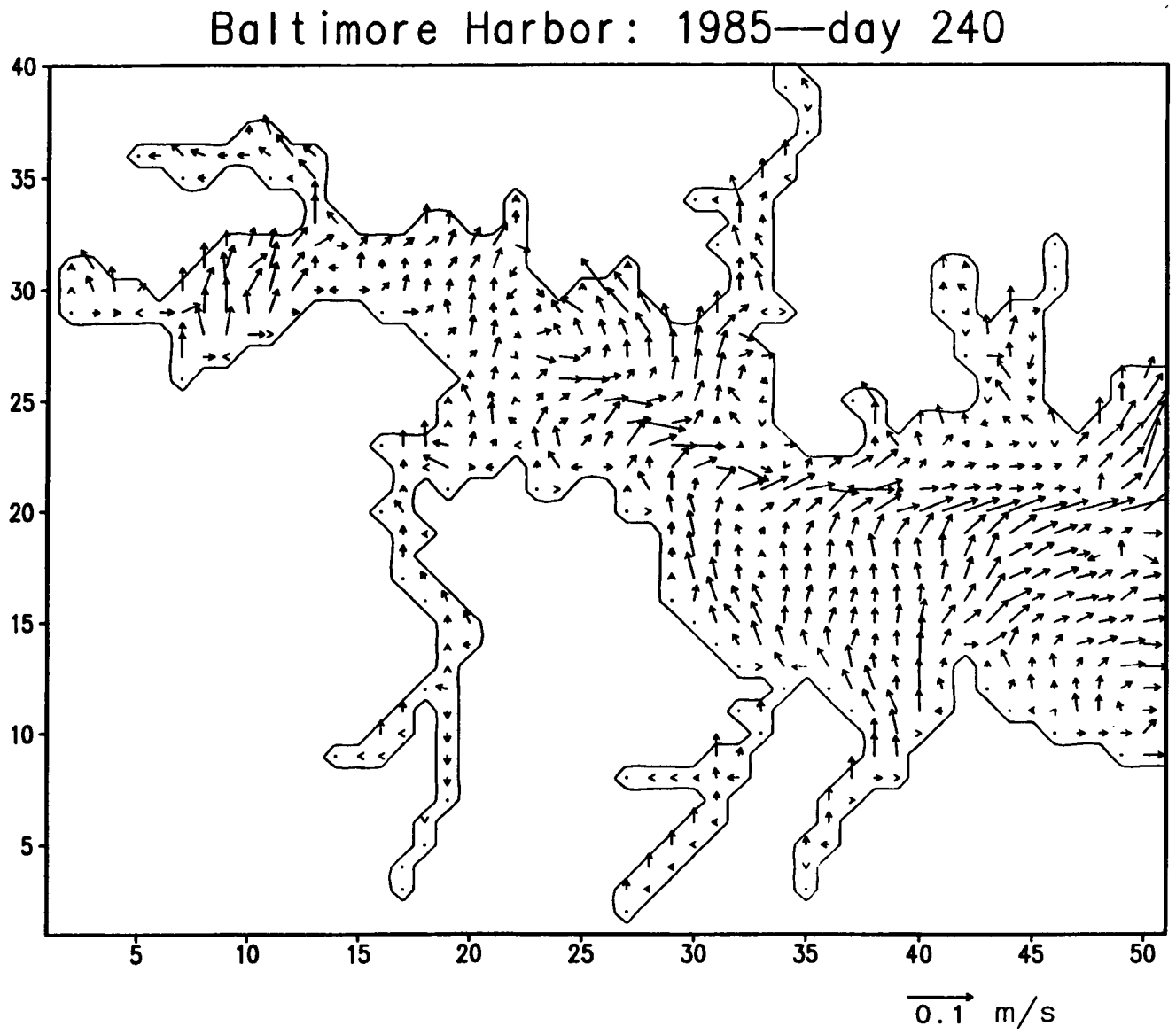

Figure 14(h). Instantaneous surface flow of the Harbor, day 240, 1985.

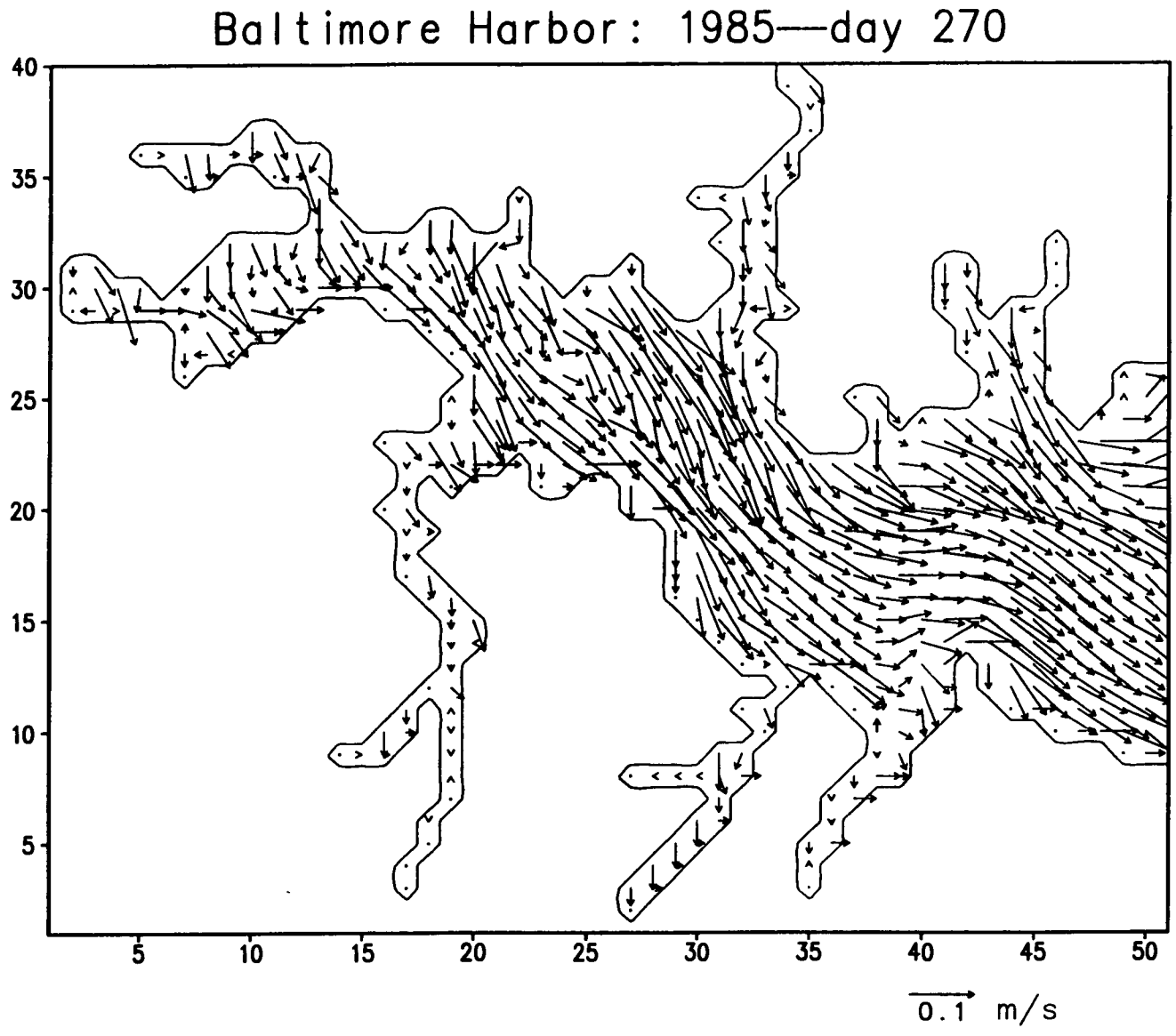

Figure 14(i). Instantaneous surface flow of the Harbor, day 270, 1985.

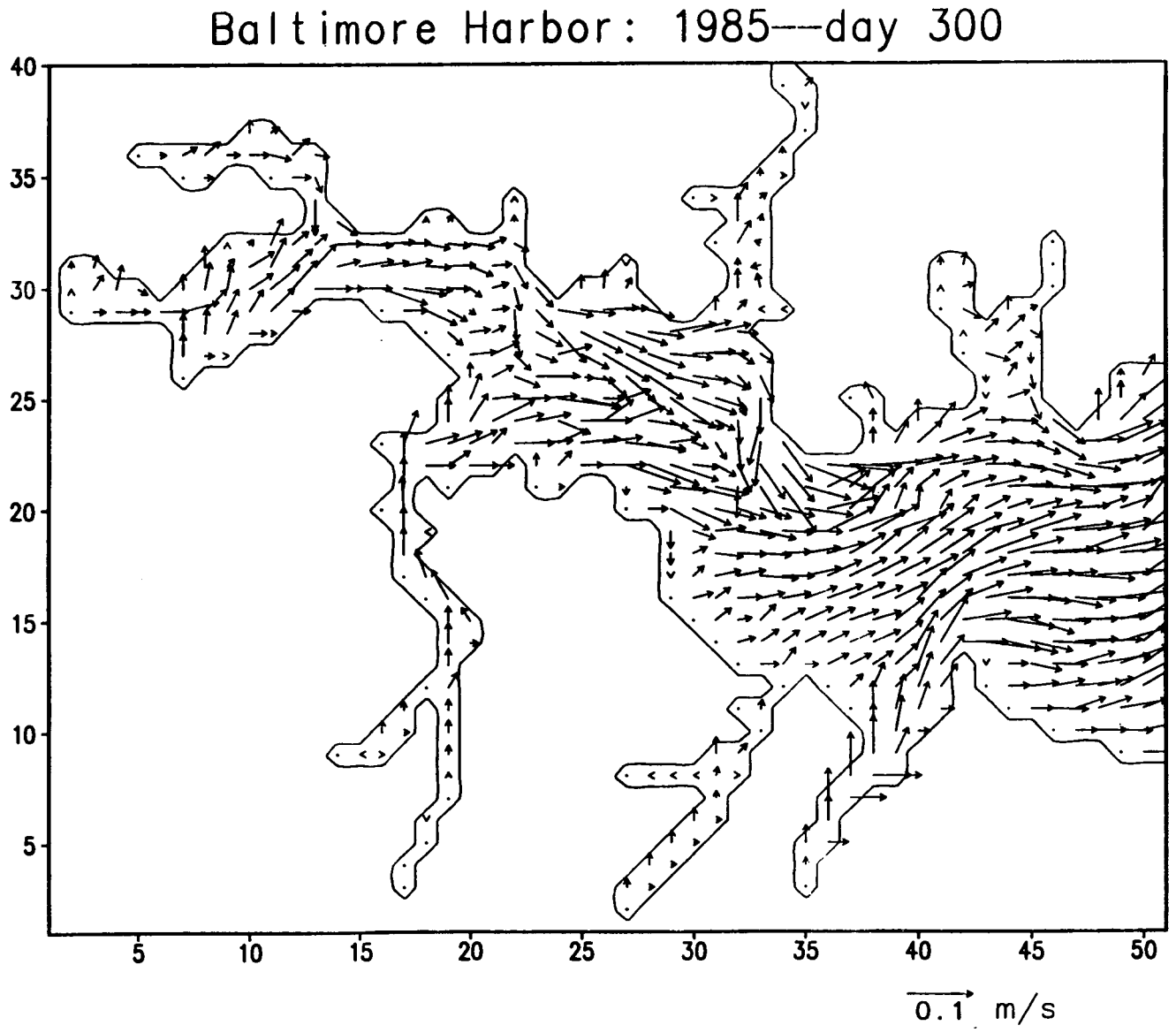

Figure 14(j). Instantaneous surface flow of the Harbor, day 300, 1985.

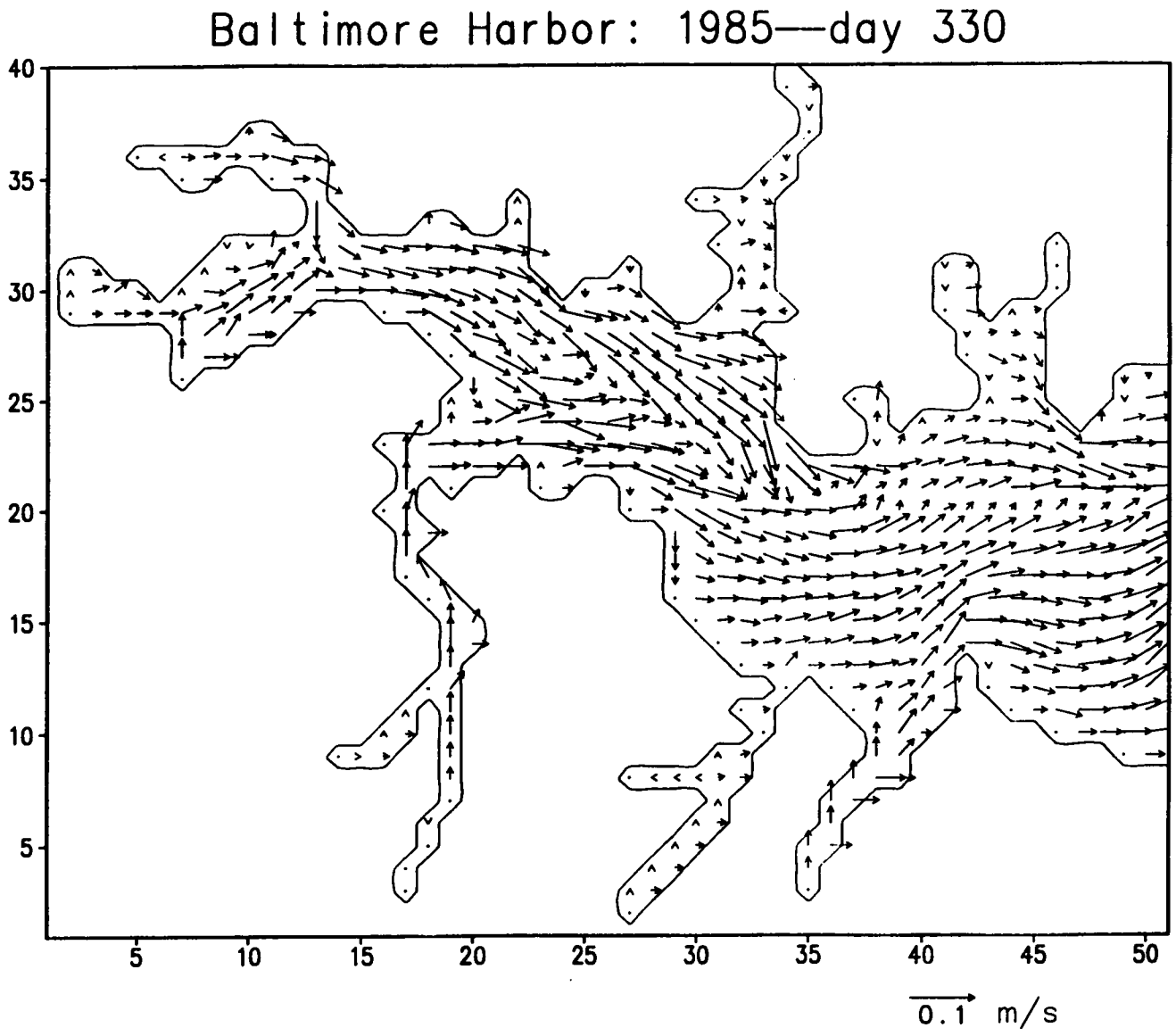

Figure 14(k). Instantaneous surface flow of the Harbor, day 330, 1985.

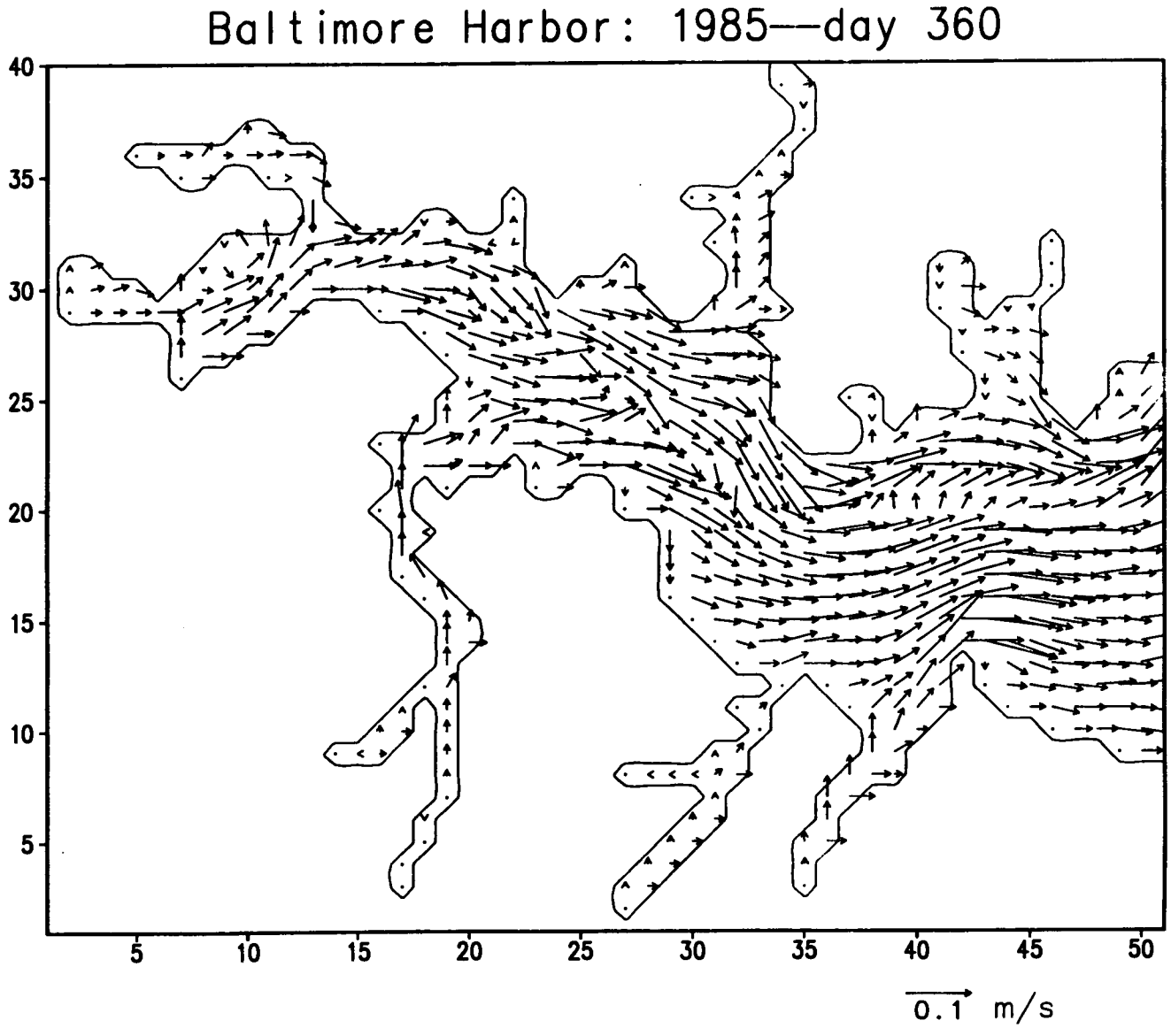

Figure 14(l). Instantaneous surface flow of the Harbor, day 360, 1985.

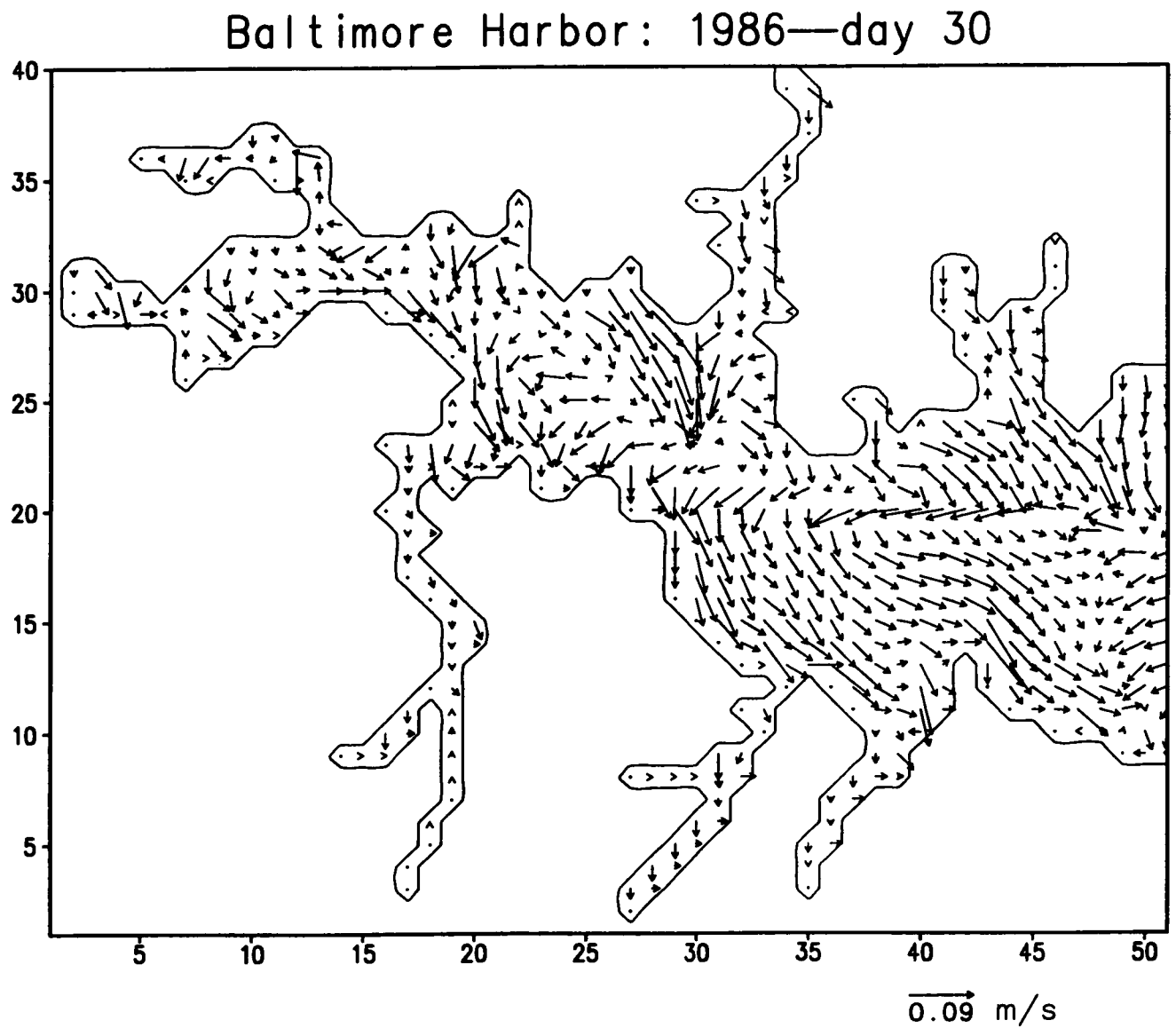

Figure 15(a). Instantaneous surface flow of the Harbor, day 30, 1986.

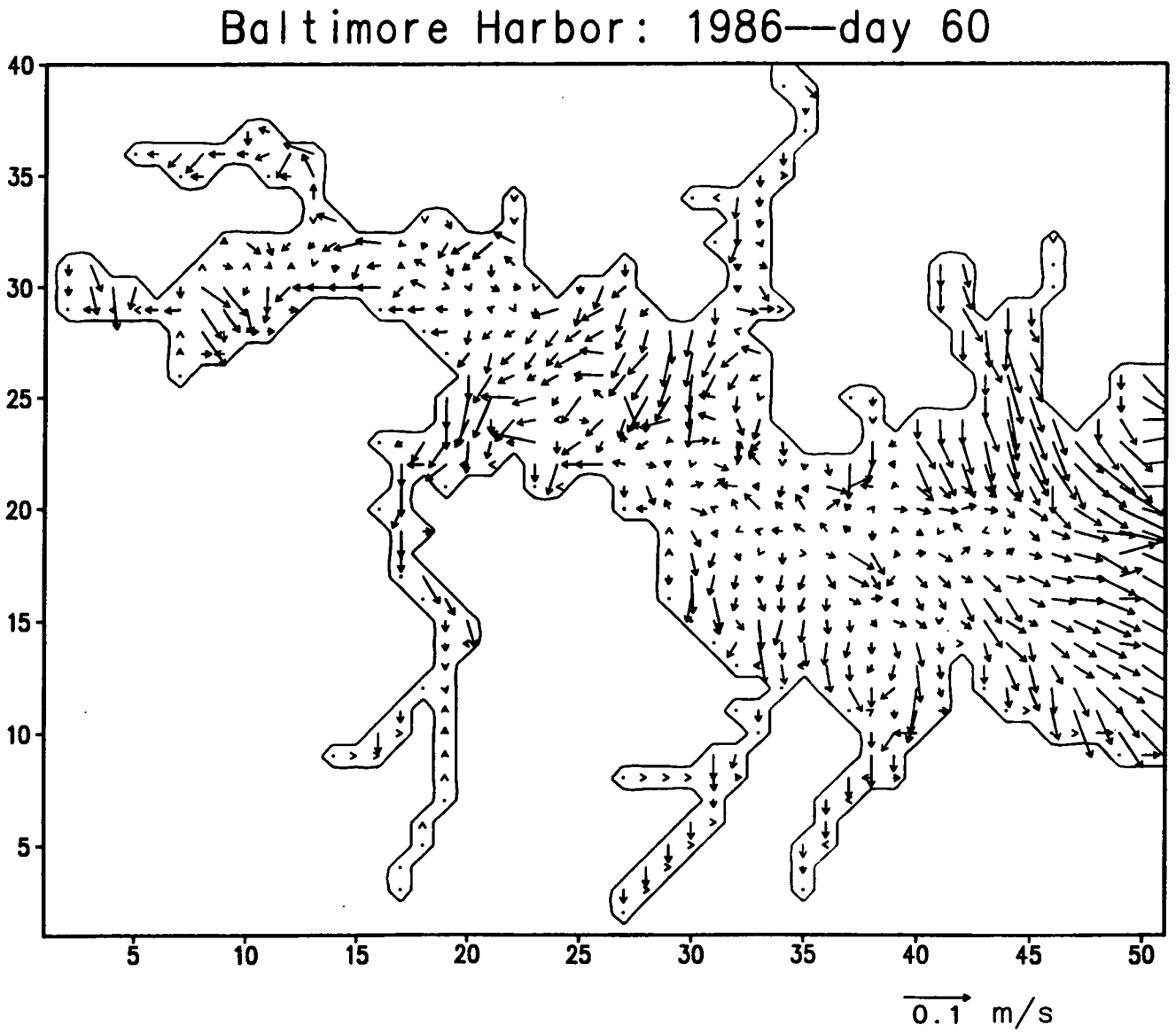

Figure 15(b). Instantaneous surface flow of the Harbor, day 60, 1986.

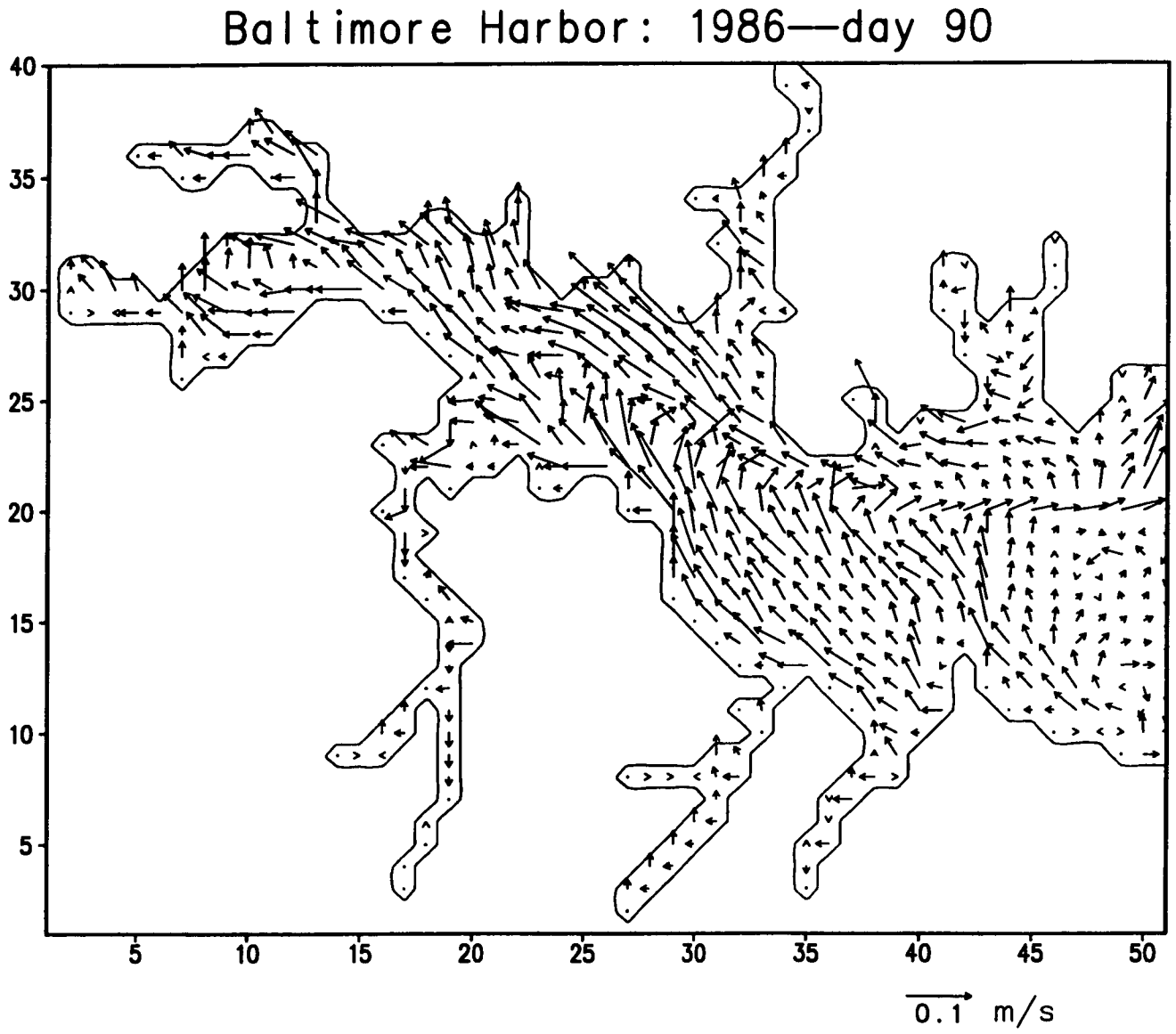

Figure 15(c). Instantaneous surface flow of the Harbor, day 90, 1986.

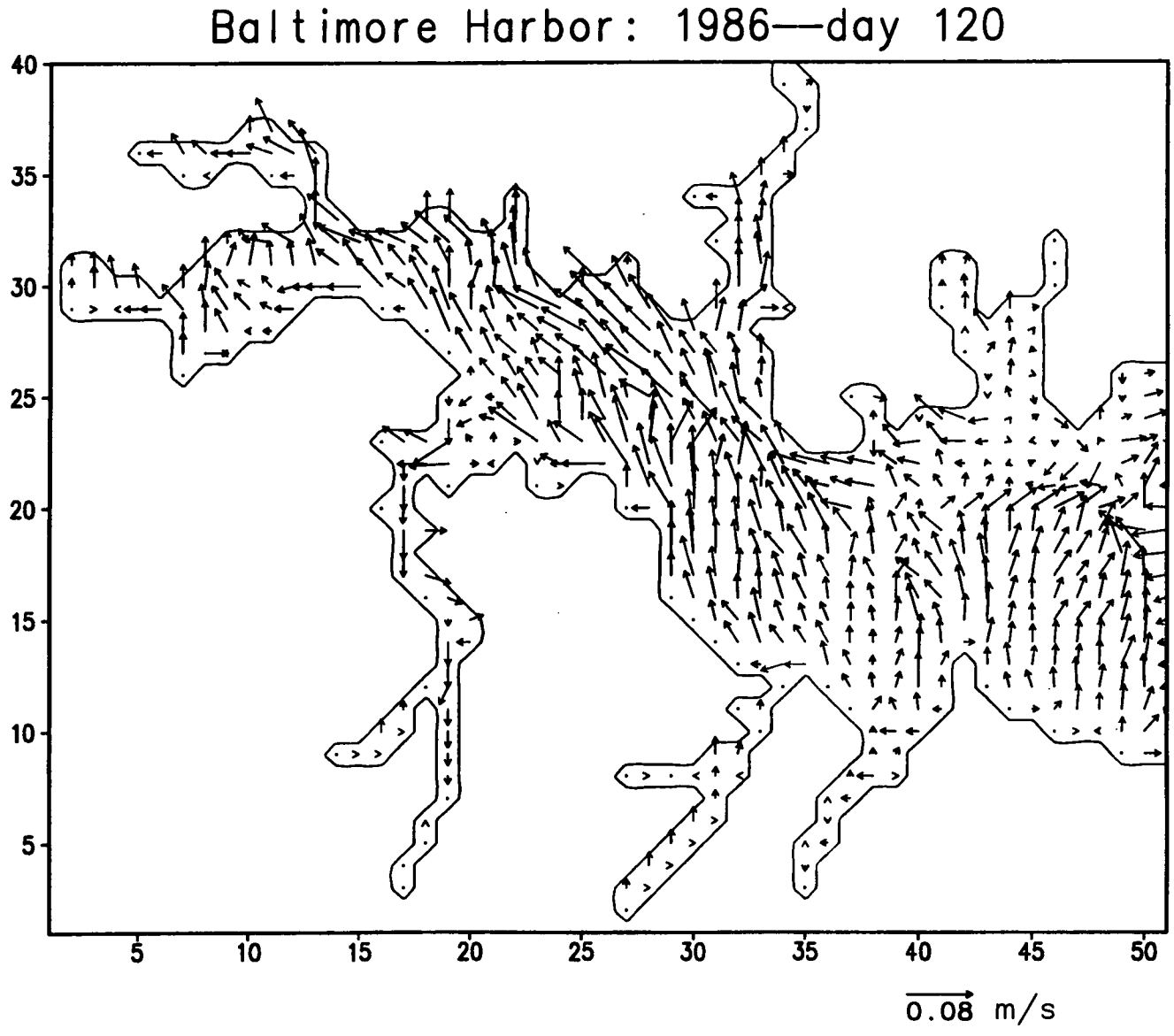

Figure 15(d). Instantaneous surface flow of the Harbor, day 120, 1986.

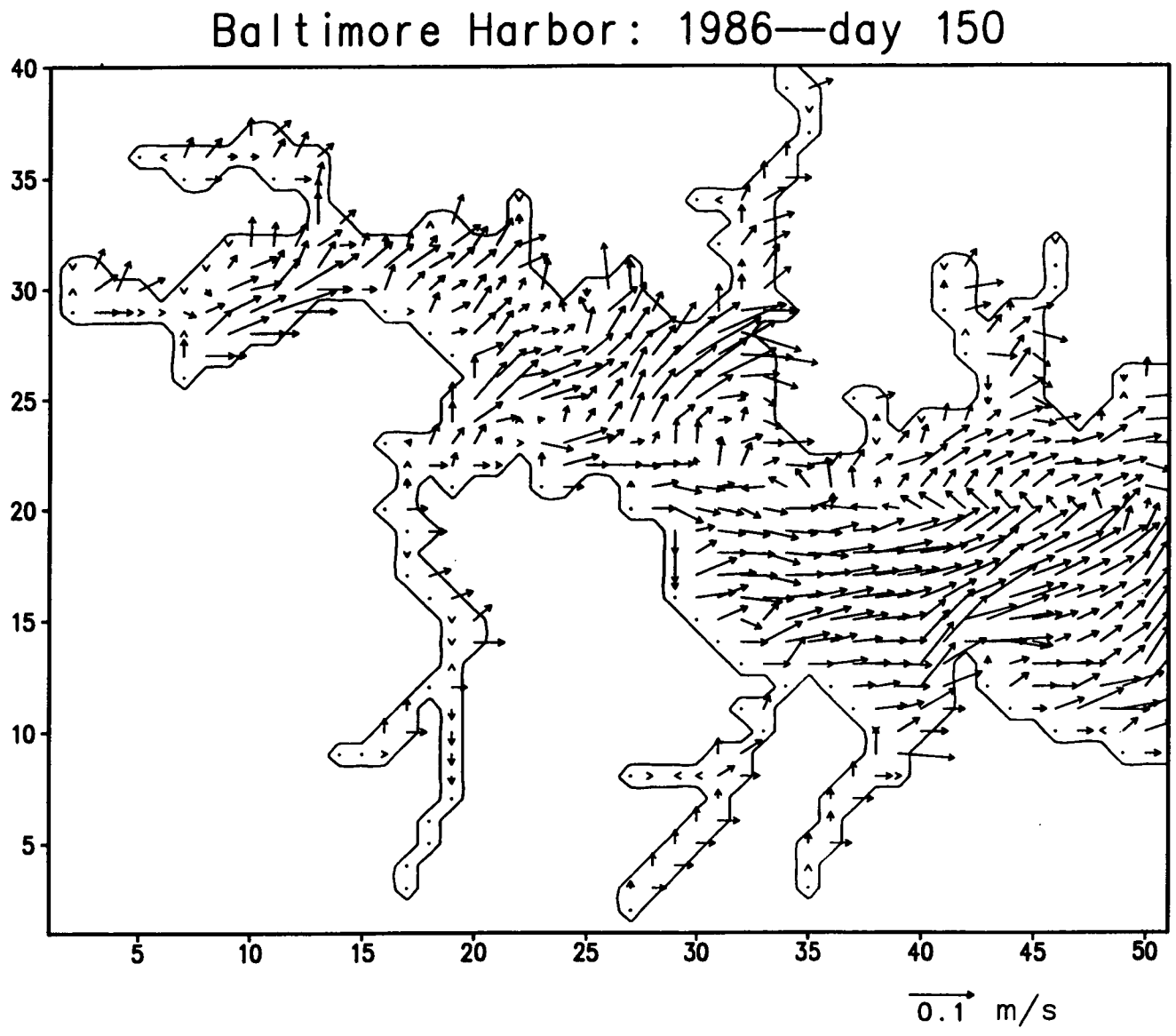

Figure 15(e). Instantaneous surface flow of the Harbor, day 150, 1986.

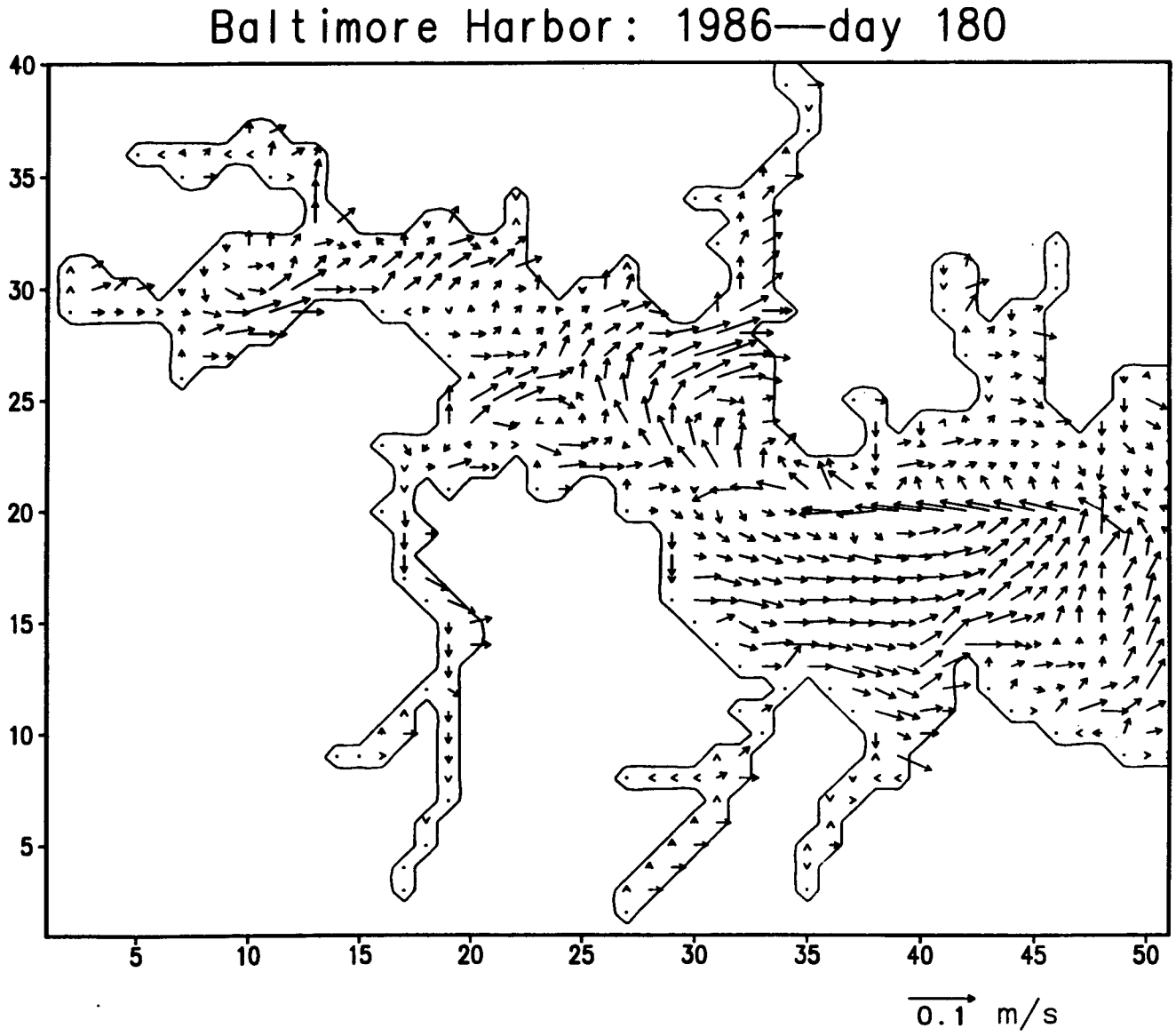

Figure 15(f). Instantaneous surface flow of the Harbor, day 180, 1986.

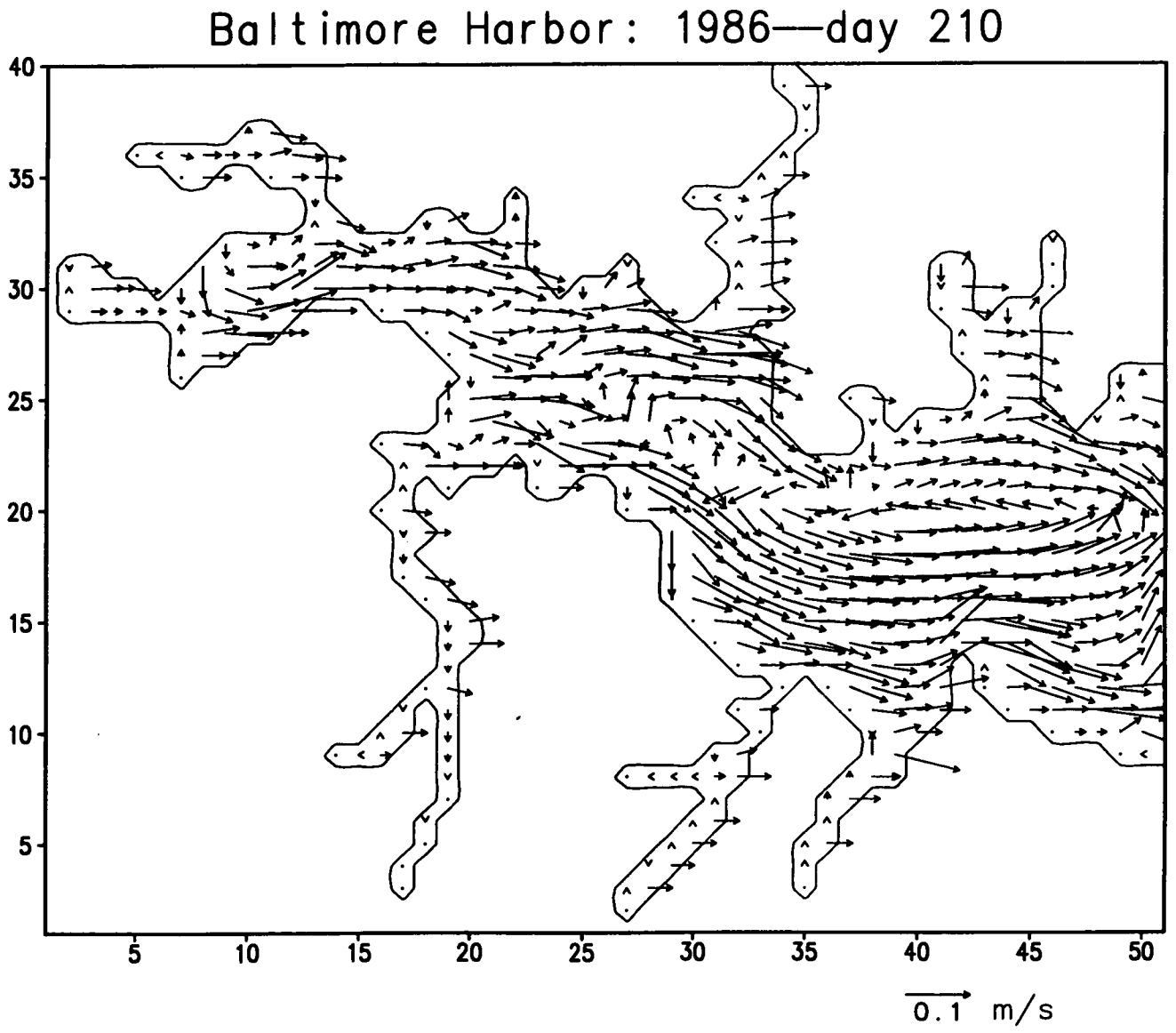

Figure 15(g). Instantaneous surface flow of the Harbor, day 210, 1986.

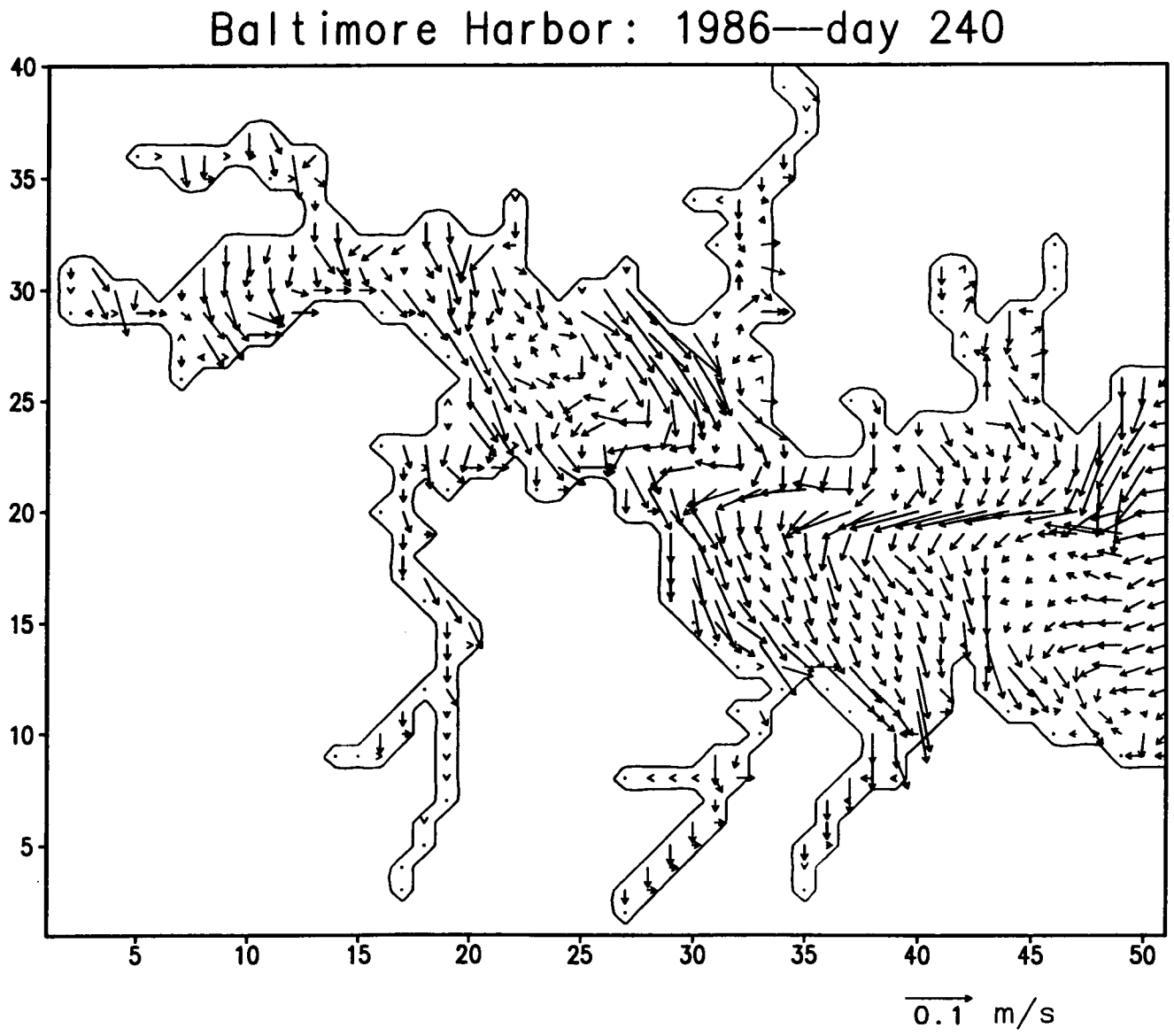

Figure 15(h). Instantaneous surface flow of the Harbor, day 240, 1986.

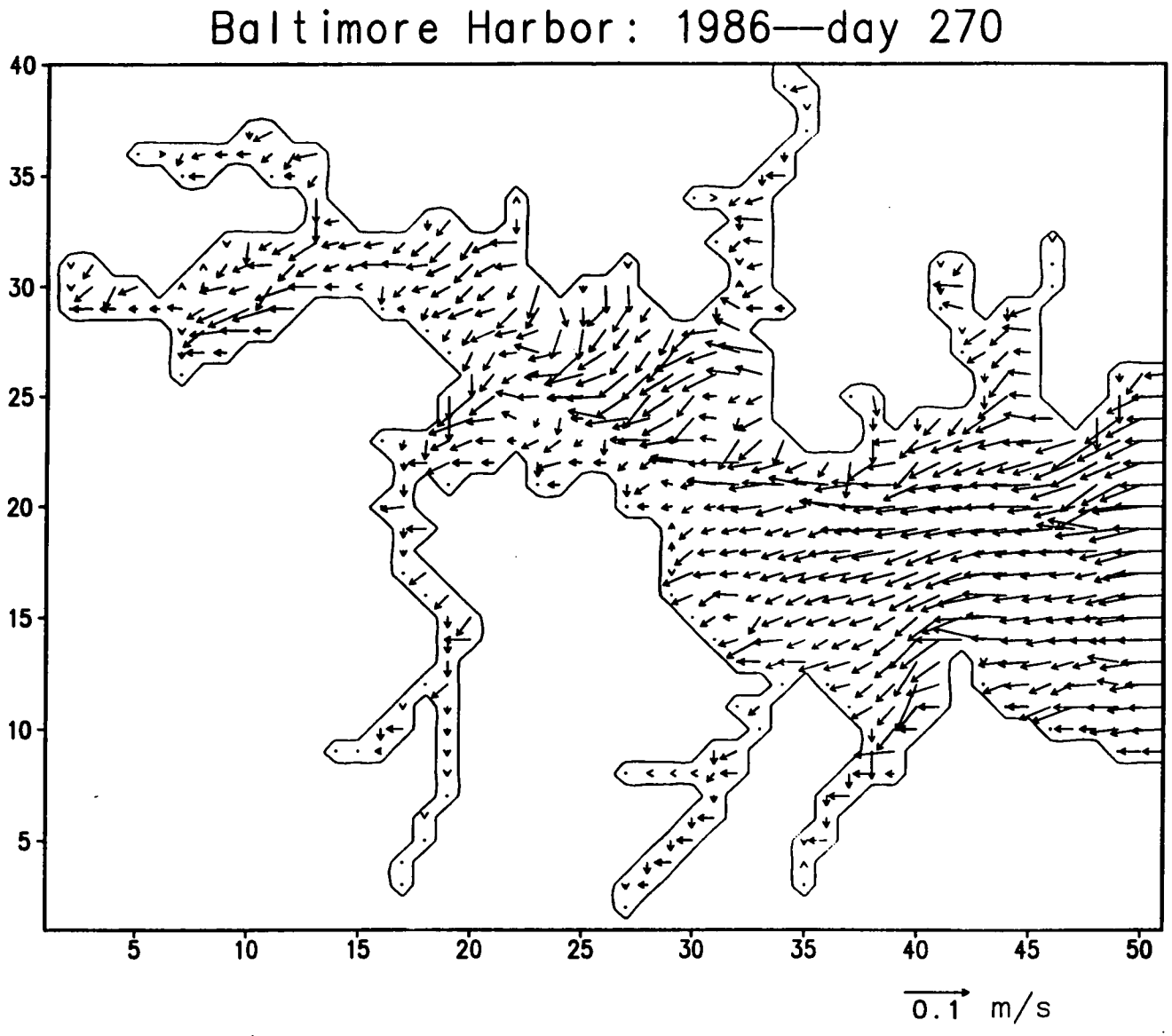

Figure 15(i). Instantaneous surface flow of the Harbor, day 270, 1986.

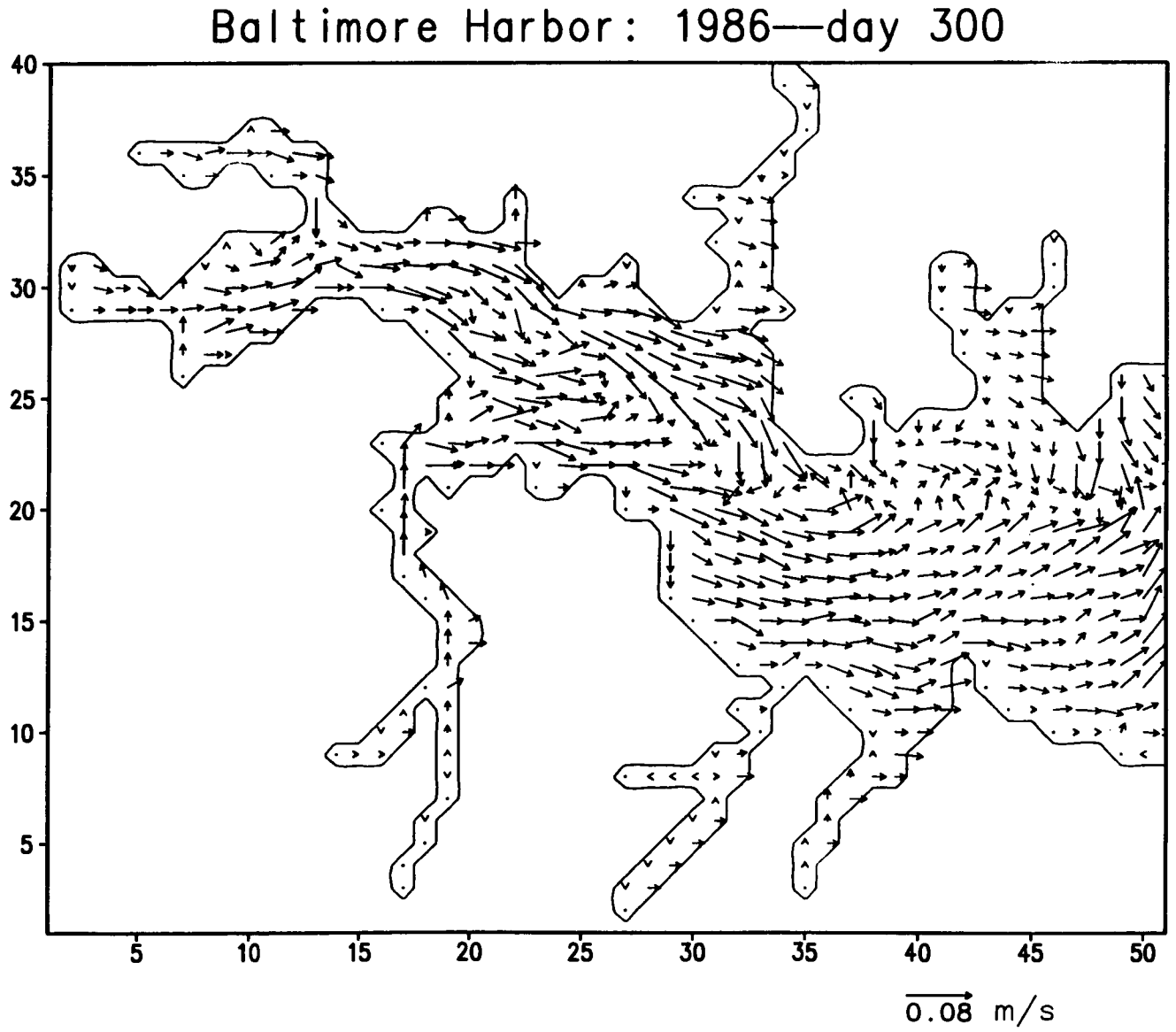

Figure 15(j). Instantaneous surface flow of the Harbor, day 300, 1986.

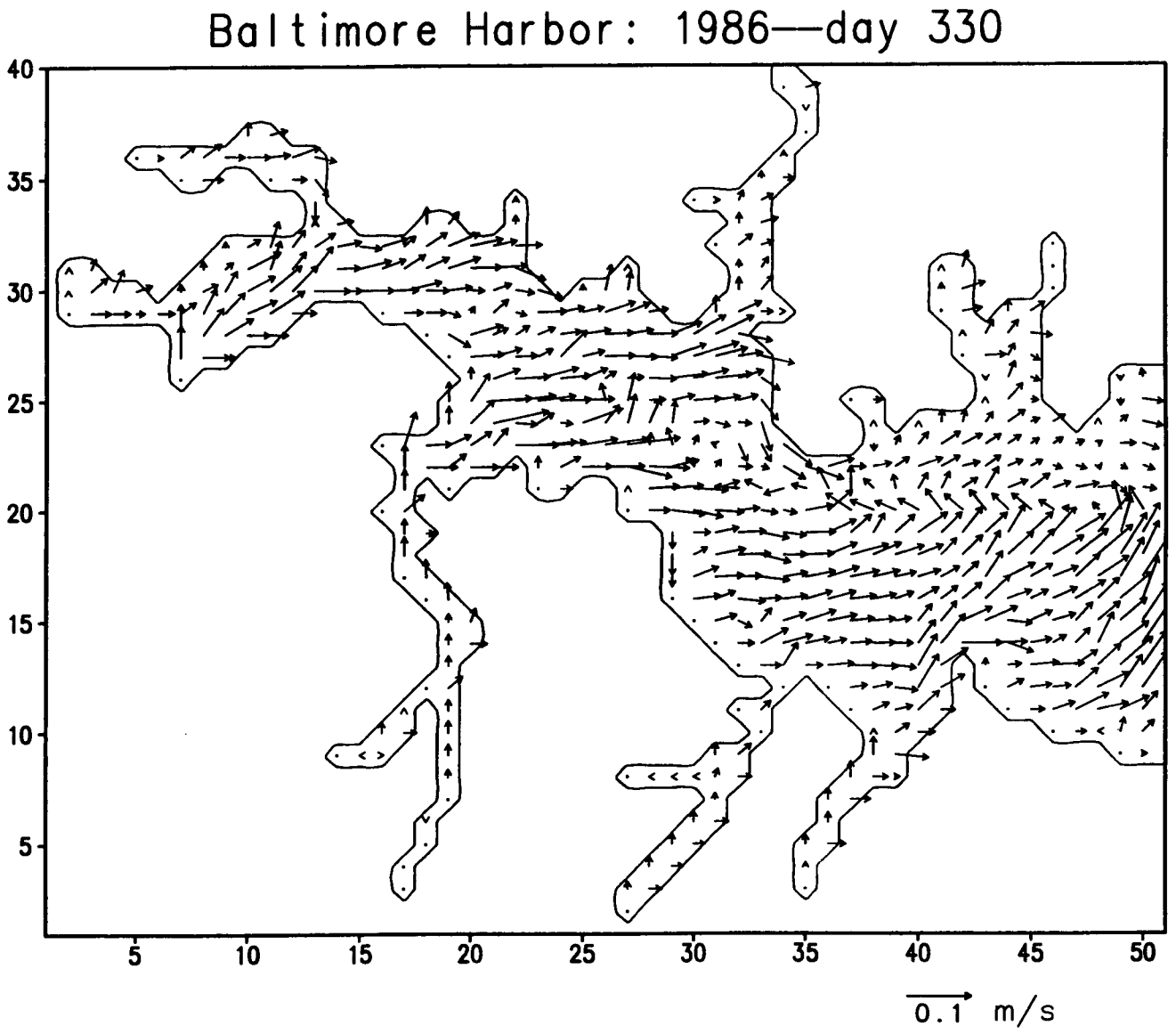

Figure 15(k). Instantaneous surface flow of the Harbor, day 330, 1986.

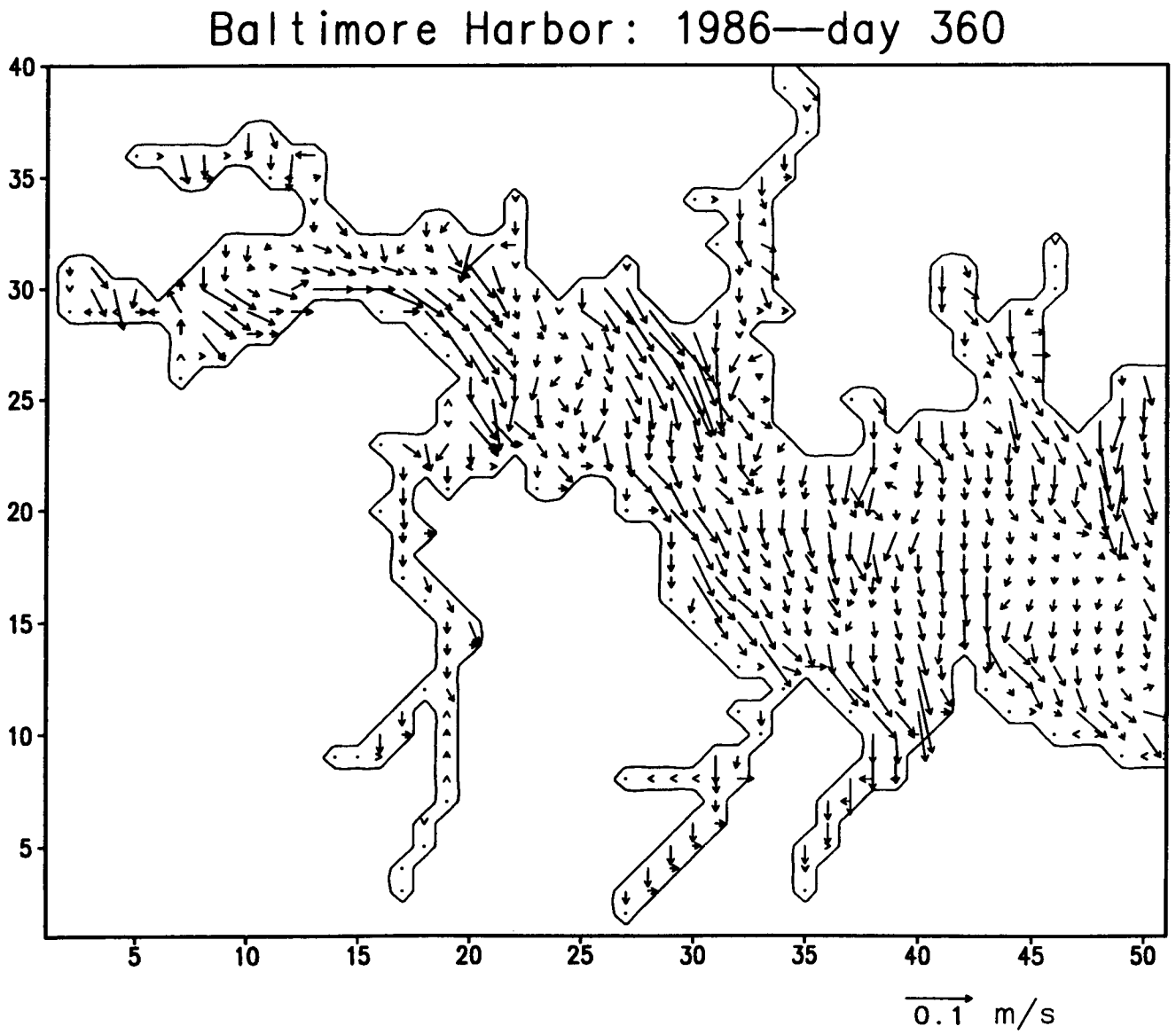

Figure 15(l). Instantaneous surface flow of the Harbor, day 360, 1986.

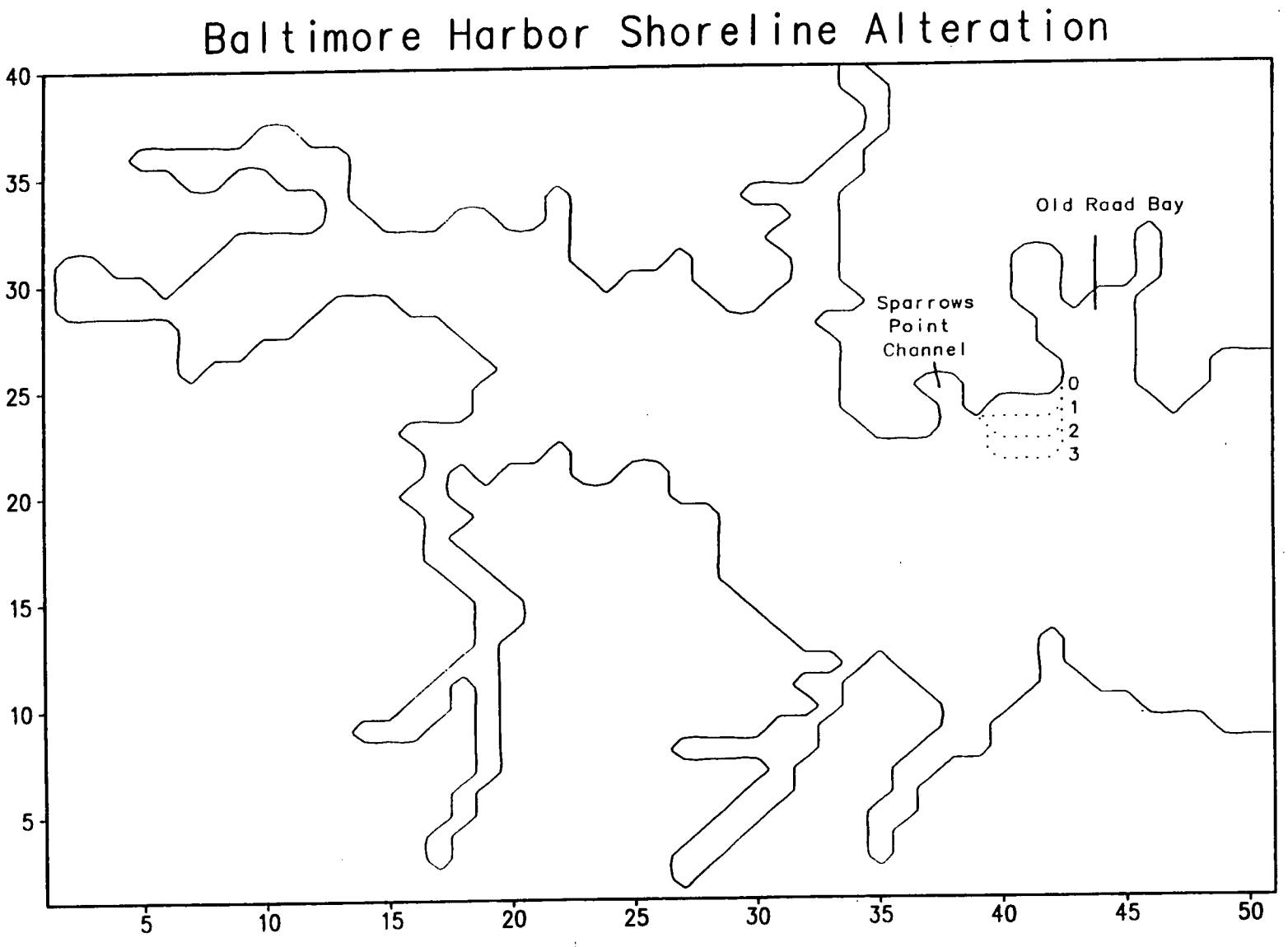

Figure 16. The existing shoreline of the Baltimore Harbor, along with three alternative shorelines south of the Sparrows Point. With a shoreline index (n=0, 1, 2, 3), each alternative shoreline pushes the coast southward by $n\Delta y$, where Δy=360 m is the grid spacing of the hydrodynamic model.

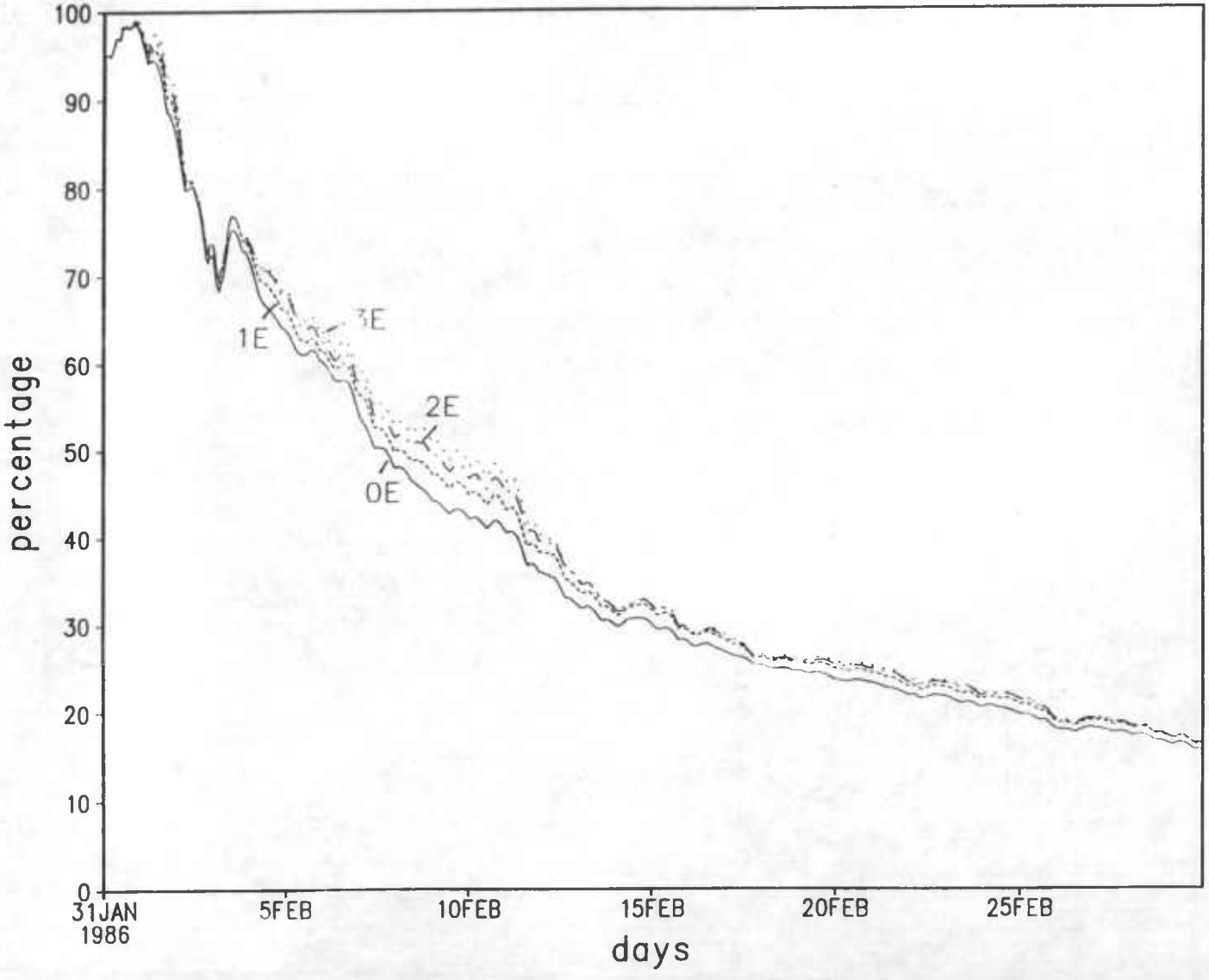

Figure 17. Percentage of total dye concentration retained in the Old Road Bay as a function of time, Feburary 1986. The initial dye concentration is uniform everywhere inside the embayment. See text for experiment indices 0E, 1E, 2E and 3E.

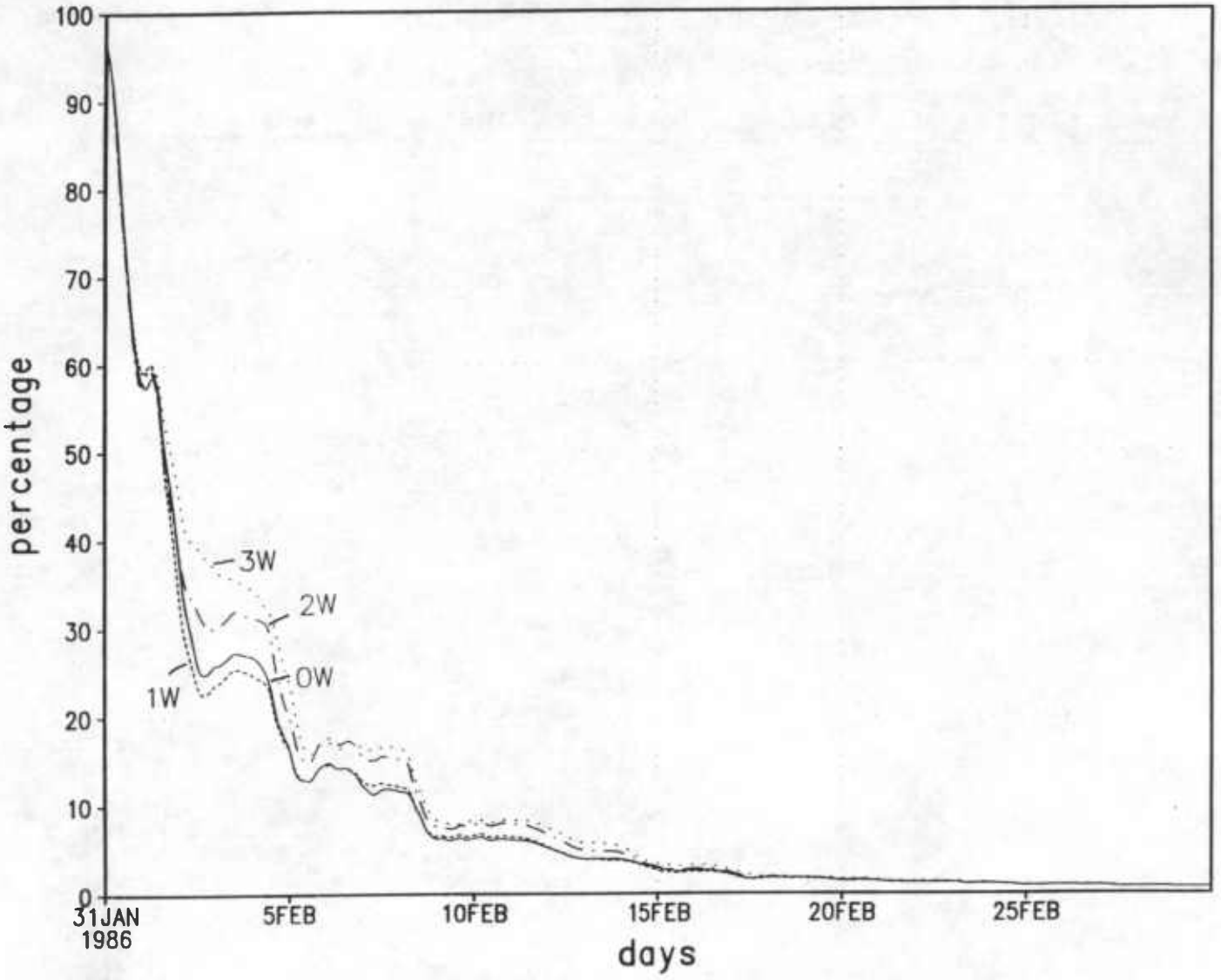

Figure 18. Percentage of total dye concentration retained in the Sparrows Point Channel as a function of time, Feburary 1986. The initial dye concentration is uniform everywhere inside the embayment. See text for experiment indices 0W, 1W, 2W and 3W.

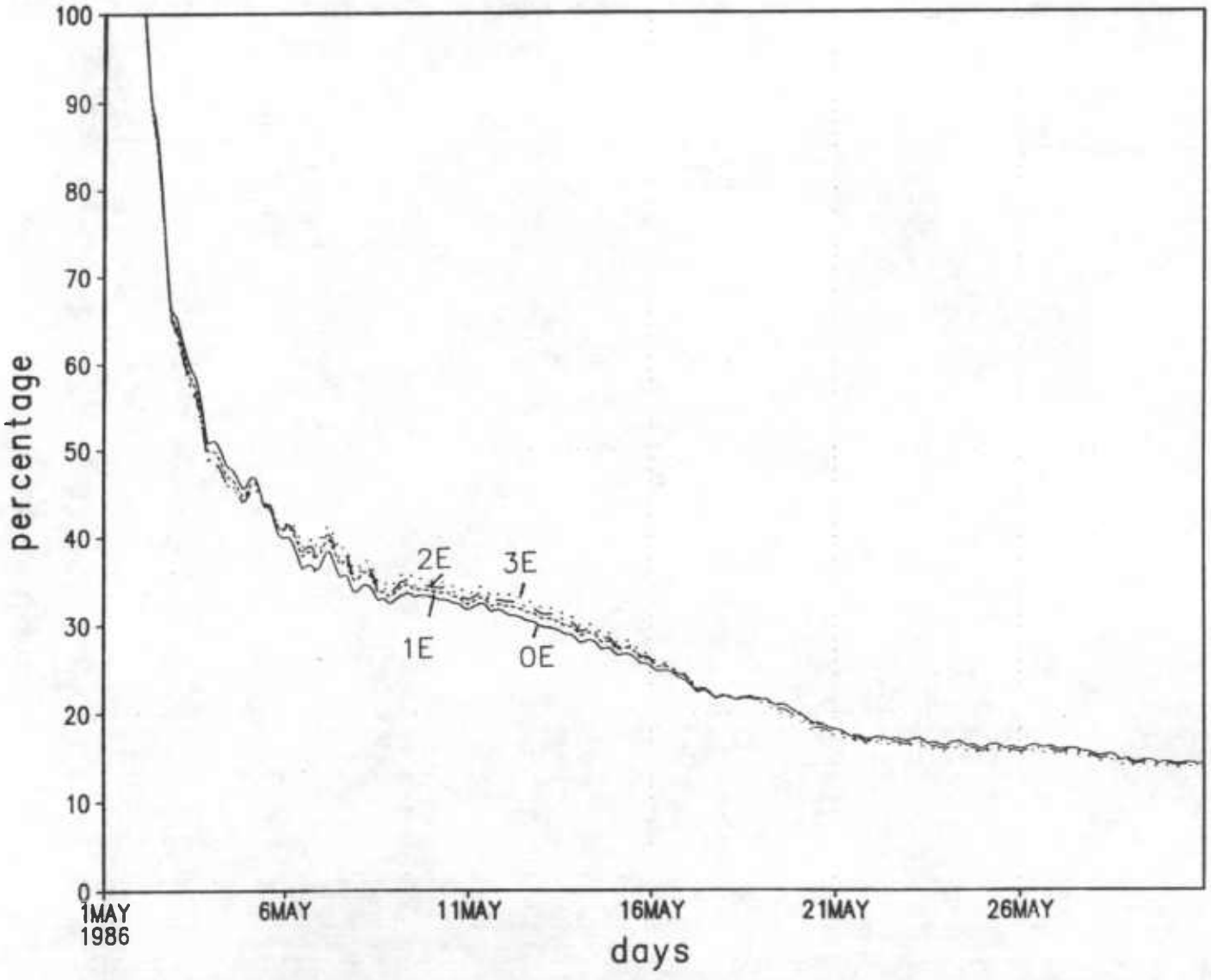

Figure 19. Percentage of total dye concentration retained in the Old Road Bay as a function of time, May 1986. The initial dye concentration is uniform everywhere inside the embayment. See text for experiment indices 0E, 1E, 2E and 3E.

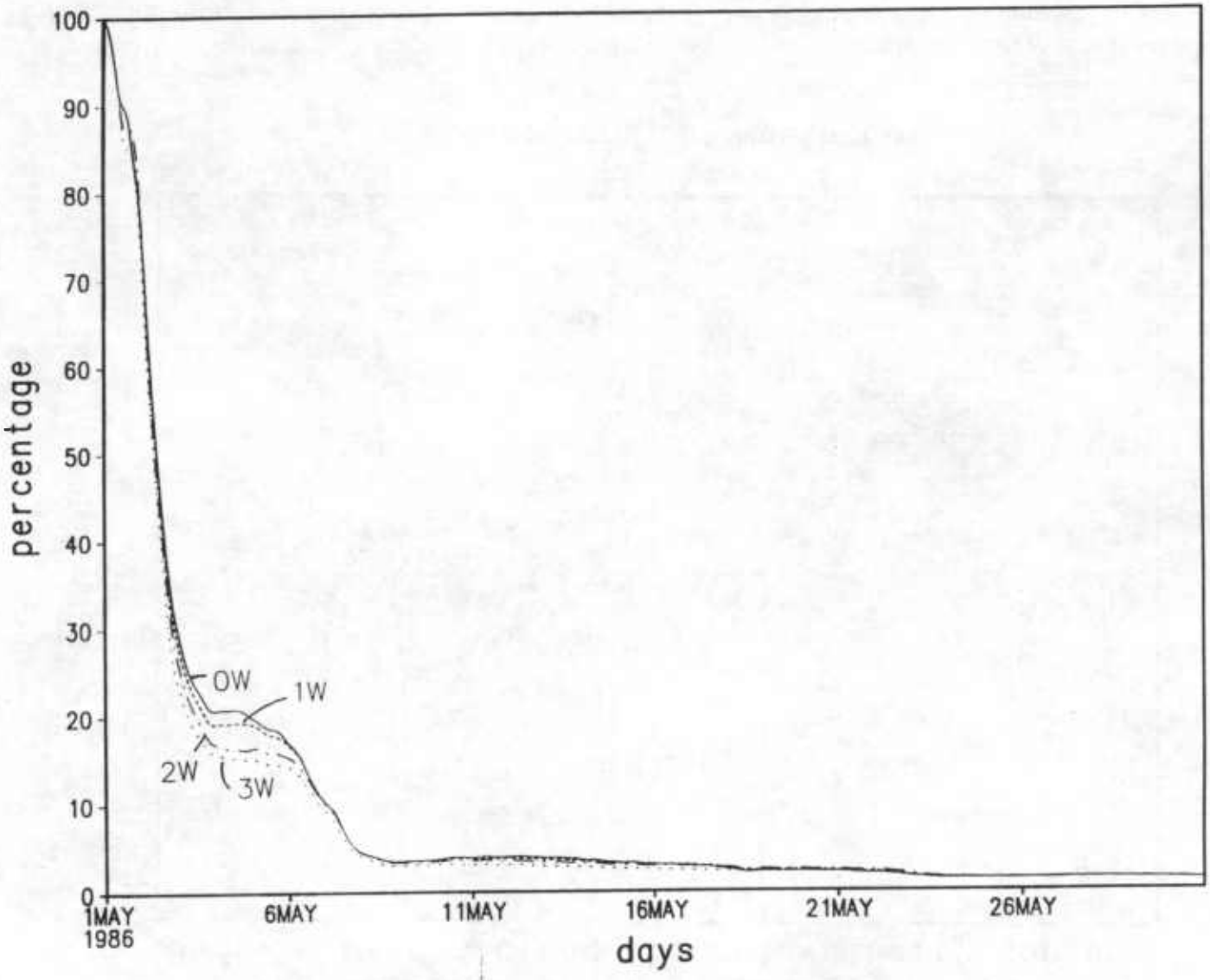

Figure 20. Percentage of total dye concentration retained in the Sparrows Point Channel as a function of time, May 1986. The initial dye concentration is uniform everywhere inside the embayment. See text for experiment indices 0W, 1W, 2W and 3W.

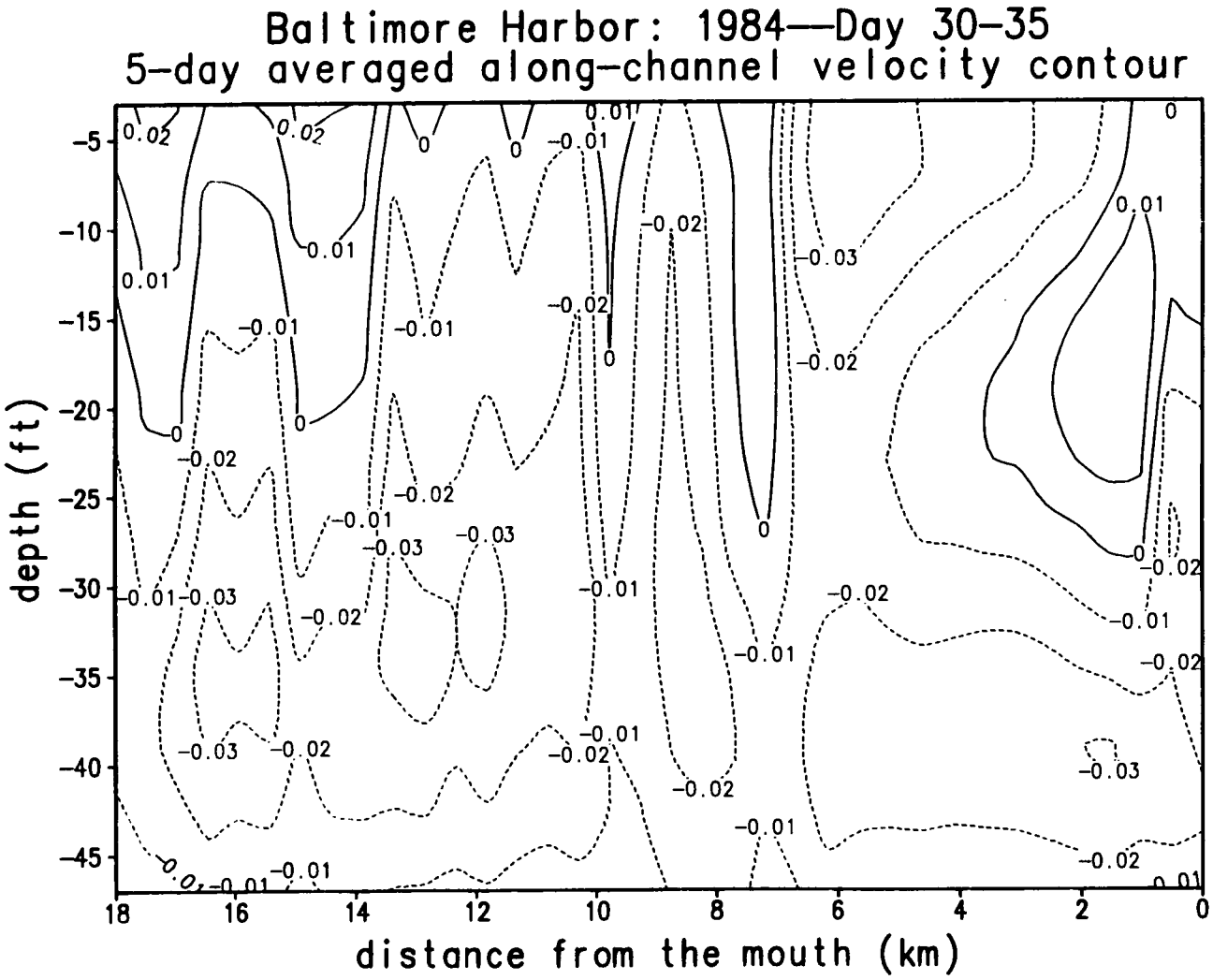

Figure 21(a). Contours of 5-day averaged longitudinal currents (m/s) on a longitudinal-vertical section following the main axis of the Harbor, days 30–35, 1985. Solid and dashed contours indicate outflows and inflows, respectively.

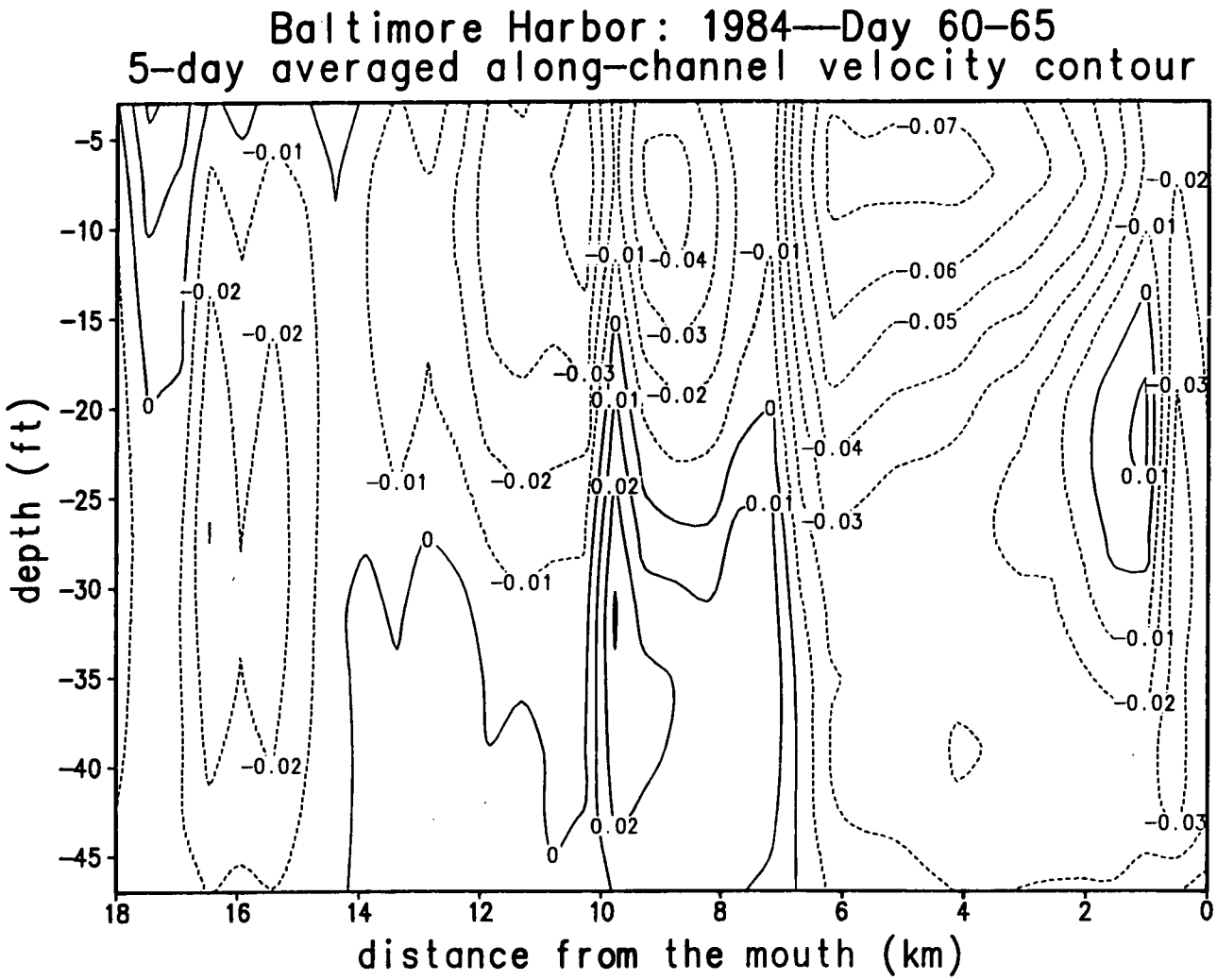

Figure 21(b). Contours of 5-day averaged longitudinal currents (m/s) on a longitudinal-vertical section following the main axis of the Harbor, days 60–65, 1985. Solid and dashed contours indicate outflows and inflows, respectively.

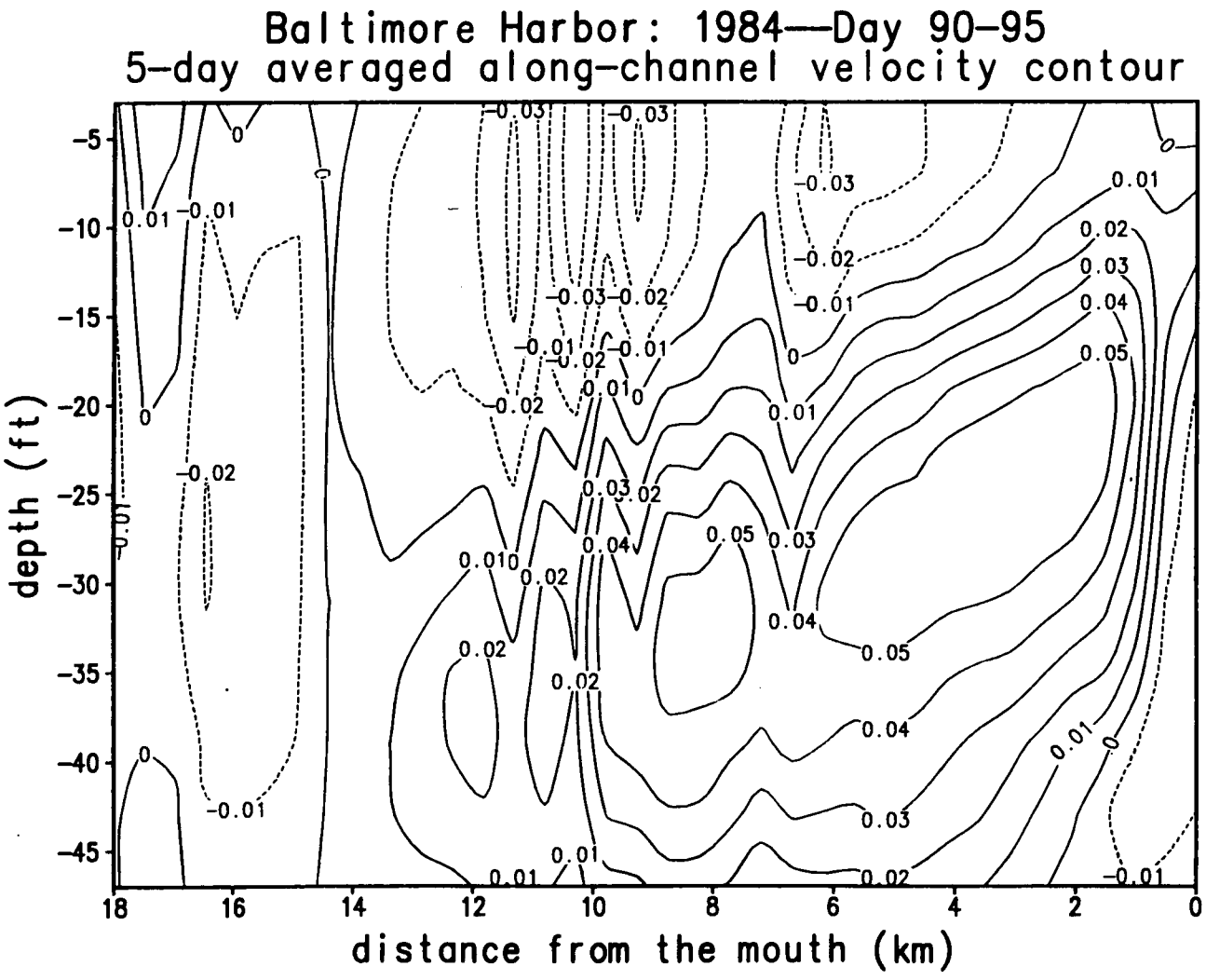

Figure 21(c). Contours of 5-day averaged longitudinal currents (m/s) on a longitudinal-vertical section following the main axis of the Harbor, days 90–95, 1985. Solid and dashed contours indicate outflows and inflows, respectively.

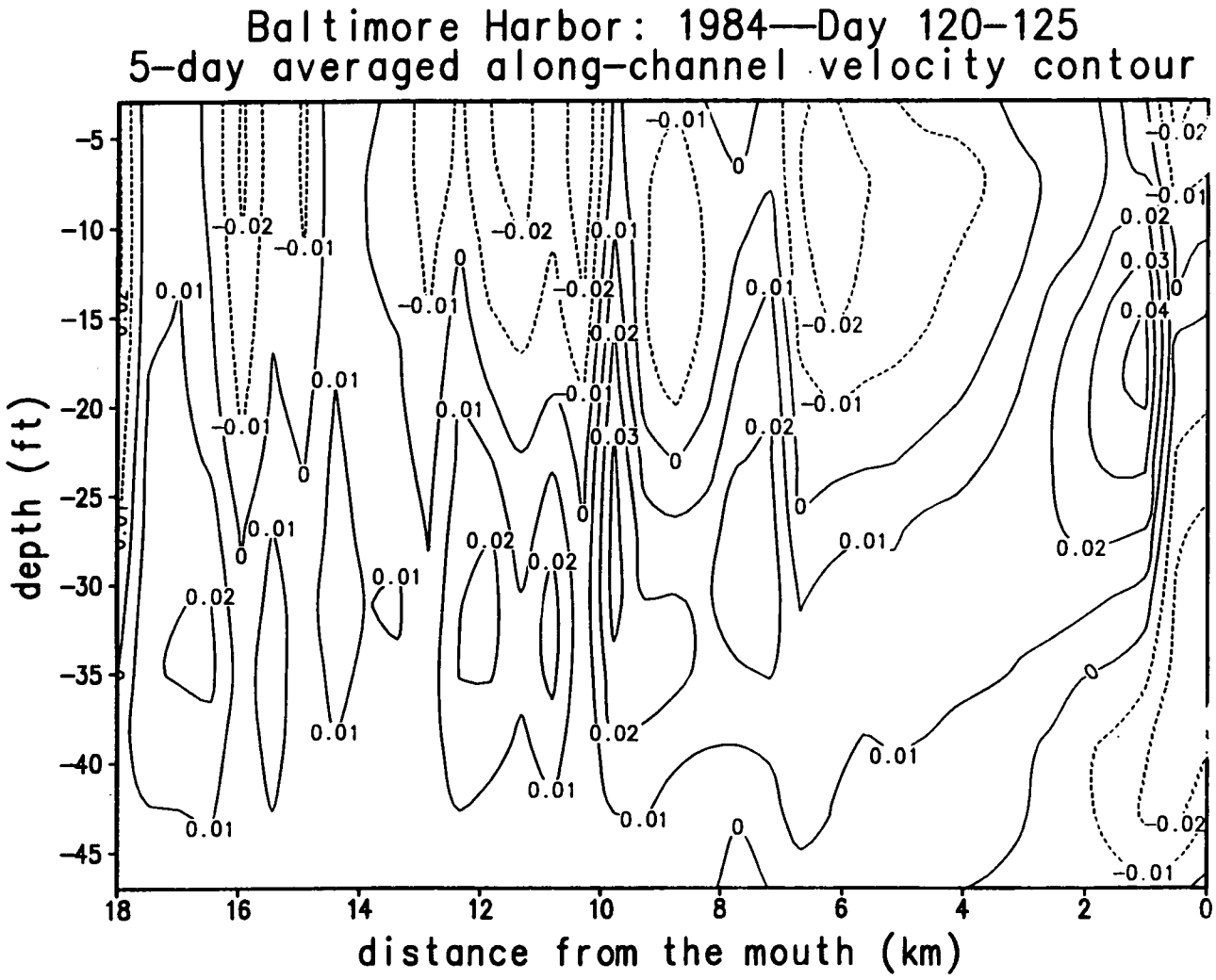

Figure 21(d). Contours of 5-day averaged longitudinal currents (m/s) on a longitudinal-vertical section following the main axis of the Harbor, days 120–125, 1985. Solid and dashed contours indicate outflows and inflows, respectively.

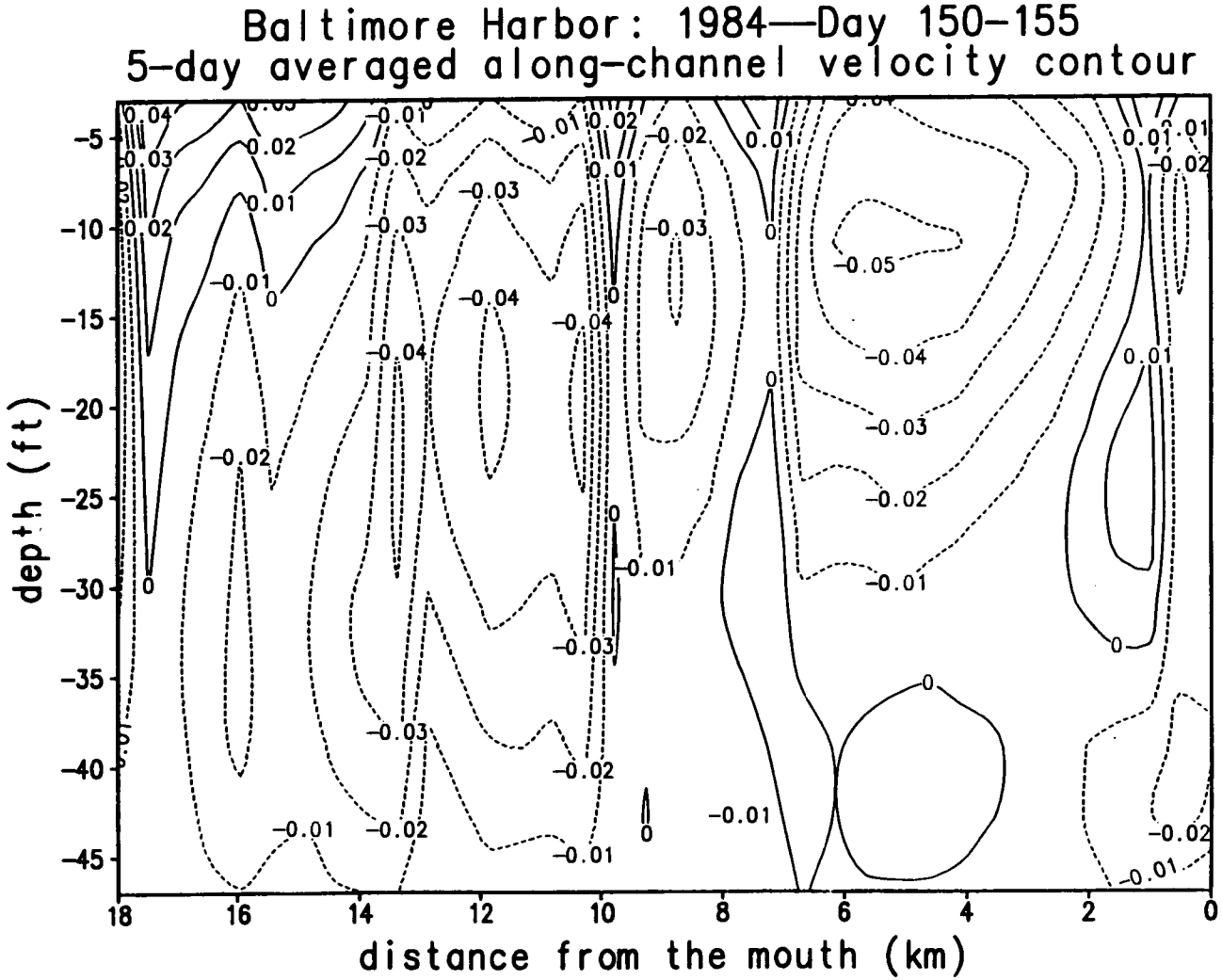

Figure 21(e). Contours of 5-day averaged longitudinal currents (m/s) on a longitudinal-vertical section following the main axis of the Harbor, days 150–155, 1985. Solid and dashed contours indicate outflows and inflows, respectively.

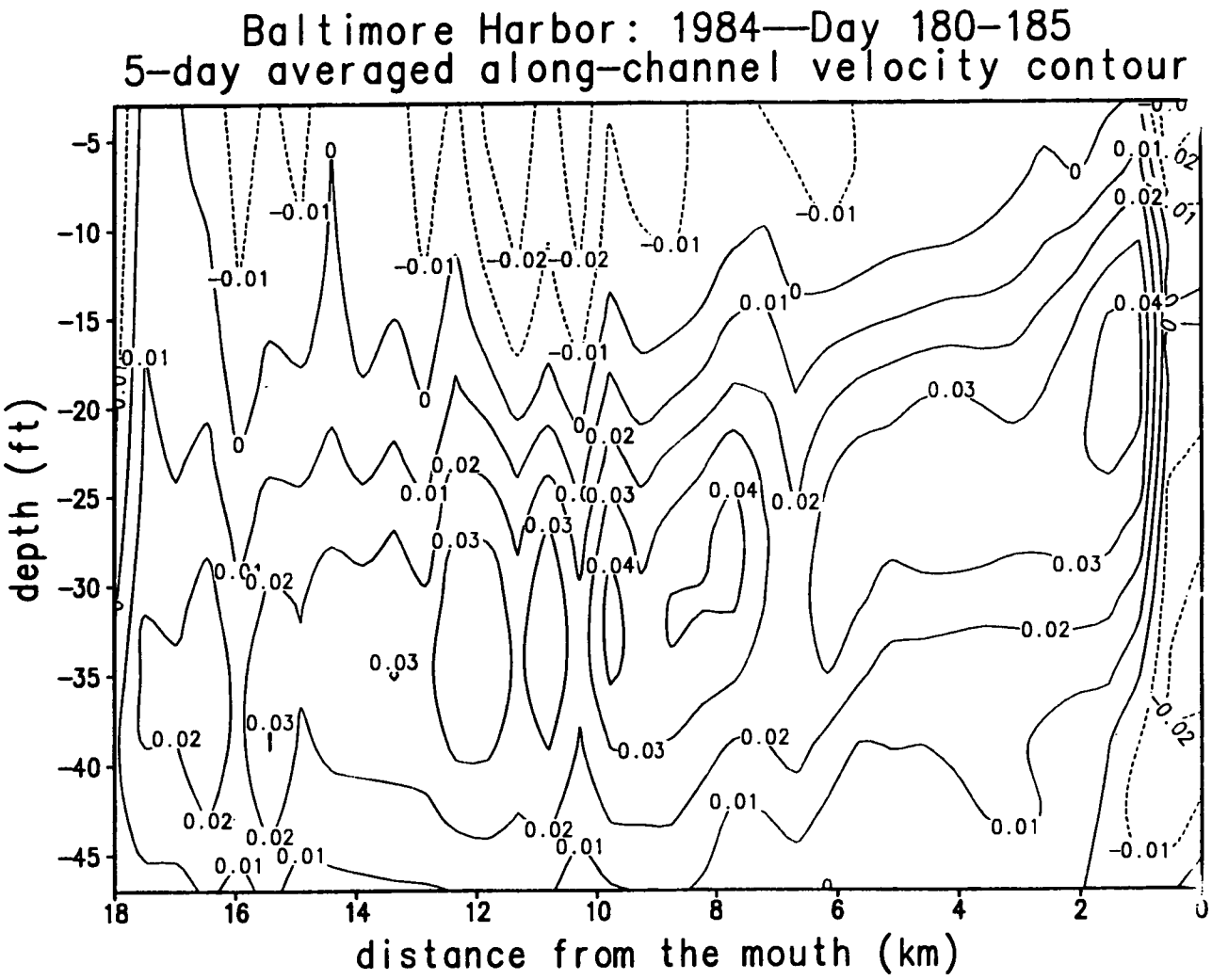

Figure 21(f). Contours of 5-day averaged longitudinal currents (m/s) on a longitudinal-vertical section following the main axis of the Harbor, days 180–185, 1985. Solid and dashed contours indicate outflows and inflows, respectively.

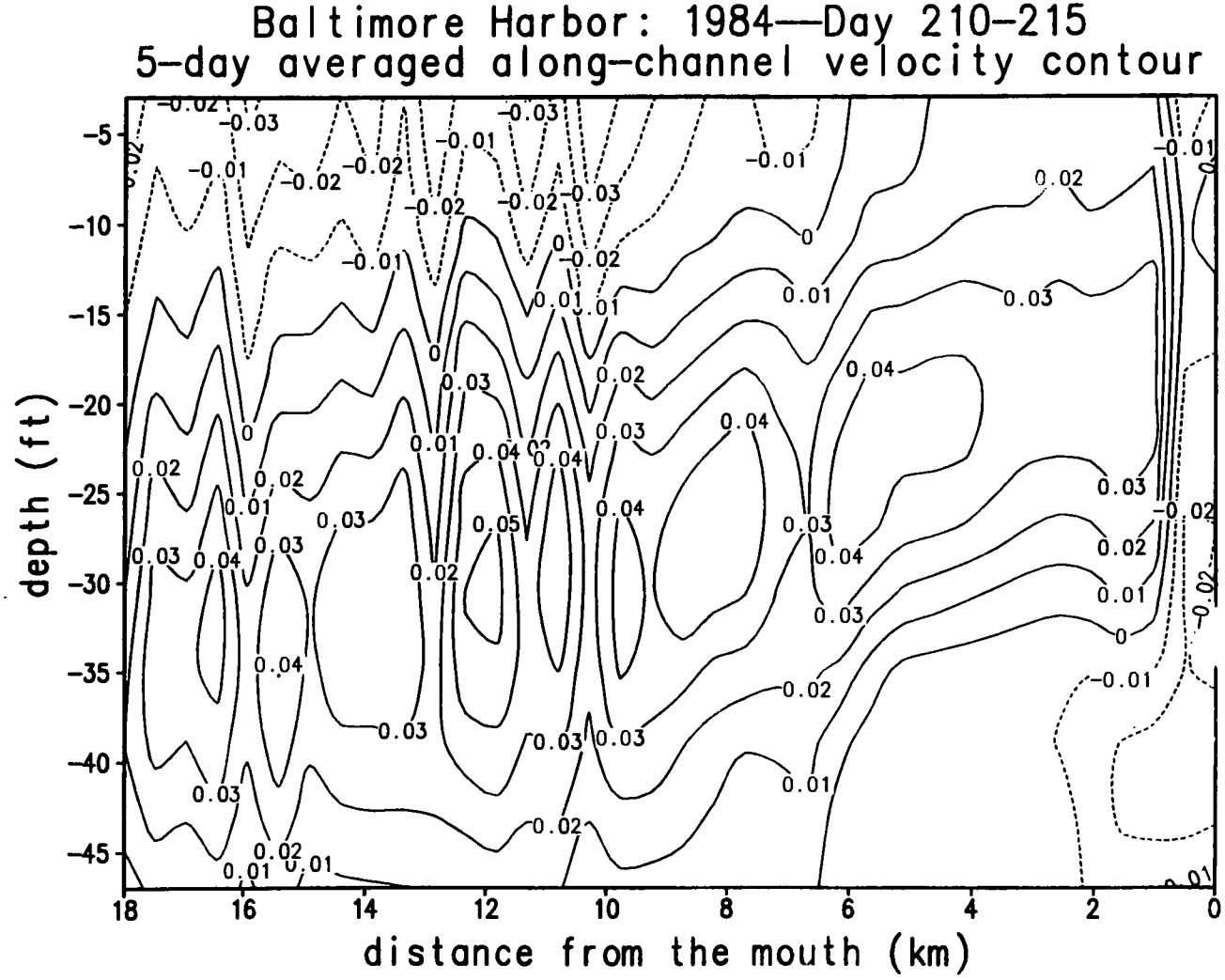

Figure 21(g). Contours of 5-day averaged longitudinal currents (m/s) on a longitudinal-vertical section following the main axis of the Harbor, days 210–215, 1985. Solid and dashed contours indicate outflows and inflows, respectively.

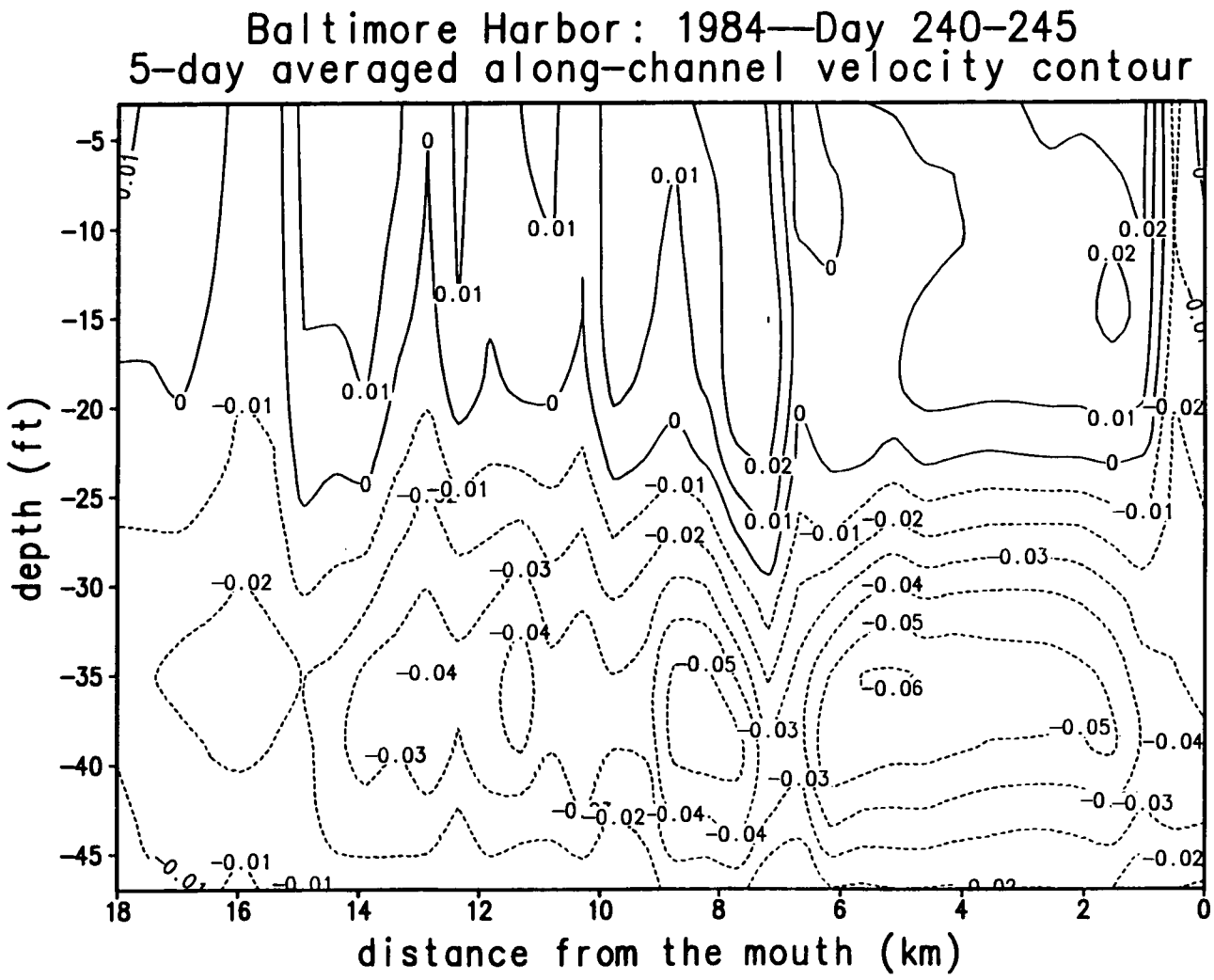

Figure 21(h). Contours of 5-day averaged longitudinal currents (m/s) on a longitudinal-vertical section following the main axis of the Harbor, days 240–245, 1985. Solid and dashed contours indicate outflows and inflows, respectively.

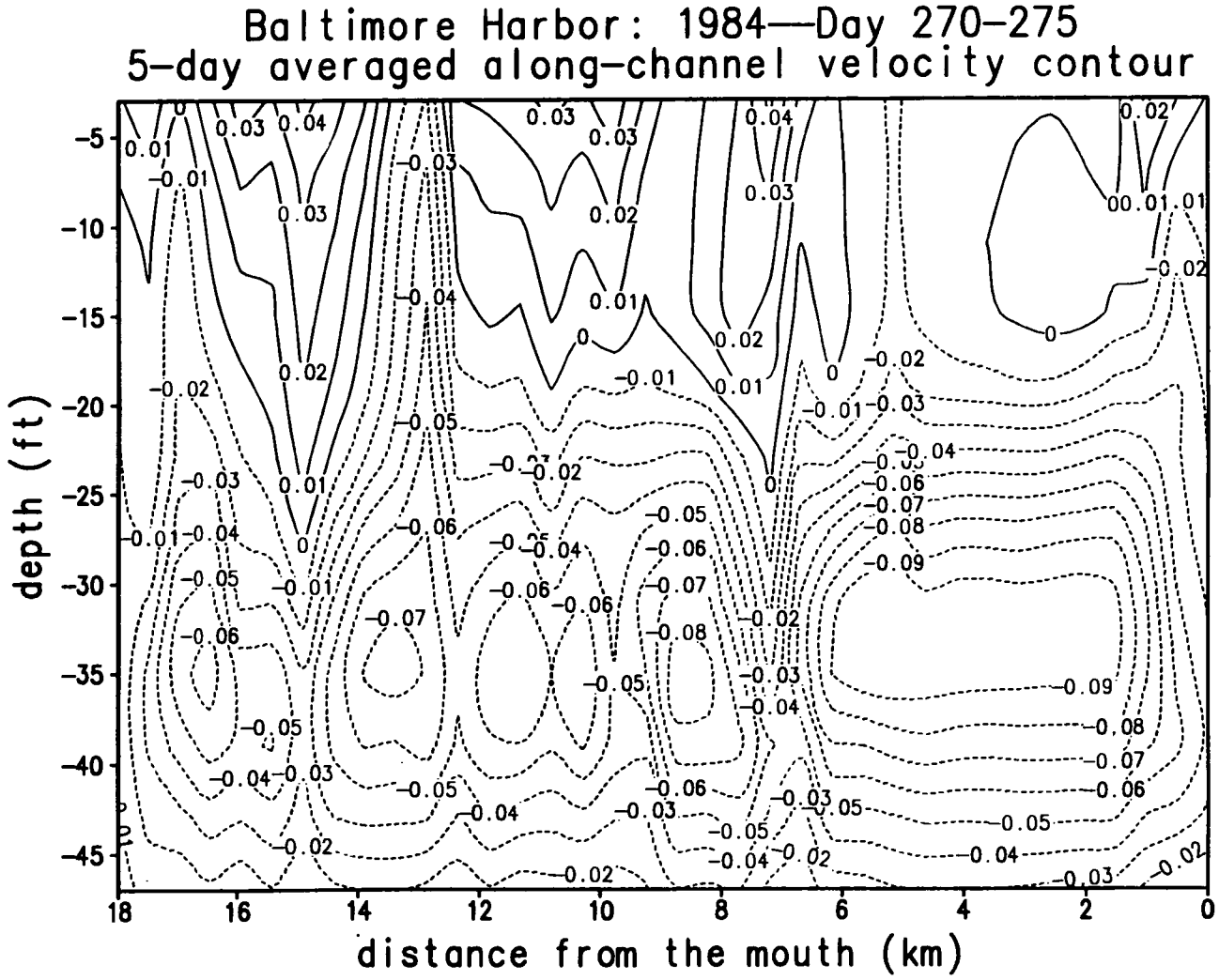

Figure 21(i). Contours of 5-day averaged longitudinal currents (m/s) on a longitudinal-vertical section following the main axis of the Harbor, days 270–275, 1985. Solid and dashed contours indicate outflows and inflows, respectively.

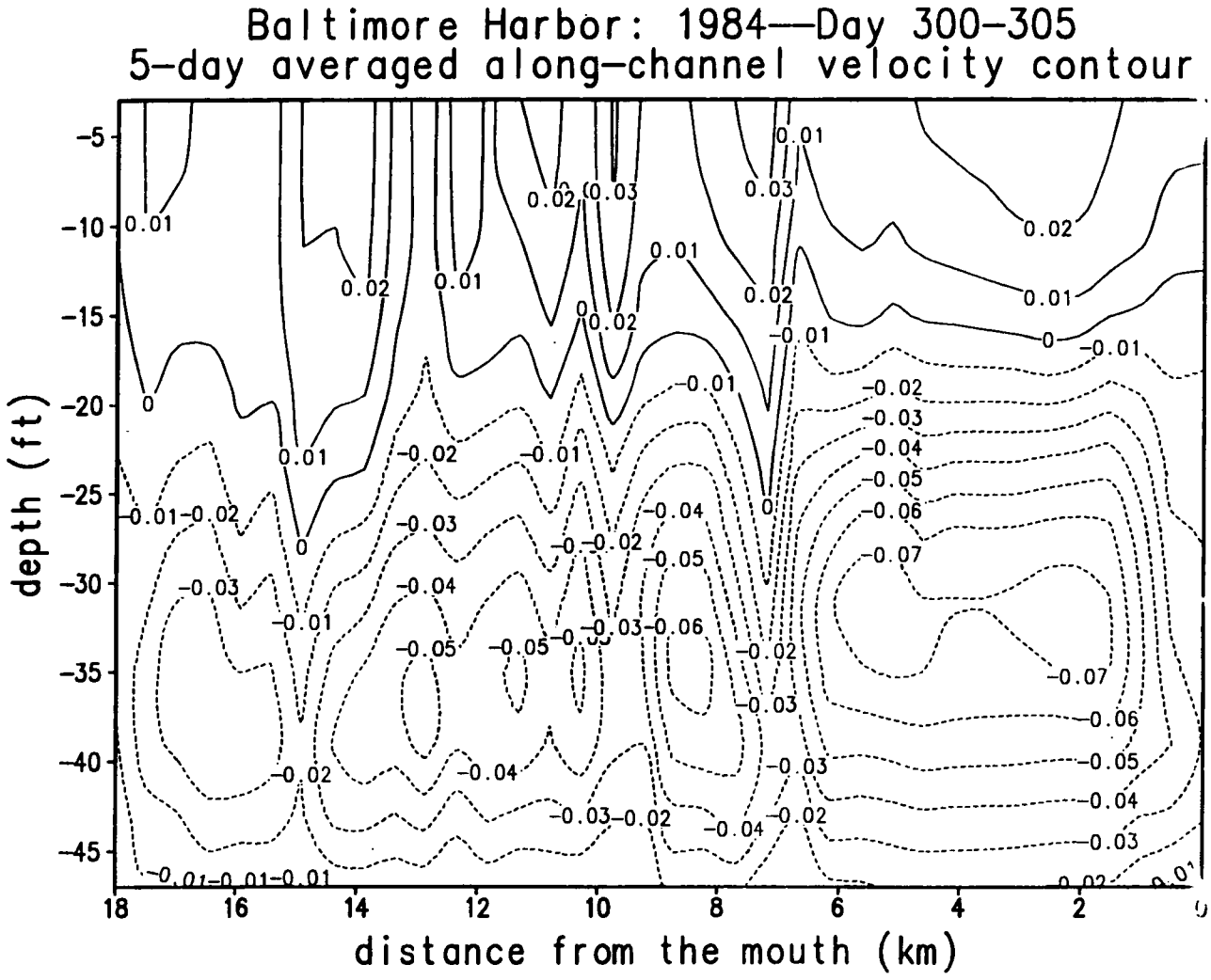

Figure 21(j). Contours of 5-day averaged longitudinal currents (m/s) on a longitudinal-vertical section following the main axis of the Harbor, days 300–305, 1985. Solid and dashed contours indicate outflows and inflows, respectively.

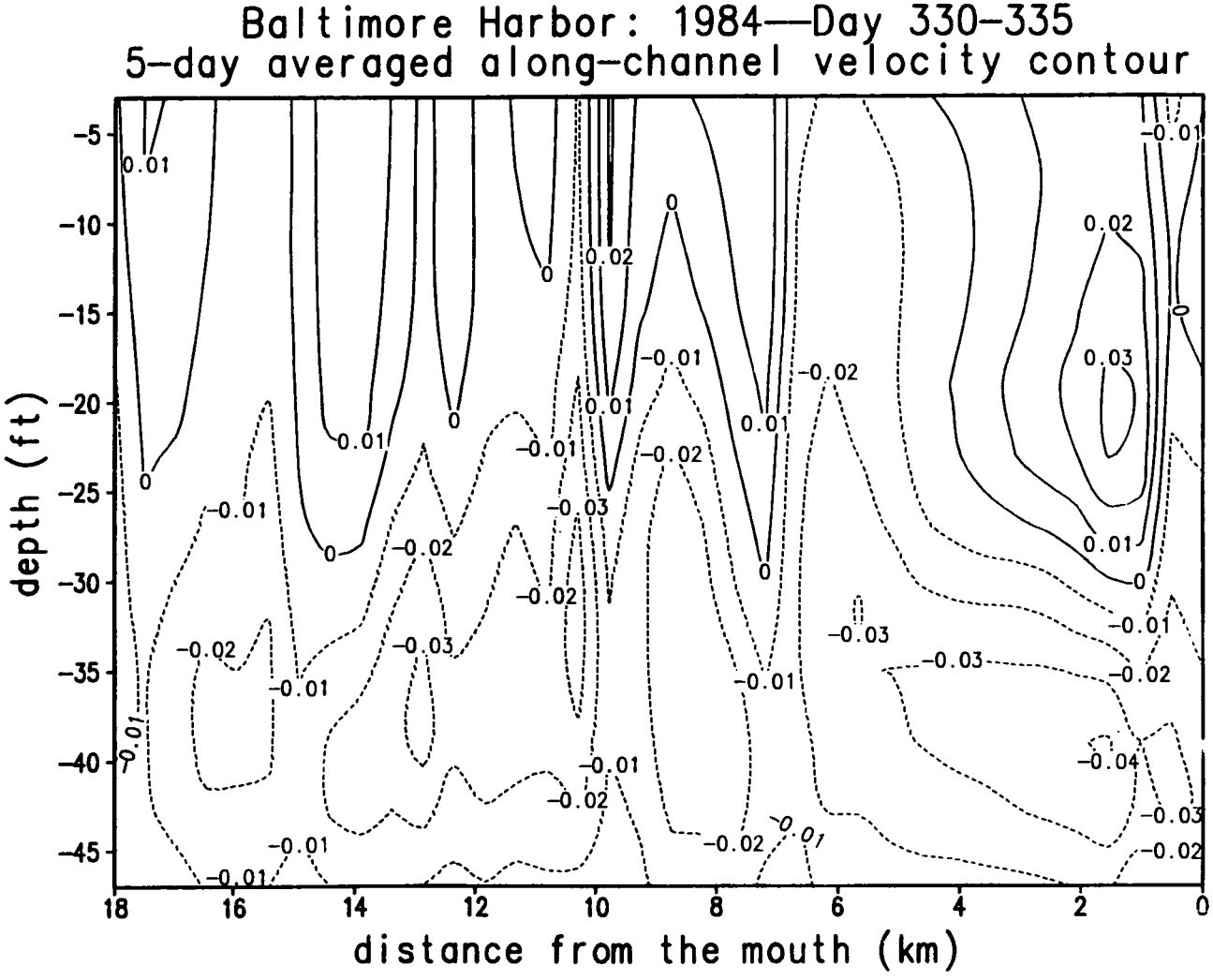

Figure 21(k). Contours of 5-day averaged longitudinal currents (m/s) on a longitudinal-vertical section following the main axis of the Harbor, days 330–335, 1985. Solid and dashed contours indicate outflows and inflows, respectively.

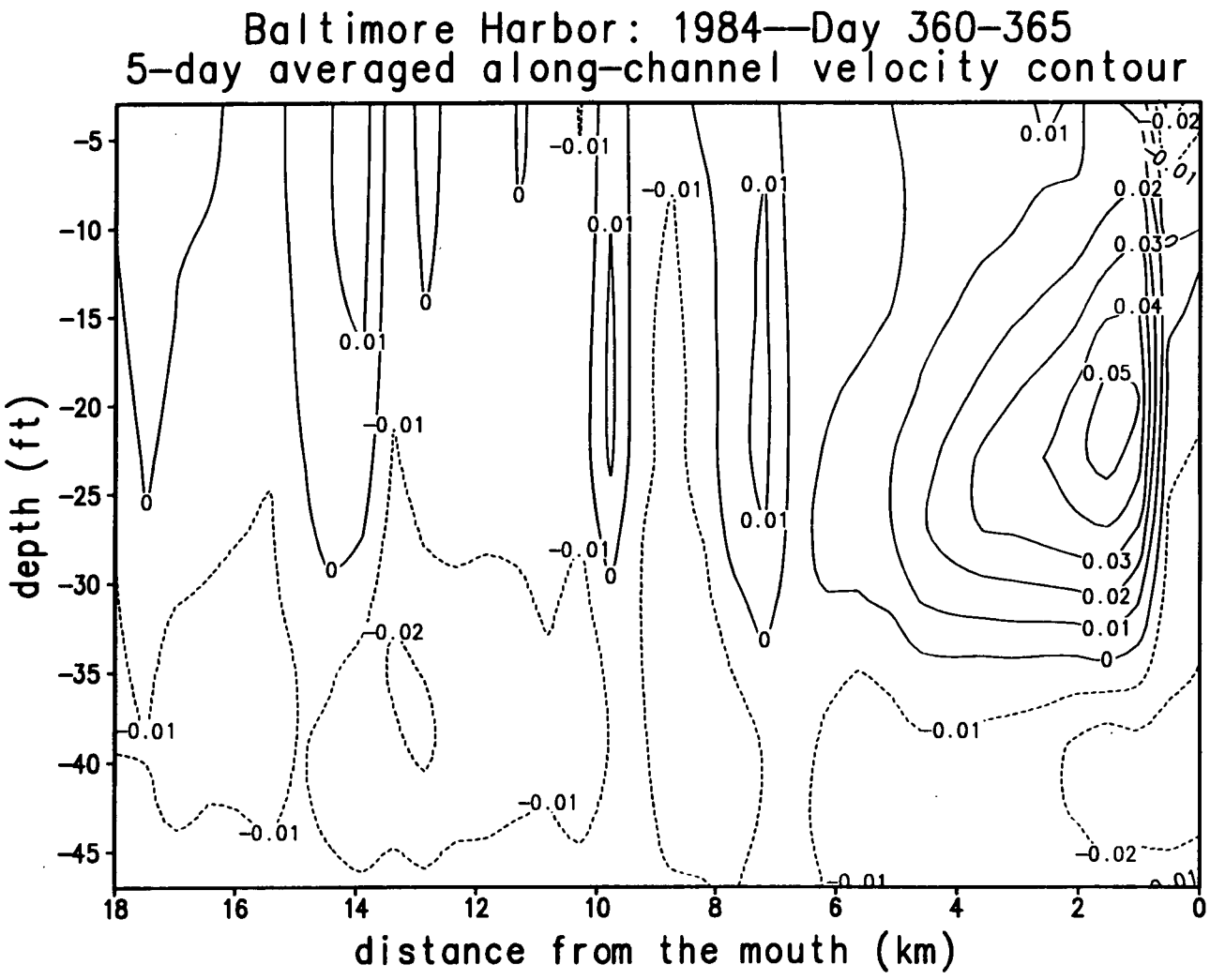

Figure 21(l). Contours of 5-day averaged longitudinal currents (m/s) on a longitudinal-vertical section following the main axis of the Harbor, days 360–365, 1985. Solid and dashed contours indicate outflows and inflows, respectively.

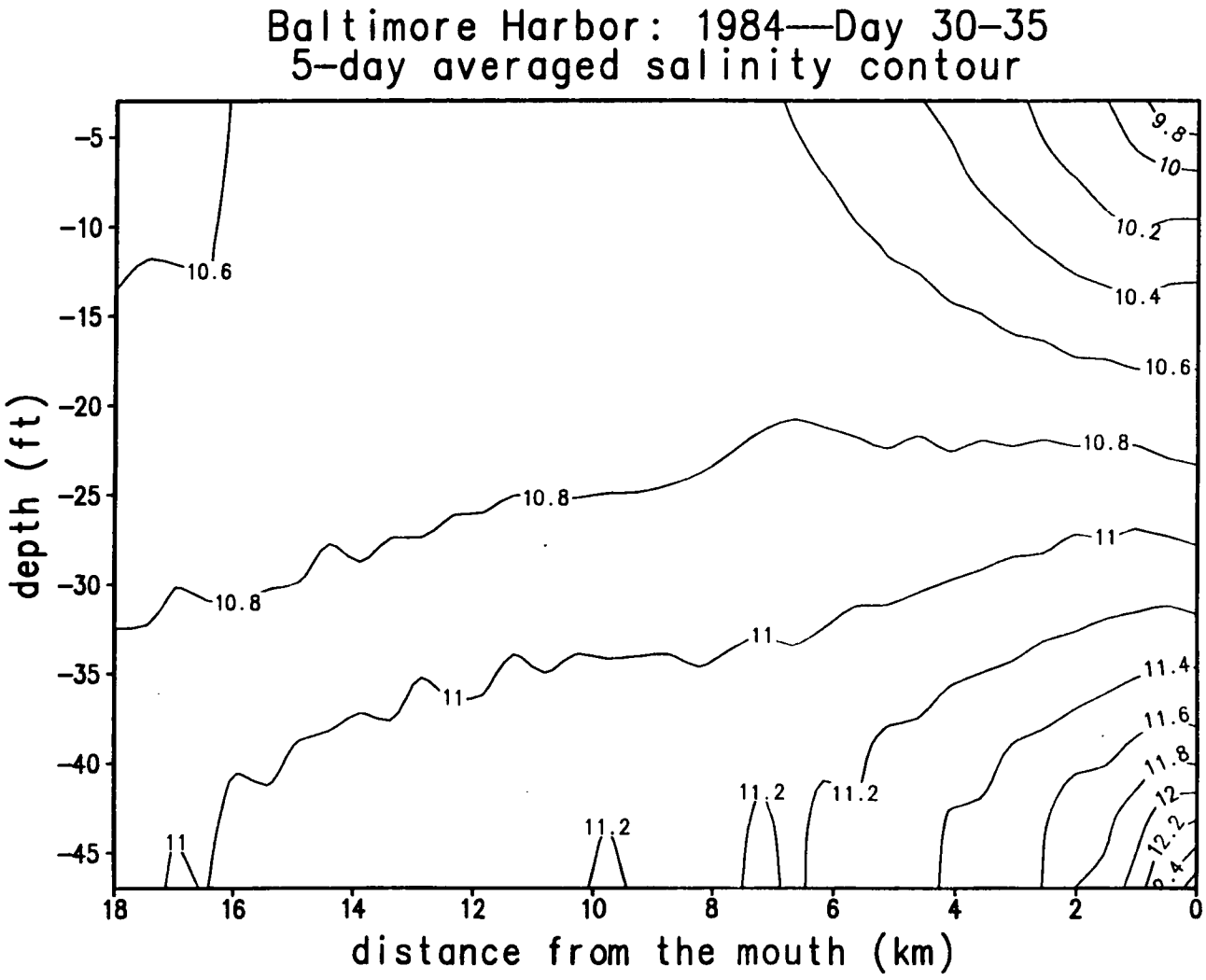

Figure 22(a). Longitudinal salinity (psu) distribution after 5-day averaging along the axis of Baltimore Harbor, days 30–35, 1984.

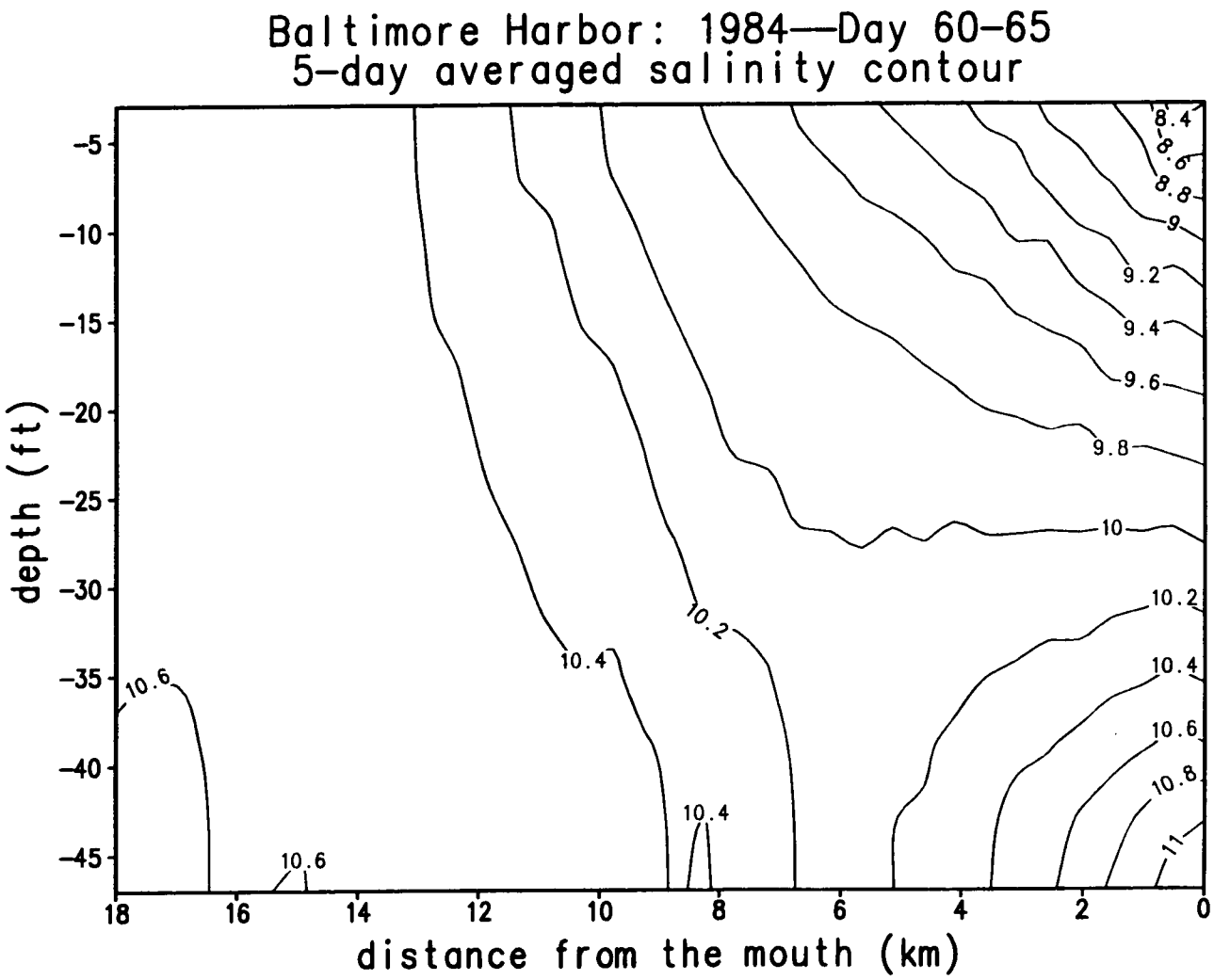

Figure 22(b). Longitudinal salinity (psu) distribution after 5-day averaging along the axis of Baltimore Harbor, days 60–65, 1984.

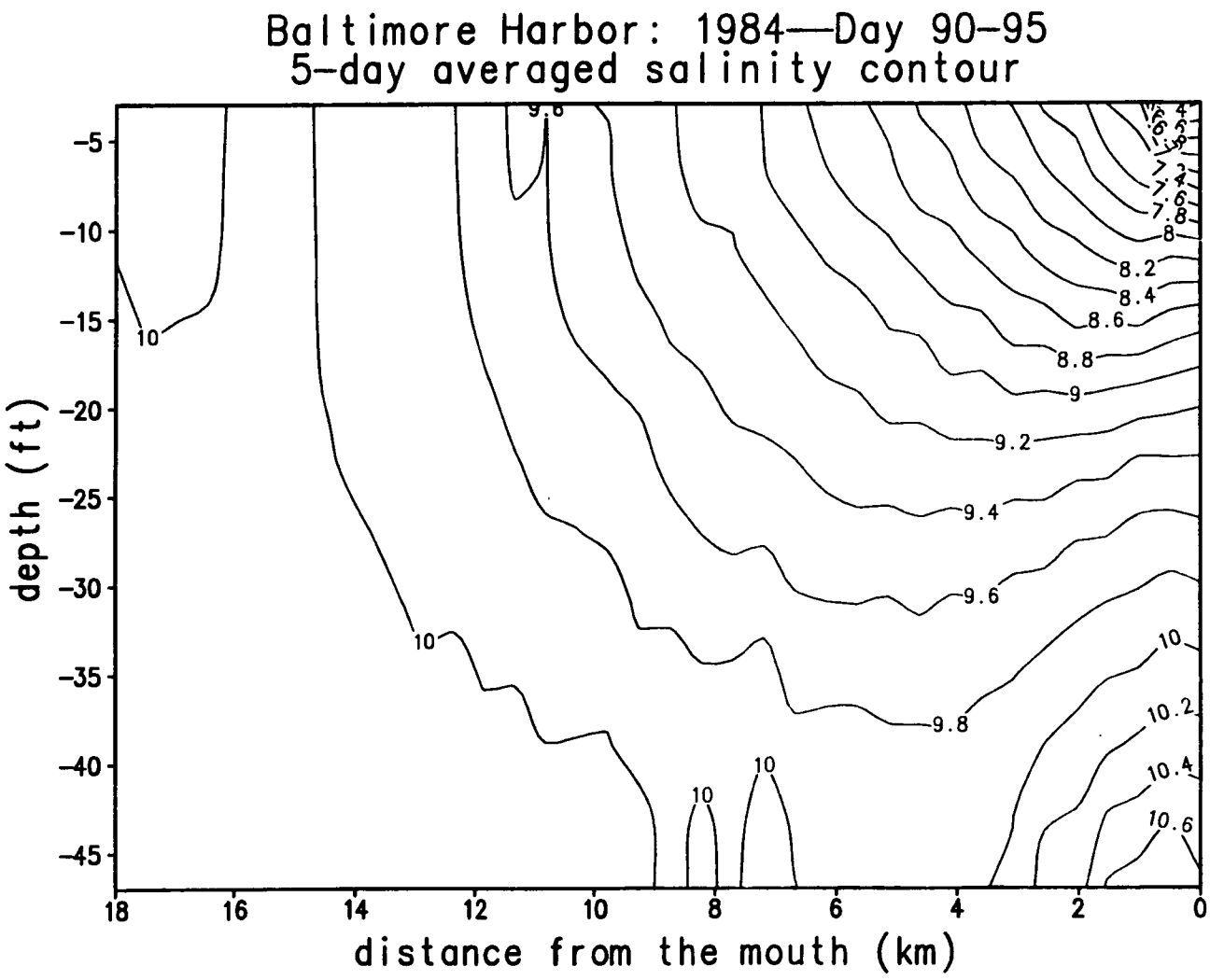

Figure 22(c). Longitudinal salinity (psu) distribution after 5-day averaging along the axis of Baltimore Harbor, days 90–95, 1984.

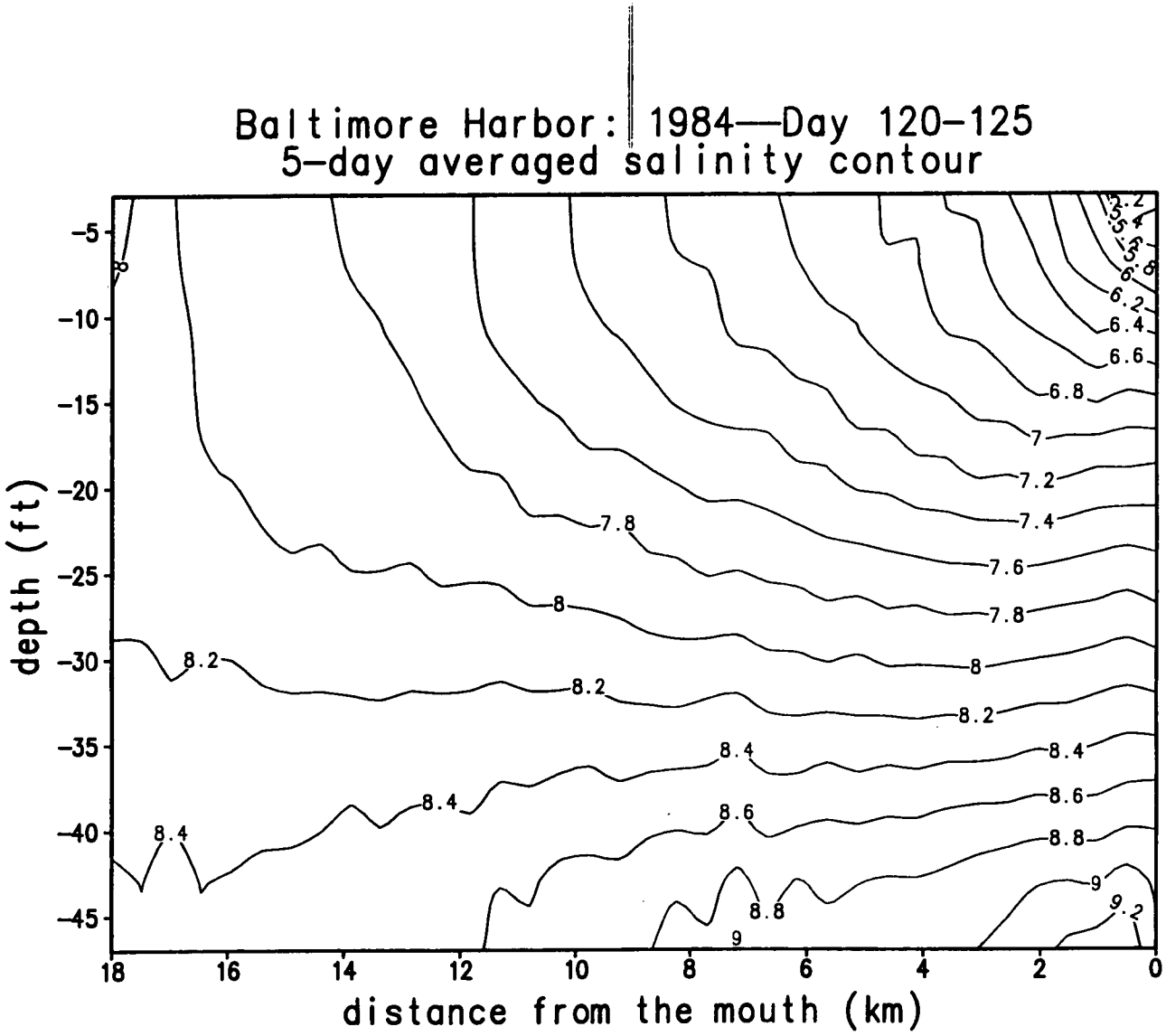

Figure 22(d). Longitudinal salinity (psu) distribution after 5-day averaging along the axis of Baltimore Harbor, days 120–125, 1984.

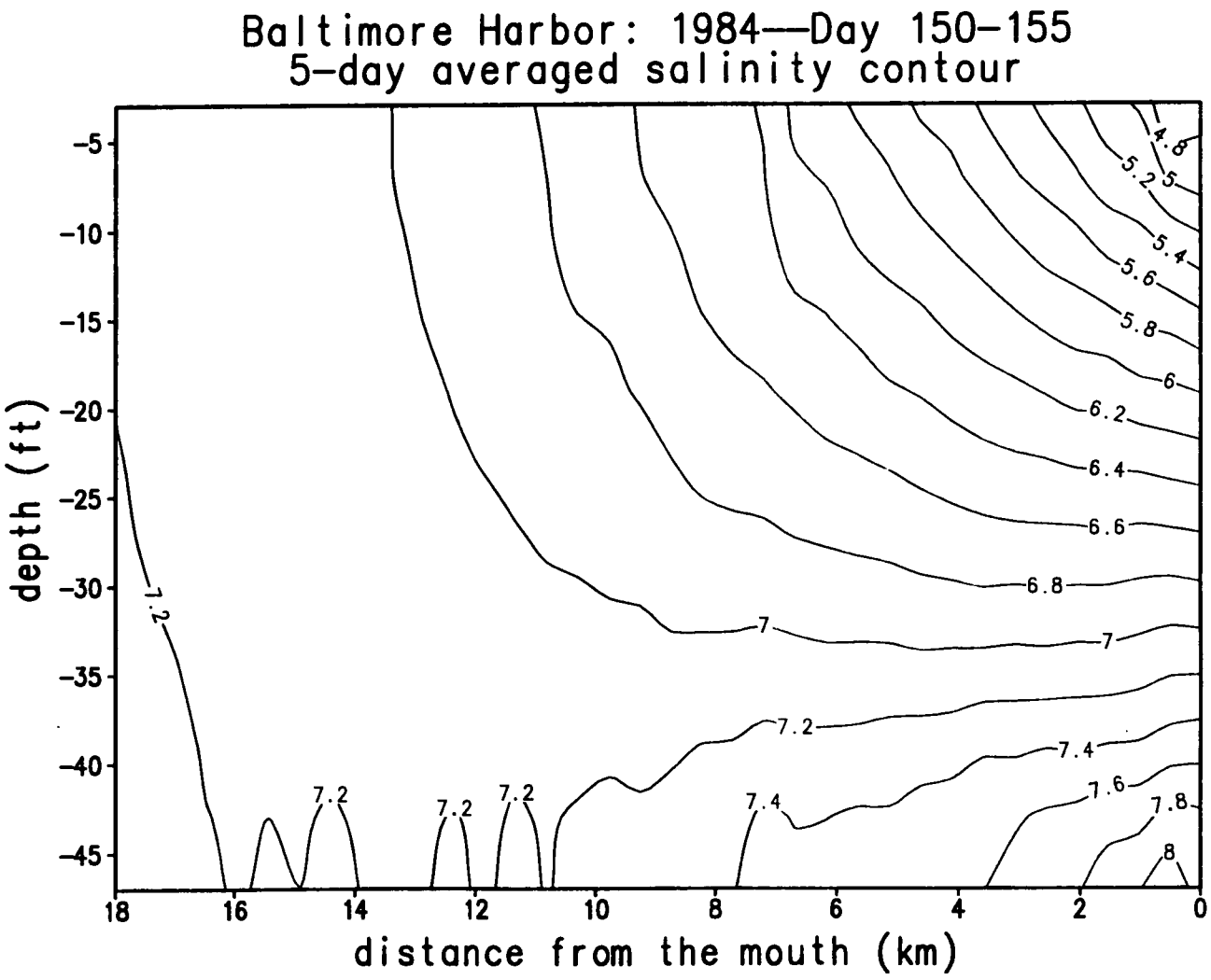

Figure 22(e). Longitudinal salinity (psu) distribution after 5-day averaging along the axis of Baltimore Harbor, days 150–155, 1984.

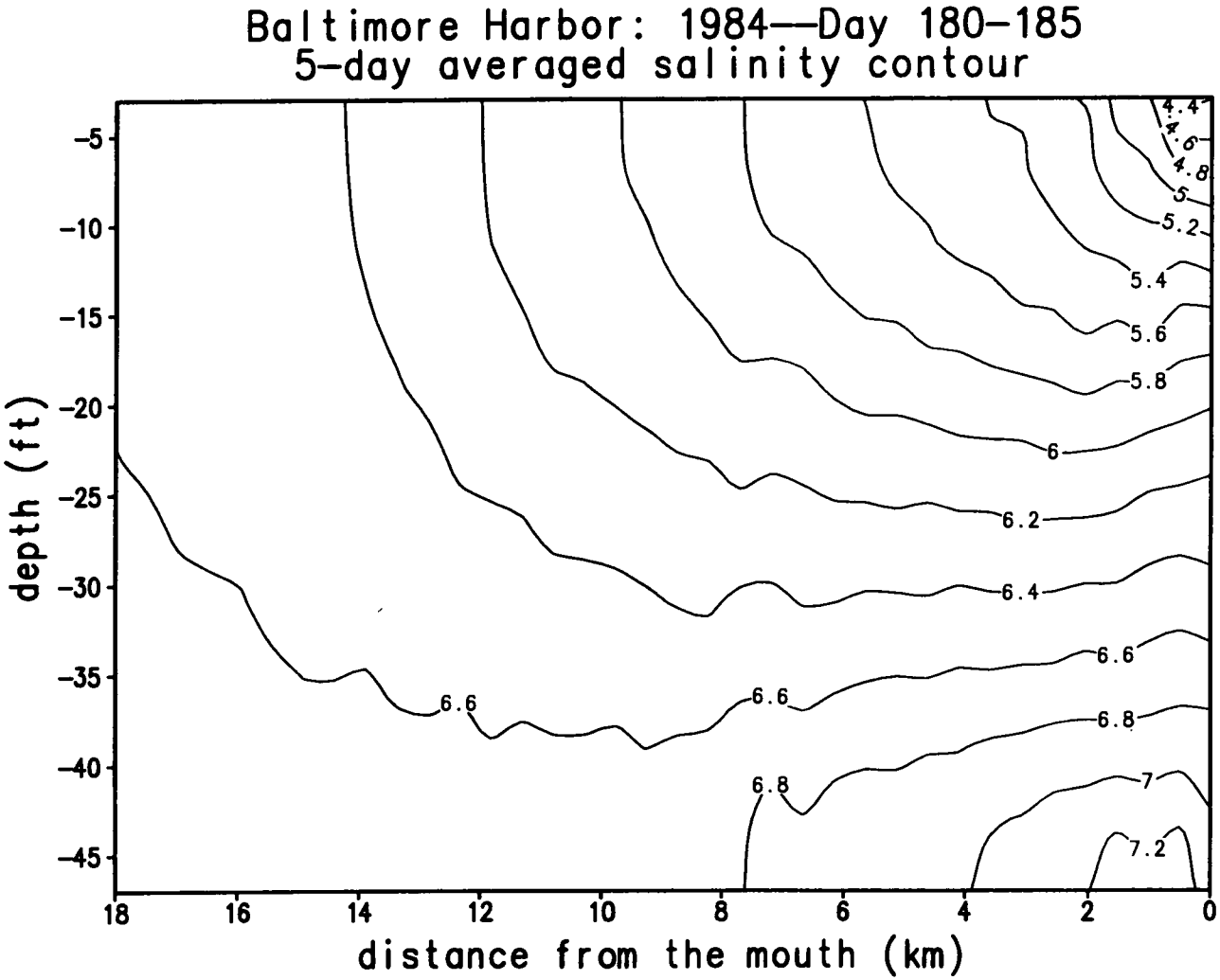

Figure 22(f). Longitudinal salinity (psu) distribution after 5-day averaging along the axis of Baltimore Harbor, days 180–185, 1984.

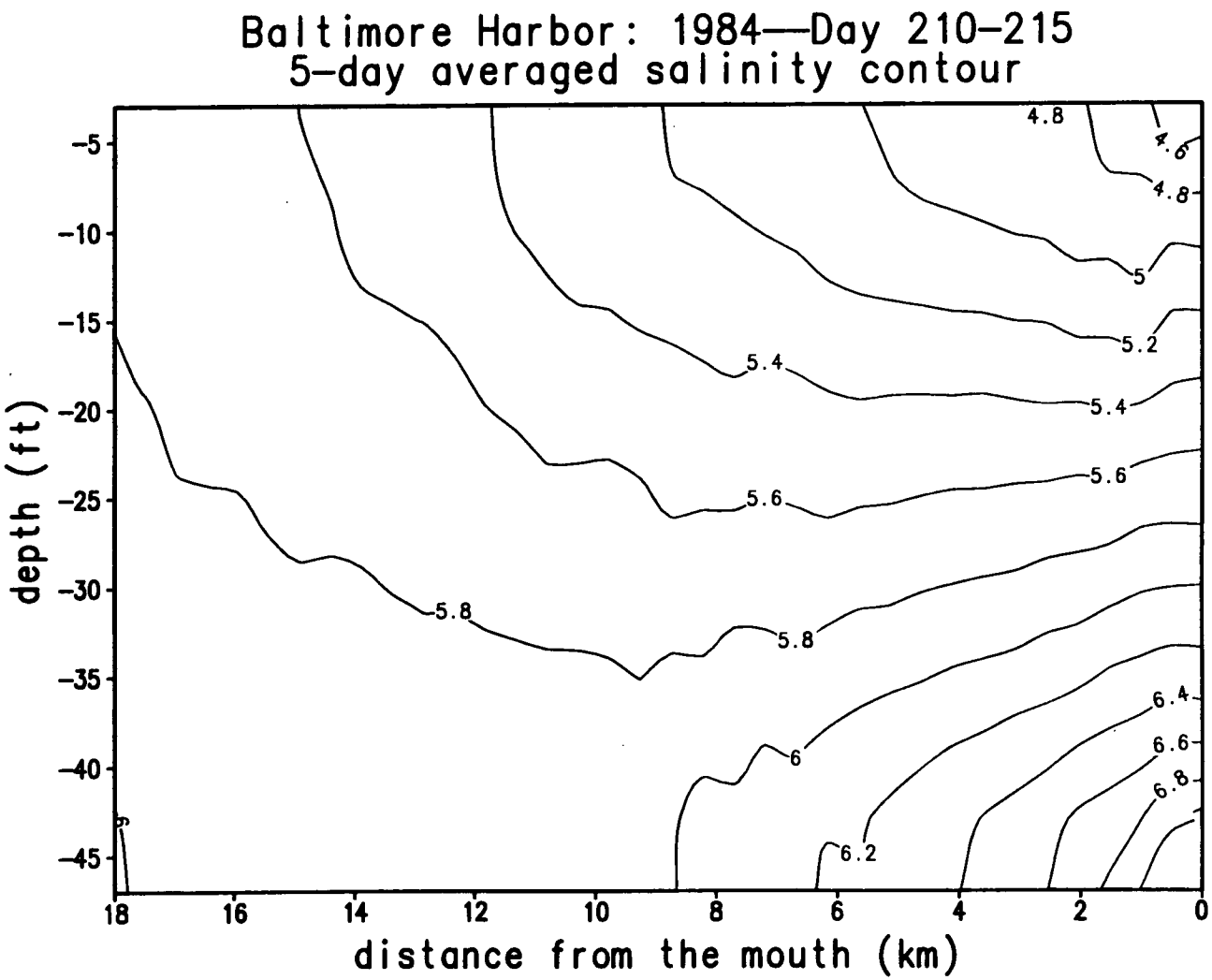

Figure 22(g). Longitudinal salinity (psu) distribution after 5-day averaging along the axis of Baltimore Harbor, days 210–215, 1984.

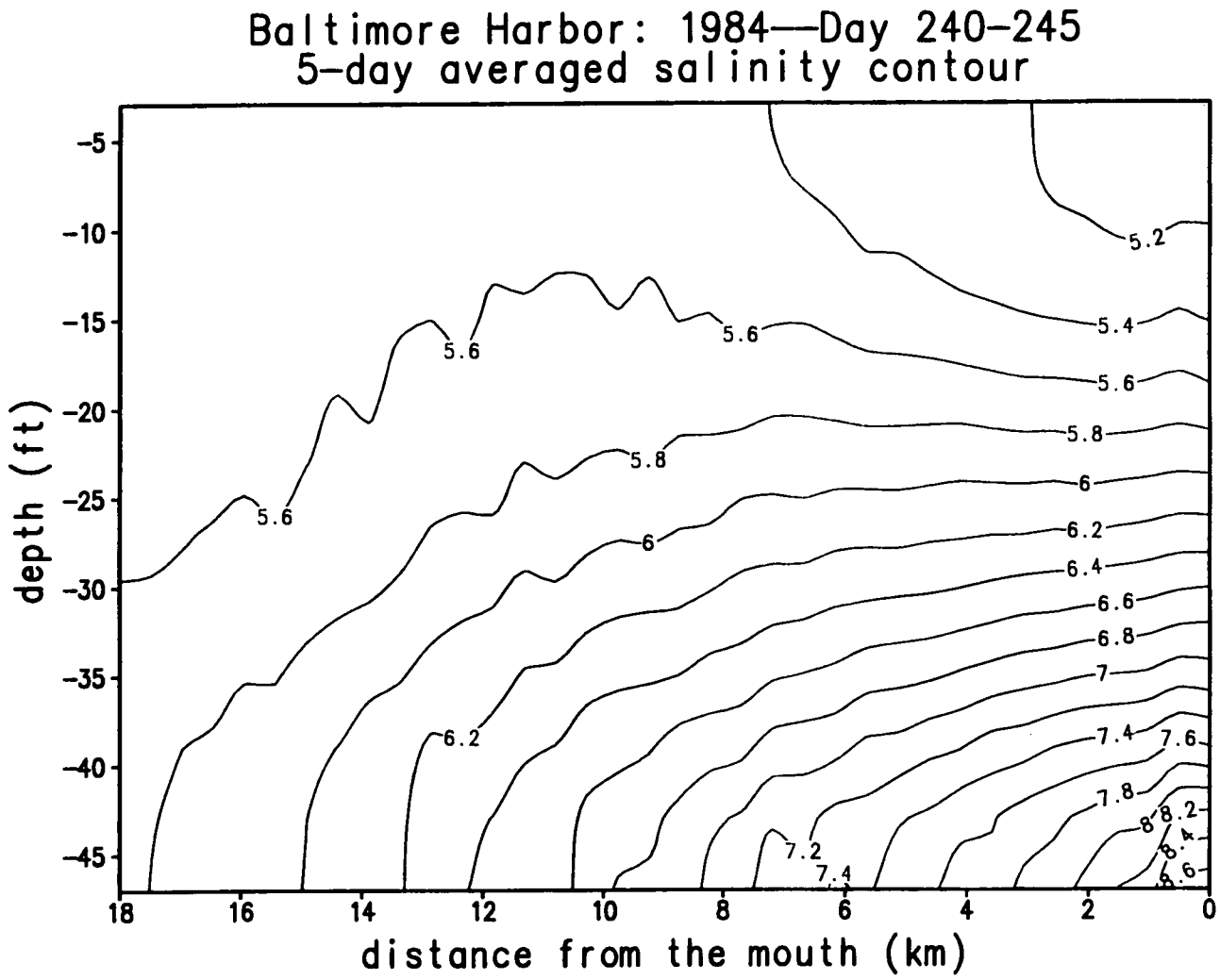

Figure 22(h). Longitudinal salinity (psu) distribution after 5-day averaging along the axis of Baltimore Harbor, days 240–245, 1984.

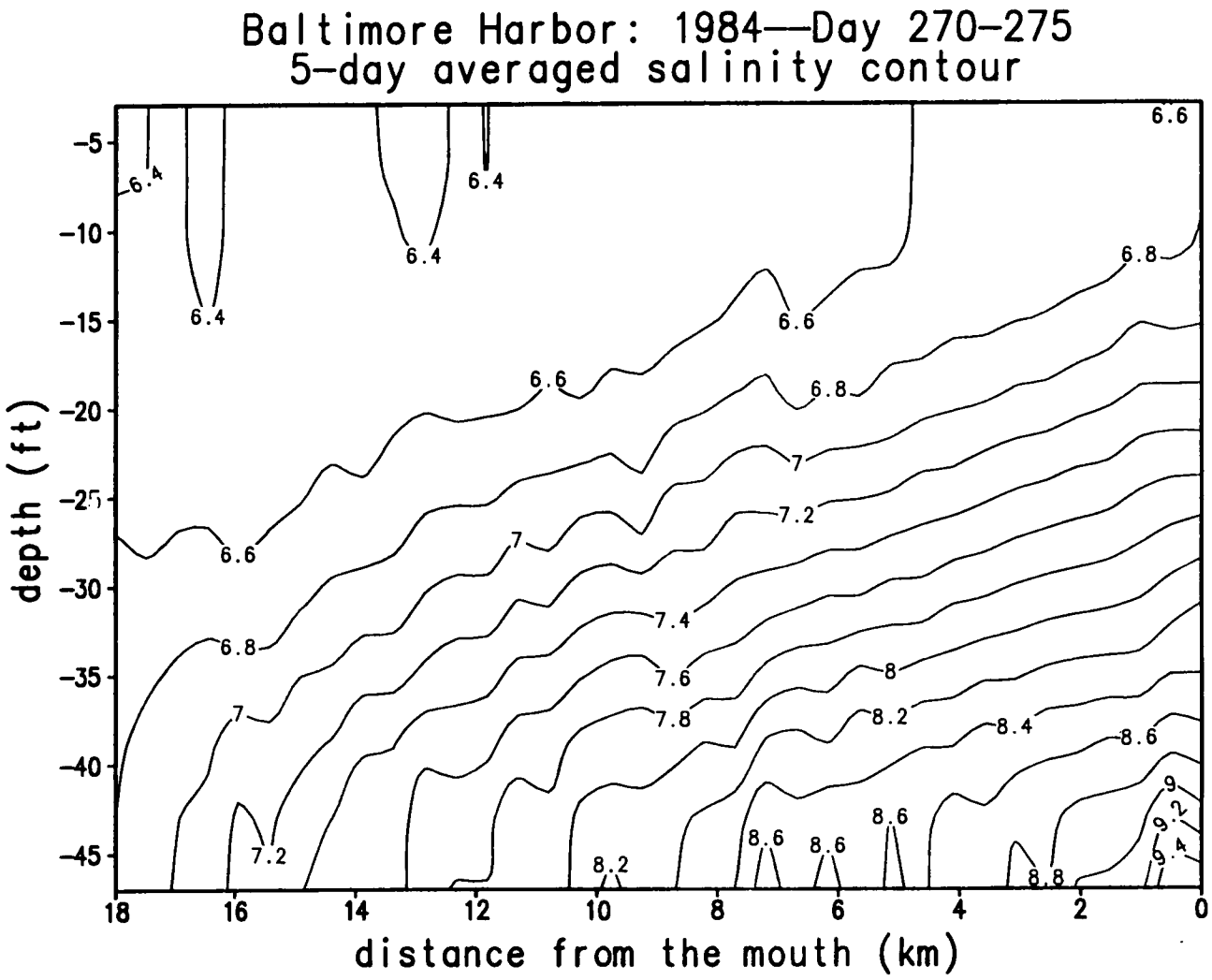

Figure 22(i). Longitudinal salinity (psu) distribution after 5-day averaging along the axis of Baltimore Harbor, days 270–275, 1984.

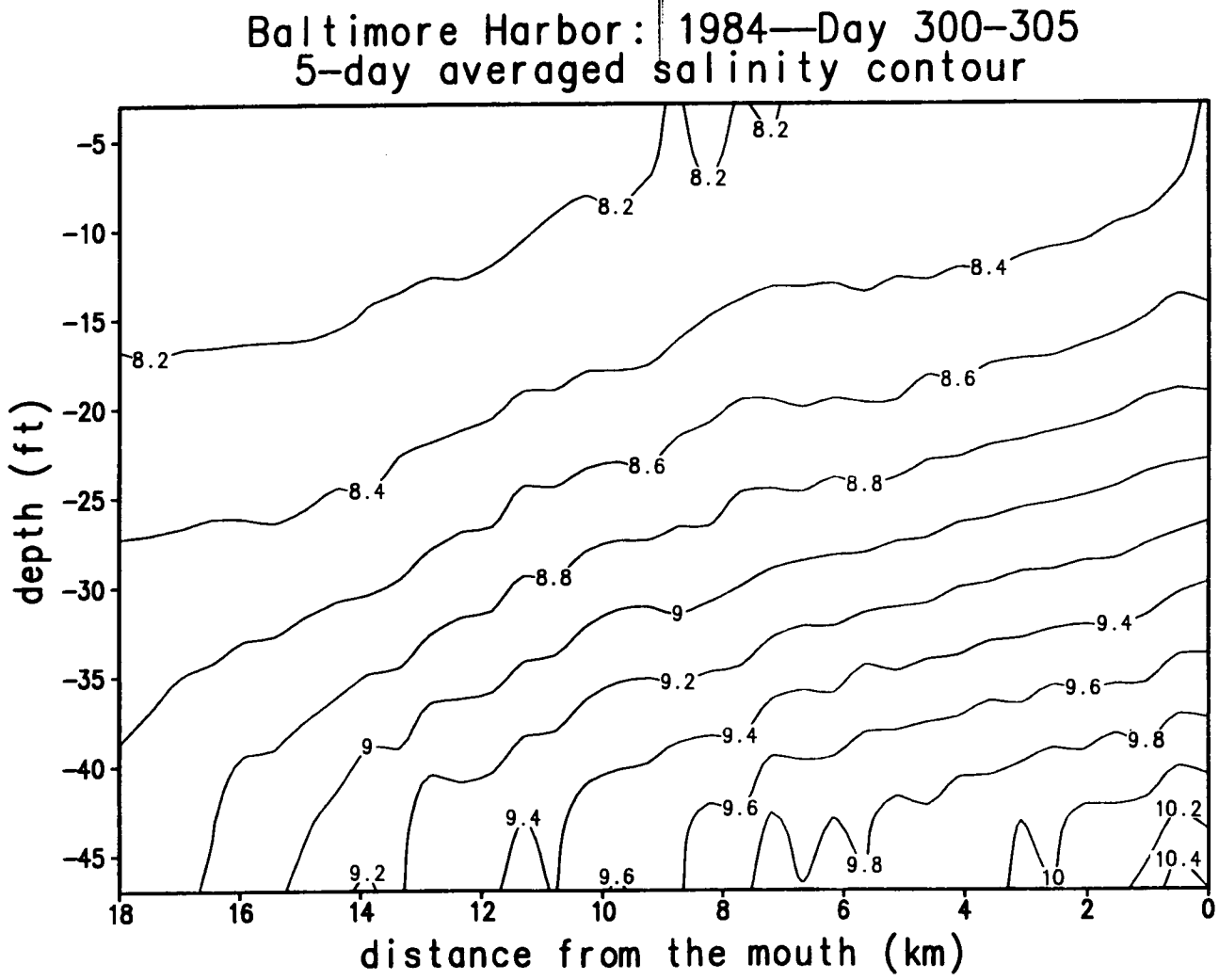

Figure 22(j). Longitudinal salinity (psu) distribution after 5-day averaging along the axis of Baltimore Harbor, days 300–305, 1984.

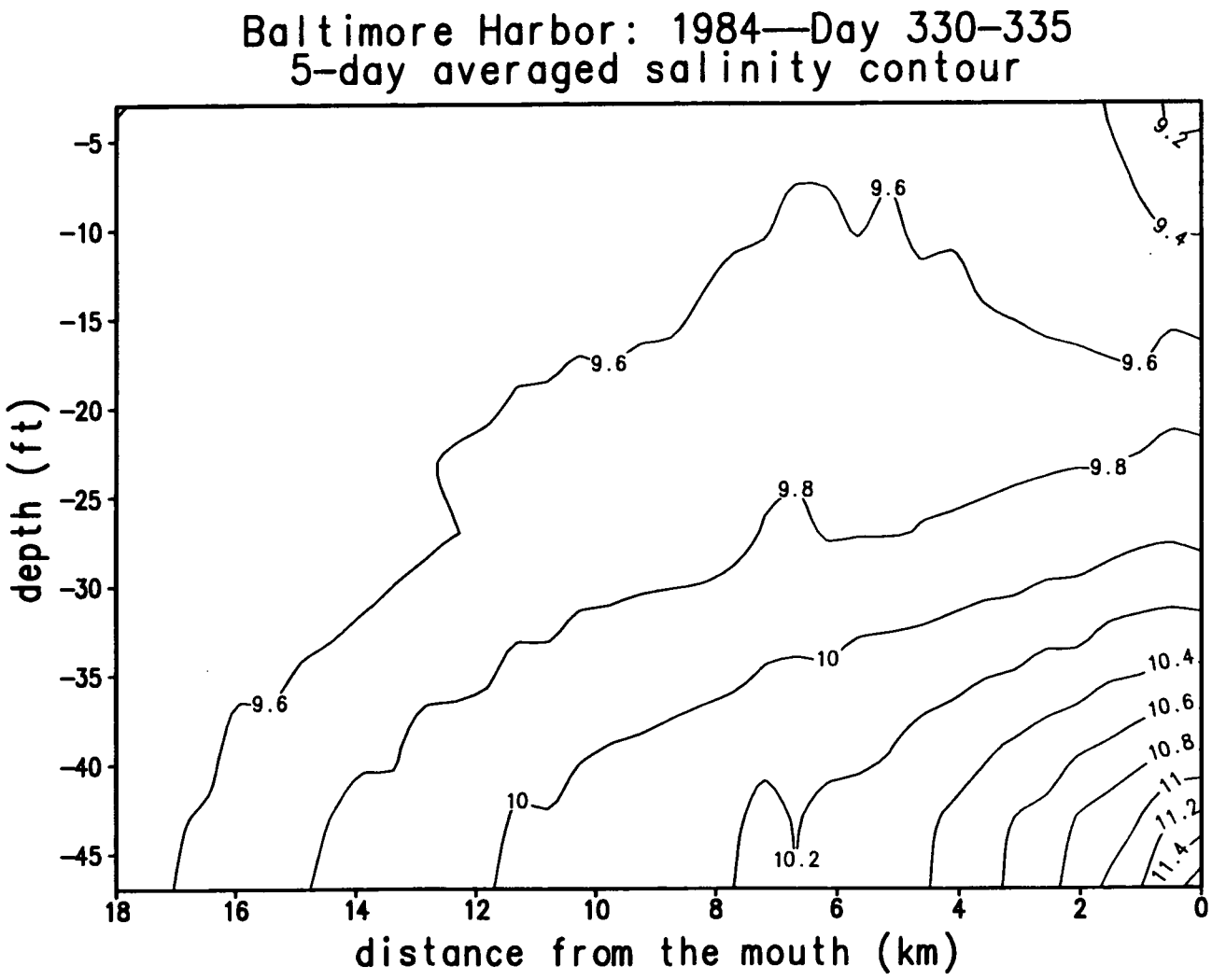

Figure 22(k). Longitudinal salinity (psu) distribution after 5-day averaging along the axis of Baltimore Harbor, days 330–335, 1984.

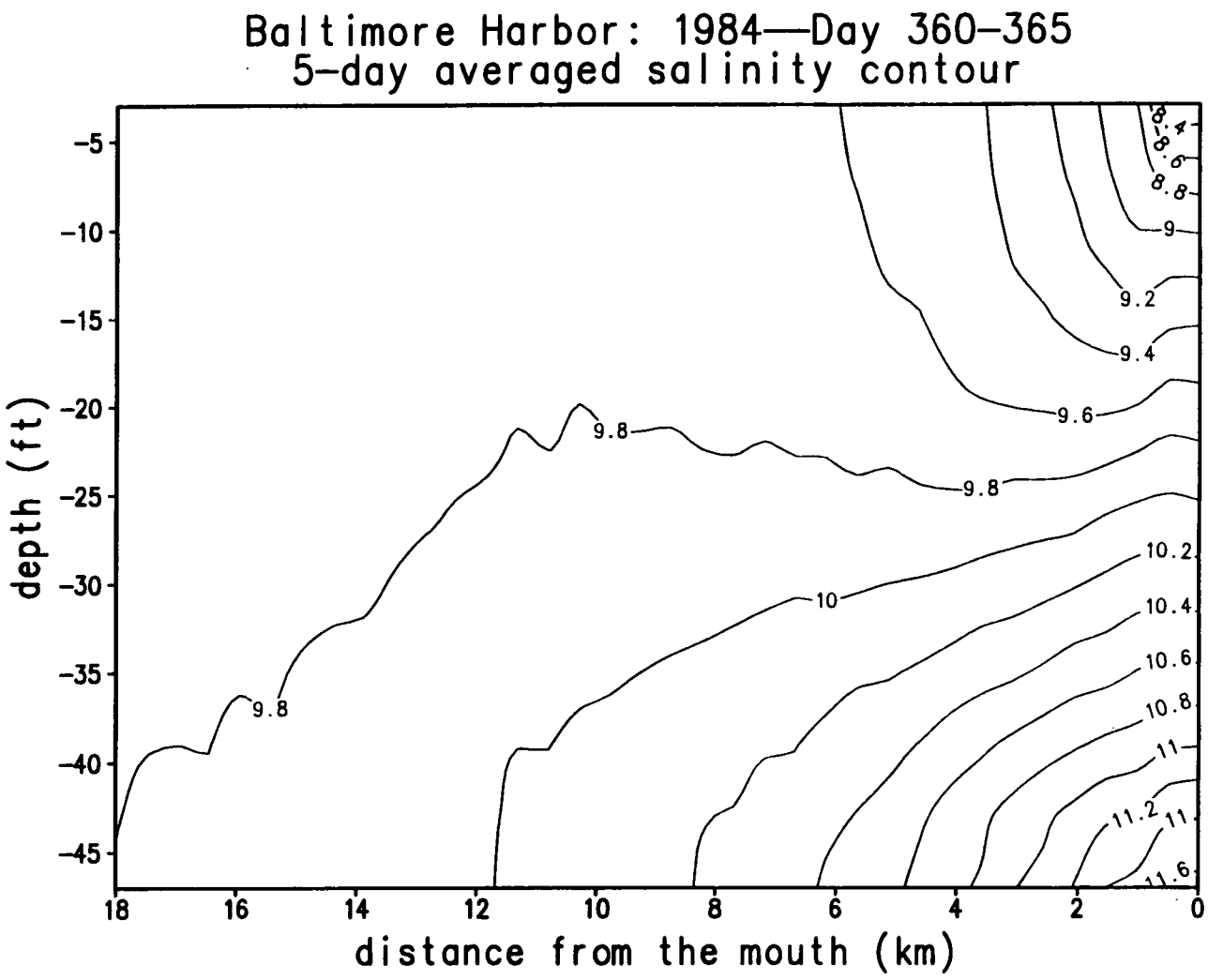

Figure 22(l). Longitudinal salinity (psu) distribution after 5-day averaging along the axis of Baltimore Harbor, days 360–365, 1984.

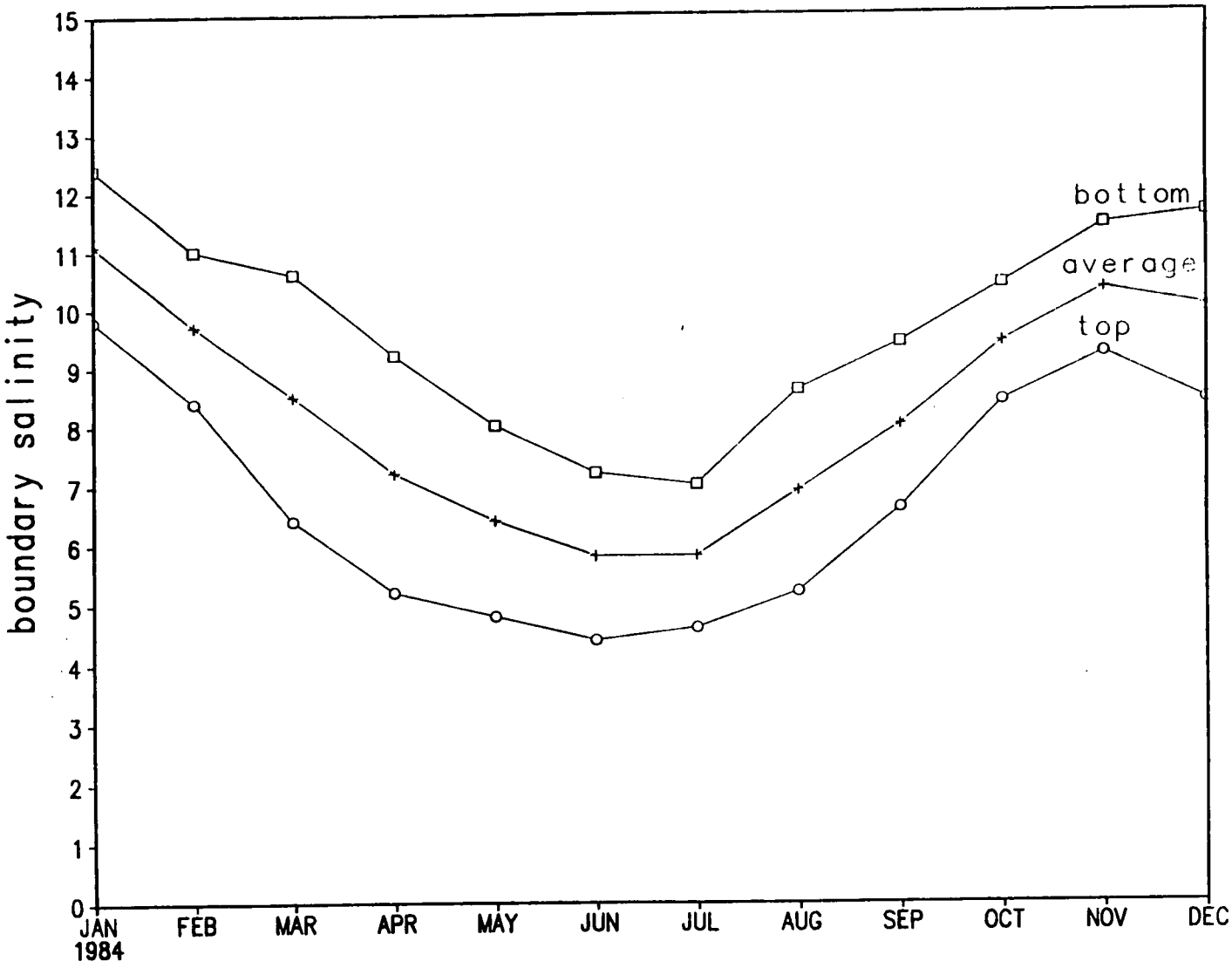

Figure 23. Five-day averaged surface and bottom salinities (psu) over the deep channel at the Harbor mouth at 30-day intervals in 1984. Between the two curves is the average of the two.

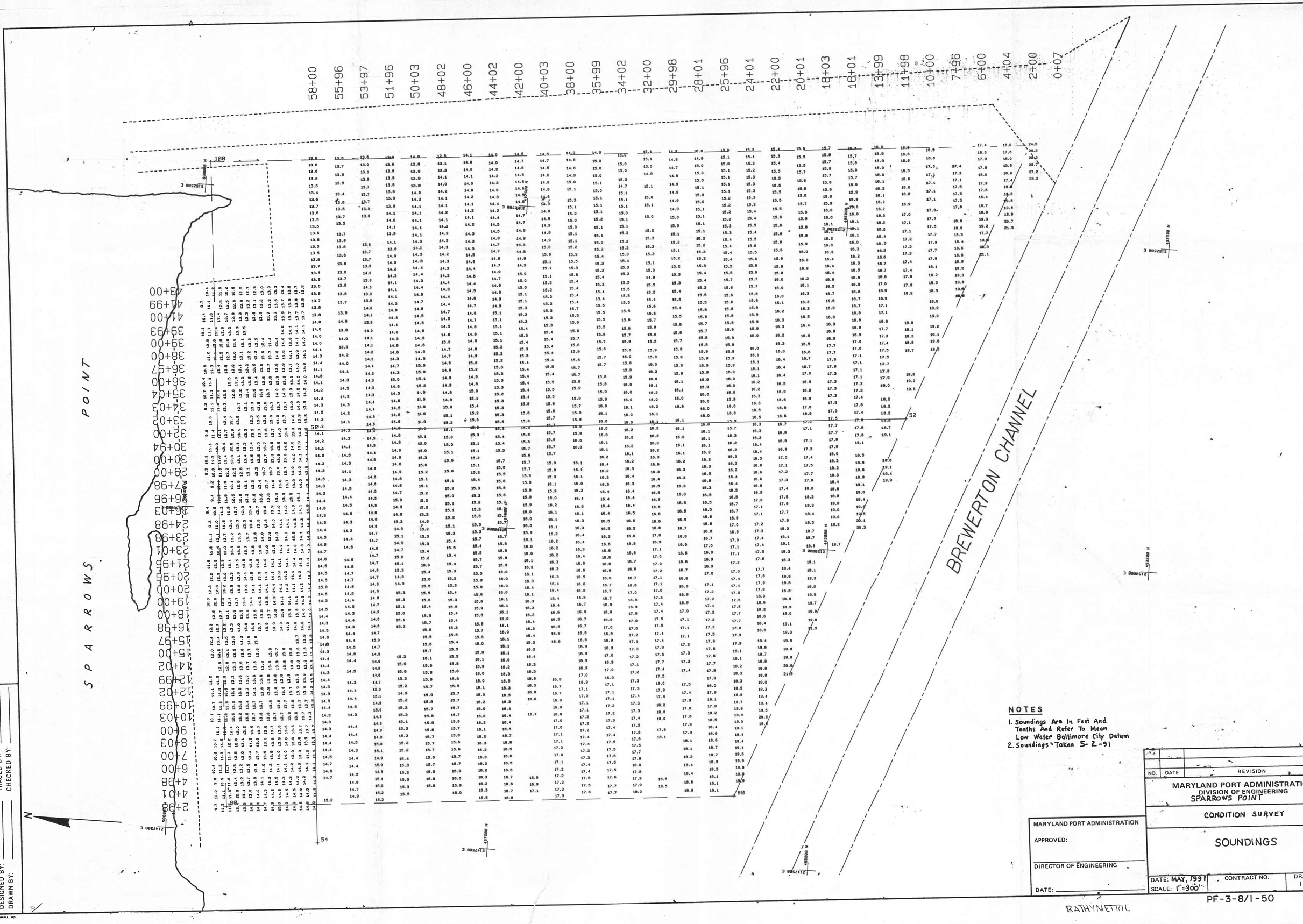

NOTES

1. Soundings Are In Feet And Tenths And Refer To Mean Low Water Baltimore City Datum
2. Soundings Taken 5-2-91

SURVEYED BY: _____ TRACED BY: _____
DESIGNED BY: _____ CHECKED BY: _____
DRAWN BY: _____

NO.	DATE	REVISION	BY

MARYLAND PORT ADMINISTRATION
DIVISION OF ENGINEERING
SPARROWS POINT

CONDITION SURVEY

SOUNDINGS

MARYLAND PORT ADMINISTRATION
APPROVED:
DIRECTOR OF ENGINEERING
DATE: _____

DATE: MAY, 1991 | SCALE: 1"=300' | CONTRACT NO. | DRAWING NO. 1 OF 1

PF-3-8/1-50

BATHYMETRIC

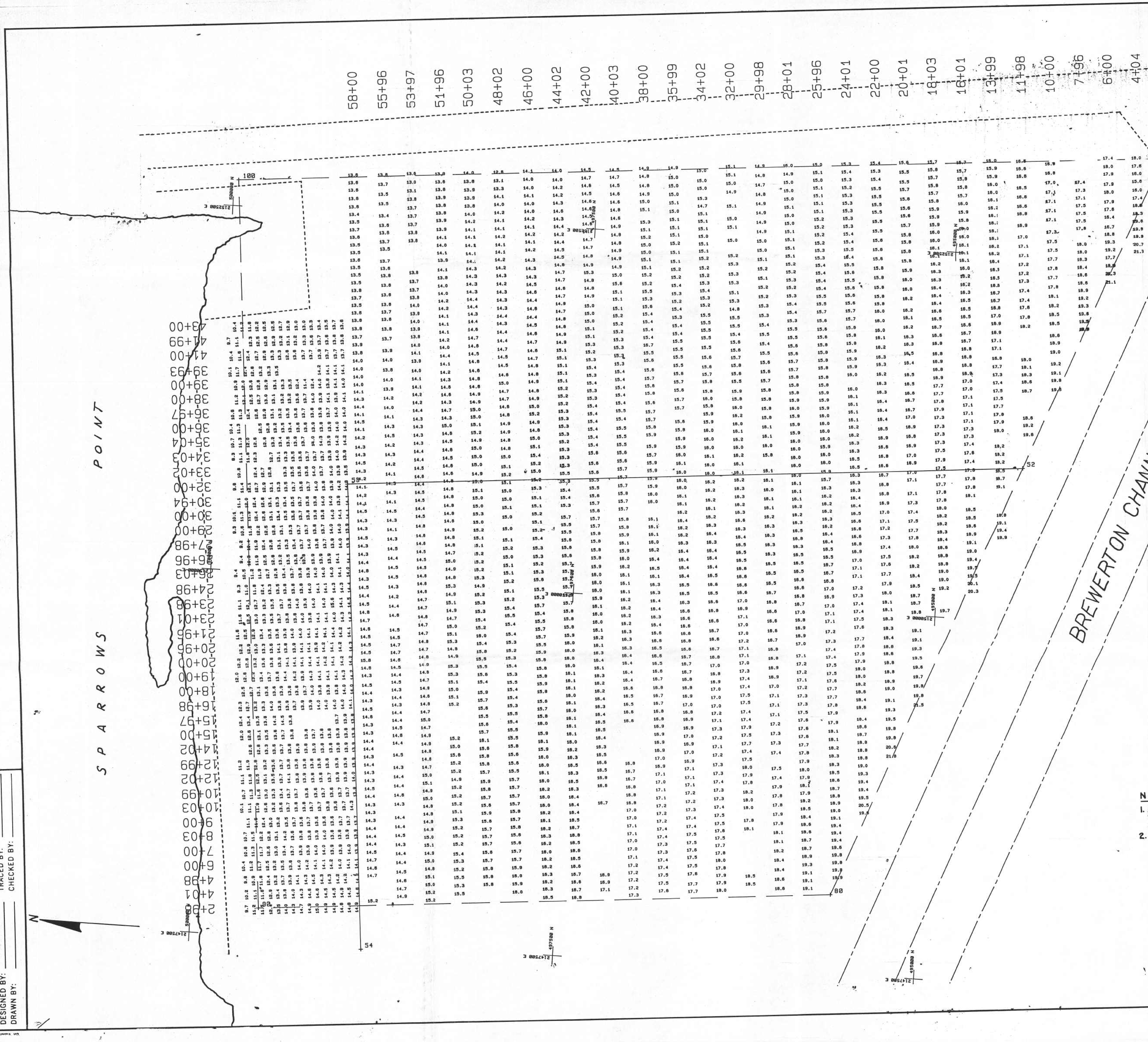

NOTES

1. Soundings Are In Feet And Tenths And Refer To Mean Low Water Baltimore City Datum
2. Soundings Taken 5-2-91

NO.	DATE	REVISION	BY

MARYLAND PORT ADMINISTRATION
DIVISION OF ENGINEERING
SPARROWS POINT

CONDITION SURVEY

SOUNDINGS

MARYLAND PORT ADMINISTRATION

APPROVED:

DIRECTOR OF ENGINEERING

DATE:

DATE: MAY, 1991
SCALE: 1"=300'

CONTRACT NO.

DRAWING NO. 1 OF 1

PF-3-8/1-50

SURVEYED BY:
DESIGNED BY:
DRAWN BY:
TRACED BY:
CHECKED BY:

BATHYMETRIC